Chemogenetic protein engineering: optimization of artificial metalloenzymes for oxidation and reduction reactions

Thèse présentée à la Faculté des Sciences
Institut de Chimie
Université de Neuchâtel

Pour l'obtention du grade de docteur ès sciences

Par

Anca Pordea

Thèse soutenue le 06 juin 2008 devant le jury composé par:

Prof. Thomas R. Ward, directeur de thèse, Université de Neuchâtel, Suisse
Prof. Donald Hilvert, rapporteur, Ecole Polytéchnique Fédérale de Zürich (ETHZ), Suisse
Prof. Robert Deschenaux, rapporteur, Université de Neuchâtel, Suisse

Université de Neuchâtel
2008

Université de Neuchâtel

FACULTE DES SCIENCES
Secrétariat-Décanat de la faculté
- Rue Emile-Argand 11
- CP 158
- CH-2009 Neuchâtel

IMPRIMATUR POUR LA THESE

Chemogenetic Protein Engineering: Optimization of Artificial Metalloenzymes for Oxidation and Reduction Reactions

Anca PORDEA

UNIVERSITE DE NEUCHATEL

FACULTE DES SCIENCES

La Faculté des sciences de l'Université de Neuchâtel,
sur le rapport des membres du jury

MM. T. Ward (directeur de thèse),
R. Deschenaux et D. Hilvert (ETH Zürich)

autorise l'impression de la présente thèse.

Neuchâtel, le 12 juin 2008

Le doyen :
F. Kessler

UNIVERSITE DE NEUCHATEL
FACULTE DES SCIENCES
Secrétariat - décanat de la faculté
Rue Emile-Argand 11 - CP 158
CH-2009 Neuchâtel

Mots clés: métalloenzymes artificielles, catalyse asymétrique, optimisation chimio-génétique, biotine-streptavidine, transfert hydrogénant, réduction de cétones, sulfoxydation, vanadium.

Keywords: artificial metalloenzymes, asymmetric catalysis, chemogenetic optimization, biotin-streptavidin, transfer hydrogenation, ketone reduction, sulfoxidation, vanadium.

This work was the object of four scientific publications:

"Artificial Transfer-Hydrogenases Based on the Biotin (Strept)avidin Technology: Fine Tuning the Selectivity by Saturation Mutagenesis of the Host Protein". C. Letondor, A. Pordea, N. Humbert, A. Ivanova, S. Mazurek, M. Novic, T. R. Ward, *J. Am. Chem. Soc.*, **2006**, *128*, 8320.

"Designed Evolution of an Artificial Transfer Hydrogenase Based on the Biotin-Streptavidin Technology". A. Pordea, M. Creus, T. Rossel, A. Sardo, C. Letondor, A. Ivanova, I. LeTrong, R. E. Stenkamp, T. R. Ward, *Angew. Chem, Int. Ed.*, **2008**, *47*, 1400.

"Artificial Metalloenzyme for Enantioselective Sulfoxidation Based on Vanadyl-loaded Streptavidin". A. Pordea, M. Creus, J. Panek, C. Duboc, D. Mathis, M. Novic, T.R. Ward, *J. Am. Chem. Soc.*, in press.

"Chemogenetic Protein Engineering: An Efficient Tool for the Optimization of Artificial Metalloenzymes". A. Pordea and T.R. Ward, *Chem. Commun.*, in press.

Table of Contents

Acknowledgements

This thesis is the expression of several years of experimental and theoretical work, but also of personal development and it would not exist without the support and assistance of different people, to whom I would like to show here my appreciation.

Foremost, I express my gratitude to Professor Thomas Ward, who guided me during these years of research and taught me that science is about privileging investigation over certainty. This work would not have been possible without his trust, encouragement and good advice.

I am grateful to Professor Donald Hilvert, Professor Robert Deschenaux and Professor Thomas Ward, who accepted to read and judge this work.

I am indebted to Mrs. Carole Duboc, Dr. Jaroslaw Panek, Dr. Sylwester Mazurek and Dr. Julien Furrer, for their kind assistance and for their scientific contribution.

I wish to thank all the collaborators from the Artificial Metalloenzymes Laboratory, my past and present colleagues, for their support and the good moments shared in and outside the lab: Nicolas, Myriem, Gérard, Julieta, Christophe M., Chris, Edy, Yves, Julien, Anita, Marc, Sabina, Thibaud, Cheikh, Alessia, Johannes, Thérèse, Jérémy, Lu and the undergraduate students Déborah, Jean-Christophe, Joanne, Fred and Christelle. Special thanks to Déborah, for her joyfulness and her work on the (schlouf)oxidation reaction, to Alessia and Thibaud, for their help with the (tedious) screening experiments and to Julieta, for her kindness and her precious advice.

I also thank all the colleagues and the administrative staff of the Institute of Chemistry and the team of biologists, who made the every day life in the lab fun and stimulating.

I would like to address a particular thank you to Christophe, who played a decisive role in this thesis journey. His passion for research, his helpful comments and his friendship have largely contributed to my forming as a scientist and as a person. As well, I am thankful to Marc for his constant joviality and for the endless discussions about science and life, which have been of great value to me.

I thank all the friends who have joined me in this discovery and have made it an unforgettable life experience: Adelina, Madelyne, Sabine, Flo, Olivier, Edith, Mimi, Josep, Fred, Luc, Johan, Egidio, Mickey, Sabina, Agathe, Mickaël, Julia, Rob, Olha, Laura, Piero and all the others. Among them, Julien has been a lab mate, a partner for scientific and personal controversies, a beer companion during long evenings of debates, a sports advisor and, above all, a good friend and I thank him for that.

I express all my appreciation to Mrs. Liliana Lupsa, who first persuaded and got me interested in the fascinating world of molecules.

Most importantly, I am grateful to my family and friends in Romania and Italy and particularly to my father and sister, as well as to my beloved mother and grandmother. They have offered me a loving and encouraging environment where to develop and taught me the values of life.

Finally, I cannot finish without addressing all my gratitude and love to Ugo, for his support and patience during all these years. His presence helped me during my worst and my best days of this beautiful adventure.

Abstract

The ability to optimize or to find new catalysts for enantioselective transformations has a major impact in today's chemistry. Artificial metalloenzymes lie at the interface between organometallic and enzymatic catalysis and have an immense optimization potential, which combines chemical and genetic methods to screen diversity space. In terms of activity, reaction repertoire, substrate range and operating conditions, they take advantage of the versatility of the organometallic chemistry. In contrast, the enantioselectivity is determined by the biomolecular scaffold, which provides a well defined second coordination sphere to the organometallic moiety, reminiscent of enzymes.

Incorporation of catalytically active biotinylated complexes within streptavidin affords artificial metalloenzymes for the transfer hydrogenation of prochiral ketones. The activity and selectivity trends of the catalysts are ensured by the choice of the chemical fragment in a first screening round. Insight into the structure of an artificial enzyme forms the basis of a designed evolution step, which relies on successive rounds of saturation mutagenesis at carefully selected positions and screening for enantioselectivity. This procedure allows the identification of highly selective scaffolds for the reduction of challenging substrates, such as dialkyl ketones.

The well-tailored hydrogen bond network of streptavidin's binding cavity can also accommodate non-biotinylated frameworks, such as catalytically active metal ions. The enantiodiscriminating environment provided by the host protein can be exploited to perform highly enantioselective vanadium-catalyzed oxidations of several prochiral sulfides, demonstrating that specific metal binding can transform a non-enzymatic protein into an enantioselective biocatalyst with synthetic utility.

Résumé

La capacité d'optimiser ou de créer de nouveaux catalyseurs pour des transformations énantioselectives a un impact majeur dans les applications de la chimie actuelle. Les métalloenzymes artificielles se situent à l'interface entre la catalyse organométallique et celle enzymatique et ont un immense potentiel d'optimisation, qui combine des méthodes chimiques et génétiques pour créer la diversité. En termes d'activité, répertoire de réactions et de substrats ou conditions opératoires, elles exploitent la versatilité de la chimie organométallique. Par contre, l'énantiosélectivité est déterminée par la protéine, qui assure une seconde sphère de coordination très bien définie, réminiscente des biocatalyseurs.

L'incorporation des complexes biotinylés catalytiquement actifs dans la streptavidine permet la création des métalloenzymes artificielles pour le transfert hydrogénant des cètones prochirales. Les tendances générales de l'activité et de la sélectivité des catalyseurs sont assurées par le choix de la partie organométallique suite à un premier criblage. L'étude de la structure d'une telle enzyme artificielle est à la base d'une « évolution rationnelle », dans laquelle des étapes successives de mutagenèse de saturation à des positions attentivement choisies sont combinées avec un criblage de l'énantiosélectivité. Cette méthode permet l'identification des catalyseurs hautement sélectifs pour la réduction de substrats difficiles, comme par exemple les dialkyl cètones.

Le réseau des liaisons hydrogène dans le site actif de la streptavidine est très bien défini et permet également l'insertion de composés non-biotinylés, tels des ions métalliques catalytiquement actifs. L'environnement asymétrique assuré par la protéine peut être exploité dans des réactions de sulfoxydation énantiosélective catalysée par du vanadium. Ces réactions montrent que l'incorporation spécifique d'un métal peut transformer une protéine sans activité enzymatique en un biocatalyseur utilisé en synthèse organique.

Curriculum Vitae

EDUCATION

2004-2008 PhD student

- Department of Chemistry, University of Neuchâtel (CH)
- Expected date of graduation: June 2008

2003-2004 DEA (equiv. Master) in Organic Chemistry

- Norman Doctoral School of Chemistry and Biology, Rouen (FR)
- Main courses: total synthesis, retrosynthesis, chemistry of heterocycles, chemistry of sulfur and selenium, chemistry of radicals, organometallic chemistry, asymmetric synthesis
- Rank: 2/22

1999-2004 Diploma in Chemical Engineering (equiv. Master)

- INSA - National Institute of Applied Sciences (Engineering School), Rouen (FR)
- Specialization (2002-2004): Organic Chemistry

1995-1999 Highschool Graduate

- German Highschool, Arad (RO)
- Specialization: Mathematics, Physics, Chemistry

RESEARCH EXPERIENCE

2004-2008 PhD Thesis

- Artificial Metalloenzymes Laboratory, University of Neuchâtel (CH)
- Thesis: "Chemogenetic Protein Engineering: Optimization of Artificial Metalloenzymes for Oxidation and Reduction Reactions"
- Supervisor: Prof. T.R. Ward
- Summary: the work consisted in developing artificial metalloenzymes for enantioselective catalysis, by incorporation of a catalytically active metal fragment within streptavidin. Using the biotin-streptavidin technology, the designed evolution of a ruthenium-dependent artificial transfer hydrogenase was implemented. By incorporation of a non-biotinylated vanadium fragment into streptavidin, a new artificial sulfoxidase was discovered.
- Technical skills:
    - Synthesis background: multi-step synthesis, work under controlled atmosphere (Schlenk techniques)
    - Catalysis background: asymmetric homogeneous organometallic catalysis, enzymatic catalysis, parallel catalyst screening using a multireactor
    - Standard purification and characterization methods: flash chromatography, NMR, MS, UV-Vis, analytical GC and HPLC

Feb.-June 2004 Pre-Doctoral Fellow

- Institute for Research in Organic Chemistry, Rouen (FR)
- Research project: "Synthesis of Huprines using Diels-Alder–Suzuki Tandem Reaction"
- Supervisor: Prof. Pierre-Yves Renard

Jan.-Mar. 2003 Research Fellow

- Institute for Research in Organic Chemistry, Rouen (FR)
- Research project: "Synthesis of a Glycosidase-resistant Glycopeptide"
- Supervisor: Prof. Jean-Charles Quirion

OTHER RESPONSIBILITIES

Laboratory Instructor (2004-2007)

- Department of Chemistry, University of Neuchâtel
- Responsibilities included supervising:
  - a laboratory section of analytical chemistry for undergraduate biology students
  - one undergraduate student during a three-month research project
  - two undergraduate chemistry students during their six-month diploma work

Private teaching (2001-2003)

- High school level in chemistry, mathematics and physics

Training as factory worker (July 2001)

- OLDHAM Arras, production of gas detection devices
- Responsibilities included manufacturing gas detectors in a team of 8 workers

AWARDS

- First prize for poster presentation at the International Symposium on Bioorganometallic Chemistry, Milano (IT), July 2006
- First prize for oral presentation at CUSO's Summer School (Conférence Universitaire de Suisse Occidentale), Villars (CH), Sept. 2006

PUBLICATIONS

- **"Artificial Transfer-Hydrogenases Based on the Biotin (Strept)avidin Technology: Fine Tuning the Selectivity by Saturation Mutagenesis of the Host Protein"**. C. Letondor, A. Pordea, N. Humbert, A. Ivanova, S. Mazurek, M. Novic, T. R. Ward, *J. Am. Chem. Soc.*, **2006**, *128*, 8320.
- **"Designed Evolution of an Artificial Transfer Hydrogenase Based on the Biotin-Streptavidin Technology"**. A. Pordea, M. Creus, T. Rossel, A. Sardo, C. Letondor, A. Ivanova, I. LeTrong, R. E. Stenkamp, T. R. Ward, *Angew. Chem, Int. Ed.*, **2008**, *47*, 1400.

- **"Artificial Metalloenzyme for Enantioselective Sulfoxidation Based on Vanadyl-loaded Streptavidin"**. A. Pordea, M. Creus, J. Panek, C. Duboc, D. Mathis, M. Novic, T.R. Ward, *J. Am. Chem. Soc.*, in press.

- **"Chemogenetic Protein Engineering: An Efficient Tool for the Optimization of Artificial Metalloenzymes"**. A. Pordea and T.R. Ward, *Chem. Commun.*, submitted.

OTHER SKILLS

Languages

- Romanian mother tongue
- French fluent
- English fluent; TOEIC score (2004): 960/990
- Italian good level
- German basic; language diploma obtained in 1999

Communication

- Good experience in oral presentations at seminars and conferences (speaker in the IBAAC mid-term meeting, Ljubljana-SLO, 2006; speaker in CUSO's Summer School, Villars-CH, 2006)
- Poster presentations in six national and international meetings

Organization

- Co-organization of the official reception for the "Remise des Diplômes" of INSA Rouen (Guests: 2000 people)

Informatics

- Scientific software: SciFinder, ChemDraw, IsisDraw, Weblab ViewerPro, DS Visualizer
- Office software: Word, Excel, PowerPoint, KaleidaGraph

List of Abbreviations

⊂	included in
Å	Angström
acac	acetylacetonate
ANS	2-anilinonaphtalene-6-sulfonic acid
APCI	Atmospheric Pressure Chemical Ionisation
Ar	arene
Avi	avidin
Aviloop	chimaeric streptavidin
BINAL-H	l,l'-binaphthalene-2,2'-diol, aluminium hydride
BINAP	2,2'-bis(diphenylphosphanyl)-1,1'-binaphtyl
BINOL	l,l'-binaphthalene-2,2'-diol
Biot	biotin(yl)
BNHS	(D)-biotinyl-*N*-hydroxysuccinimide ester
BPFB	(D)-biotin pentafluorophenyl ester
BSA	bovine serum albumin
t-Bu	*tert*-butyl
C	catalyst
CAMP	methylcyclohexyl-*o*-anisylphosphine
Conv.	conversion
CPO	chloroperoxidase
DET	diethyl tartrate
DIOP	2,3-*O*-isopropylidene-2,3-dihydroxy-1,4-bis(diphenylphosphino)butane
DIPAMP	1,2-bis(*o*-anisylphenylphosphinyl)ethane
DMF	dimethylformamide
DMSO	dimethylsulfoxide
DNA	deoxyribonucleic acid
DOPA	3,4-dihydroxyphenylalanine
E	enzyme
EDC	*N*-(3-dimethylaminopropyl)-*N'*-ethylcarbodiimide

e. g.	*exempli gratia*, for example
ee	enantiomeric excess
EPR	Electron Paramagnetic Resonance
eq.	equivalent(s)
ESI	Electron Spray Ionisation
Et	ethyl
GC	Gas Chromatography
HABA	4-hydroxyazobenzene-2-carboxylic acid
HOBT	1-hydroxybenzotriazole
HPLC	High Performance Liquid Chromatography
i. e.	*id est*, that is
M	metal
Me	methyl
min.	minute(s)
MOPS	3-(*N*-morpholino)propanesulfonic acid
MS	Mass Spectrometry
NADH	nicotinamide adenine dinucleotide
NADPH	nicotinamide adenine dinucleotide phosphate
NMR	Nuclear Magnetic Resonance
P	product
PCR	polymerase chain reaction
PDB	Protein Data Bank
i-Pr	*iso*-propyl
RMS	root mean square
r.t.	room temperature
Sav	streptavidin
t_1, t_2	retention times (min.)
TADDOL	*trans*-α,α'-(dimethyl-1,3-dioxolane-4,5-diyl)bis(diphenylmethanol)
Temp.	temperature
THF	tetrahydrofurane
TOF	turnover number
TON	turnover frequency

TS	transition state
TsDPEN	*N*-(*p*-toluenesulfony1)-1,2-diphenylethylenediamine
v / v	volume / volume ratio
vs.	*versus*
WT	wild-type

Chapter 1 Introduction

1 Asymmetric Catalysis

Catalysis is the phenomenon by which a substance, called a catalyst, accelerates a chemical reaction without undergoing any permanent chemical change.

Catalysis plays an important role in many aspects of human progress: in the efficient manufacture of many kinds of materials, from fuels to plastics, in creating new energy sources and protecting the environment and in developing effective, safer medicines. Over recent decades, there has been enormous progress in understanding the molecular mechanisms leading to efficient catalytic reactions and this has had an explosive effect on developing new catalytic systems. Since a large number of processes in the chemical industry now depend on catalysts to work efficiently, it is not surprising that catalysis is an extremely active research area.

1.1 Generalities on Catalysis

Catalysts participate in chemical reactions by changing the kinetics, while the reaction result and the overall thermodynamics are the same (Figure 1).

The following factors can explain the effect of the catalyst on the reaction:

- stabilization of the transition state;
- decreasing the entropy of the reactants, by interactions that force their proximity and favourable spatial orientation;
- selective enhancement of one specific pathway over the competing, undesired ones.

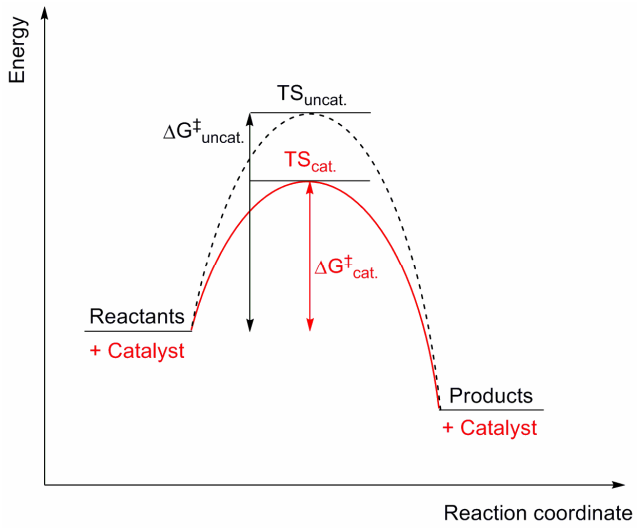

Figure 1. Effect of a catalyst on the reaction's Gibbs energy of activation.

Catalysis is a phenomenon of crucial importance not only for chemical and biochemical reactions occurring in nature, but also for chemical laboratories and industry. The production of a variety of chemicals involves catalytic reactions, as they consume less energy and generate less waste than stoichiometric ones.

Although catalysis, as a tool for performing reactions, had already been exploited much earlier, the term "catalysis" was first introduced by Jöns Jakob Berzelius, who in 1835 noted that certain chemicals have the property of accelerating a reaction. Later, Humphry Davy discovered that the oxidation of coal gas is catalyzed by platinum. In the 1880's, Wilhelm Ostwald at the Leipzig University gave the definition that a catalyst does not influence the thermodynamic equilibrium, but only affects the chemical rate of the reaction. For this work, Ostwald received in 1909 the Nobel Price in Chemistry.[1]

From a physical point of view, catalysts have traditionally been divided into two groups:

- homogeneous catalysts: they are present in the reaction mixture in the same phase as the reactants / products. As a result, they have good contact with the reactants and therefore a high efficiency, allowing the use of mild reaction conditions.
- heterogeneous catalysts: they are present in a different phase than the reactants. They offer the advantage of easy separation and recycling.

According to their chemical nature, homogeneous catalysts can also be classified into organocatalysts and organometallic catalysts (transition metal complexes). One special class of homogeneous catalysis is the enzymatic catalysis.

Homogeneous catalysis by transition metal complexes has been intensely studied since the 1940's. The pioneering work of G. Wilkinson[2] on alkene hydrogenation using a rhodium-based catalyst (Scheme 1) had a considerable impact on the development of homogeneous catalysis for the synthesis of organic compounds.[3]

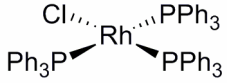

chlorotris-(triphenylphosphine)rhodium
Wilkinson's catalyst

Scheme 1. Wilkinson's catalyst for alkene hydrogenation.

Even though it was early discovered that fermentation processes are of catalytic nature, it was not until about one hundred years ago that biocatalysis started to be employed to perform

chemical transformations on non-natural organic compounds. In the past decades there has been an enormous increase in the application of enzymes to produce fine chemicals, especially in the pharmaceutical industry.[4]

1.2 Catalyst Performance

The successful application of a catalytic transformation for organic synthesis depends on several key parameters that influence the total cost of the process. The activity of a catalyst is defined as the amount of product produced by a unit weight of catalyst in a certain time. In chemocatalysis, the degree of activity is described in terms of turnover frequency (TOF, moles product formed by a mole of catalyst per unit time), while in biocatalysis the term employed is the specific activity (μmoles of product formed per unit mass of enzyme per unit time).

Knowledge of enzyme kinetics is useful to understand the enzymatic activity. The basic equation of enzyme kinetics follows Michaelis-Menten theory, which divides the catalytic reaction into two steps (Equation 1). First, the enzyme (E) and the substrate (S) associate in a rapid and reversible step to give the enzyme-substrate complex (ES, dissociation constant K_S). The chemical processes take place during the second step with formation of the product (rate constant k_2). Other enzyme-bound intermediates can also occur during the reaction, like for example the enzyme-product complex. An apparent dissociation constant can be defined, K_M, which can be treated as the overall dissociation constant of all the enzyme-bound species.[5] In the simple Michaelis-Menten mechanism, in which there is only one ES complex and the binding steps are fast, k_2 can be assimilated with the overall catalytic rate constant, k_{cat}, while $K_M = K_S$.

$$E + S \underset{}{\overset{K_S}{\rightleftharpoons}} ES \xrightarrow{k_2} E + P \qquad v = \frac{[E]_0[S]k_{cat}}{K_M + [S]} \qquad \text{(Equation 1)}$$

If the purity and the molecular mass of the enzyme are known, the specific activity of the enzyme is determined by the value of k_{cat} (moles of converted substrate per moles of catalyst per time unit). The k_{cat}/K_M constant determines the specificity of the enzyme for competing substrates and thus its general synthetic utility. For application in a catalytic process, an ideal enzyme would have a high specific activity and would be subject to minimal substrate inhibition.[5]

Another parameter that affects the practicality of a catalyst is its stability. This factor is associated with the turnover number (TON, moles of product formed per mol of catalyst), which reflects the amount of product formed before inactivation of the catalyst.

1.3 Chirality: Importance and Synthesis of Chiral Compounds

Chirality is defined as the geometric property of a rigid object of not being superimposable on its mirror image, called enantiomer. Chirality is a property of matter that can be found in biological systems, from the basic building blocks such as amino acids, carbohydrates and lipids to the layout of the entire organism. Life is based on chirality at the molecular level and therefore understanding and creating chiral processes is one of the most challenging areas in organic chemistry.

To date, chiral compounds have mostly gained attention in pharmaceutical industry.[6] Enantiomers of a chiral molecule have identical physical and chemical properties in an achiral environment. However, because living systems are chiral, each of the enantiomers of a chiral drug can behave very differently *in vivo*, thus displaying different pharmacologic activities (see Scheme 2 for an example of two enantiomers with different effects).[7] In addition to pharmaceuticals, chiral technology is important in other industries, *e.g.* biochemicals, pesticides, aroma and flavour compounds, dyes and pigments, liquid crystals, nonlinear optical materials, polymers and others.

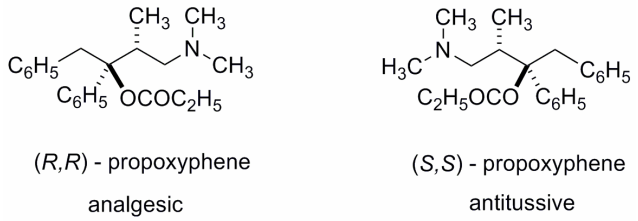

Scheme 2. The two enantiomers of propoxyphene display different biologic activities: the (*R*,*R*)-isomer is an analgesic, while the (*S*,*S*)-isomer has antitussive effect.

The combination of both enantiomers of a chiral compound in equal amounts forms a racemic mixture. The degree of enantiomeric enrichment of a non-racemic mixture can be analyzed using polarimetric, spectroscopic (NMR) or chromatographic techniques with a chiral stationary phase and is usually expressed in terms of enantiomeric excess (ee = ([*R*]-[*S*]) / ([*R*]+[*S*]) × 100).

Several different strategies are available for the preparation of enantiopure compounds, the most obvious being the chemical modification of “chiral pool” molecules, *i.e.* naturally

occurring chiral molecules such as amino acids, carbohydrates, terpenes, alkaloids etc. Resolution techniques (diastereomeric crystallization or enzymatic kinetic resolution) are widely used methods, especially on an industrial scale.[6] The recently developed dynamic kinetic resolution techniques (Scheme 3) are of particular interest in this area, as they allow the transformation of a racemic starting material into a single enantiomer.[8]

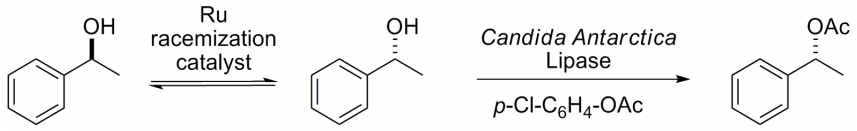

Scheme 3. Chemoenzymatic dynamic kinetic resolution of racemic 1-phenylethanol.

Asymmetric synthesis refers to synthetic paths starting from achiral compounds. There are four main approaches in asymmetric synthesis, all of which involve the use of chiral material (Scheme 4).[7] The asymmetric catalysis approach, in which the chirality is amplified rather than transferred, has clear economic advantages over the stoichiometric methods for the preparation of enantiomers.

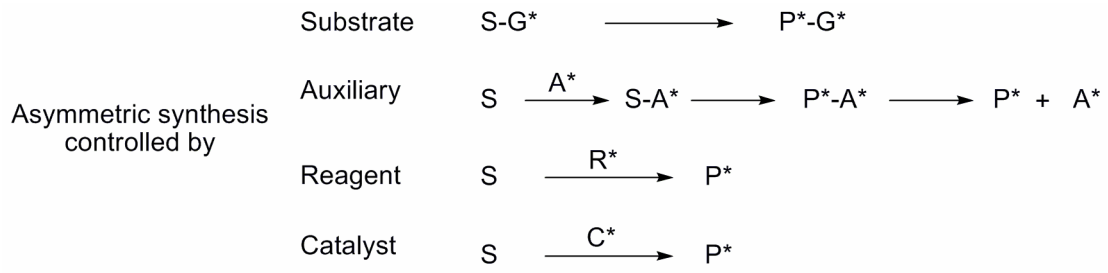

Scheme 4. Asymmetric synthesis of chiral compounds.

1.4 Homogeneous Asymmetric Catalysis

. There are three types of homogeneous asymmetric catalysts:

- organometallic catalysts
- biocatalysts: enzymes or whole cells
- organocatalysts

The first two categories have found most applications in enantioselective synthesis.[4,9-11] A complementary method, which has attracted renewed interest in recent years, is the enantioselective organocatalysis, in which the reaction is mediated by a small chiral organic molecule.[12]

1.4.1 Transition Metal-Mediated Enantioselective Catalysis

1.4.1.1 Historical Perspective

The development of chiral catalysts started in the 1960's with the pioneering work of William S. Knowles, who extended the use of Wilkinson's catalyst by placing the rhodium metal in a chiral environment provided by enantiopure phosphine ligands.[13] Knowles exploited the chirality at the phosphorous atom to obtain the first transition metal catalysts for the asymmetric hydrogenation of dehydro amino acids. A major breakthrough in this area was provided by Kagan, who showed that the chirality can be transferred from ligands bearing the asymmetry at the carbon backbone, like the bidentate C_2-symmetric diphosphine DIOP.[14] For the commercial synthesis of L-DOPA (a drug useful in treating Parkinson disease) through rhodium-catalyzed asymmetric hydrogenation, up to 95% ee was obtained using the chelating biphosphane ligand DIPAMP (Scheme 5).[15]

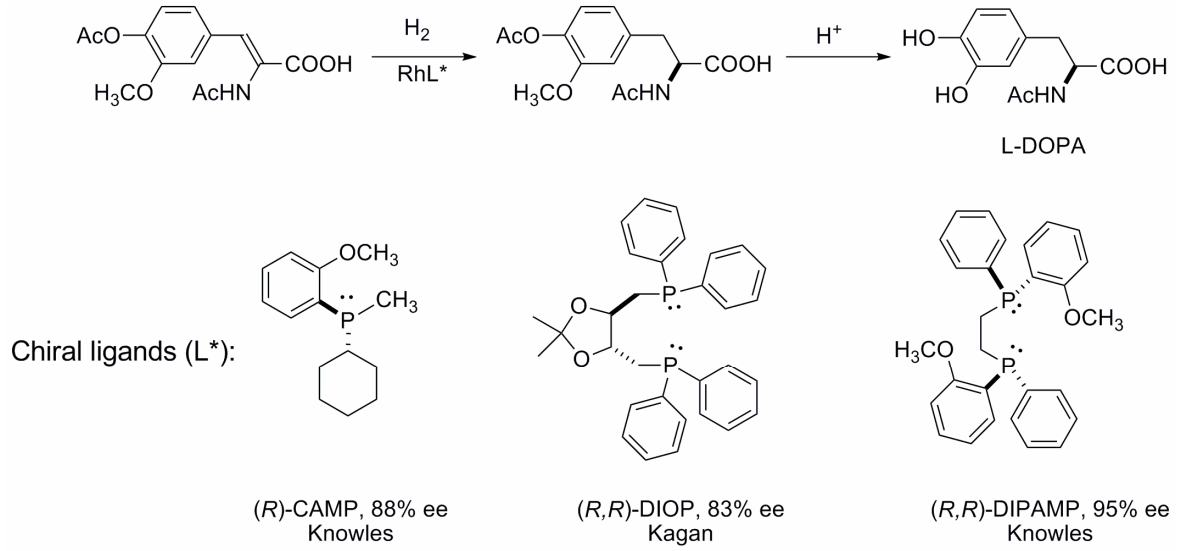

Scheme 5. Synthesis of L-DOPA and some chiral phosphine ligands used for the catalytic hydrogenation.

The soluble metal-ligand complexes for asymmetric hydrogenation have started a new era in catalytic processes. Ryoji Noyori discovered the BINAP-ruthenium(II) complexes, which proved to be excellent catalysts in the asymmetric hydrogenation of various functionalized alkenes and ketones with very high enantioselectivities.[16] Parallel to the progress in catalytic asymmetric hydrogenation, Barry K. Sharpless developed chiral catalysts for asymmetric oxidation reactions.[17] For their work in the field of asymmetric catalysis, W. Knowles, R. Noyori and B.K. Sharpless were awarded the 2001 Nobel Prize in Chemistry. Their

discoveries have had a significant impact on academic and industrial efforts to obtain chiral compounds.

1.4.1.2 General Principles

A variety of transition metals and chiral ligands have been used in the past decades to develop asymmetric catalysts.[18] The design of active and selective catalysts relies on a successful combination of metal centre, which interacts with the substrate and is responsible for the activity, and ligand, which modulates the steric and electronic properties of the catalyst and determines the selectivity. Some important trends in metal-ligand stabilities are outlined in Figure 2.[10]

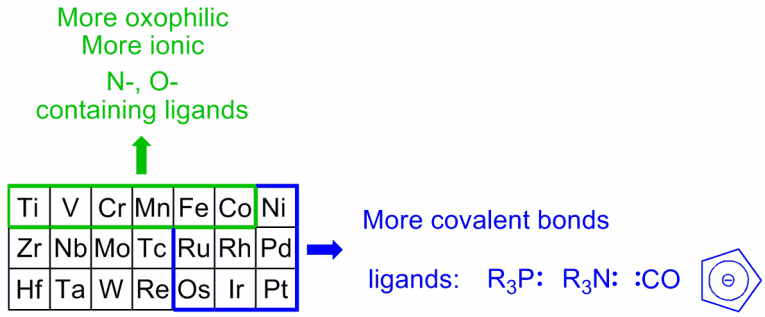

Figure 2. General trends in σ-bonding of early and late transition metals to common ligands.

In terms of ligand choice, in most cases chemists design their systems inspired by nature's catalysts, the enzymes. However, unlike enzymes, certain synthetic catalysts are not limited to a specific class of substrates, but display high activity and selectivity for a large panel of substrates and, more interestingly, for a wide range of different reactions. The discovery of such "privileged" ligands (named by analogy with the pharmaceutical compounds that are active against several biological targets) has greatly contributed to the rapid development of practical catalytic asymmetric processes (Scheme 6).[19]

The interactions that take place in the immediate vicinity of the metal are called first coordination sphere interactions. They are usually well-defined and can account for the enantioselectivity of the reaction. Yet, despite intensive computational, structural and mechanistic studies, predicting the outcome of an enantioselective catalytic transformation remains very challenging, since the difference in the two transition state energies leading to the two possible enantiomers is too small to be reliably computed (at 0°C, 95% ee represents a difference in energy of about 2 kcal / mole).[20] Moreover, the enantioselection path is decisively influenced by weak, non-bonding contacts between the substrate and the catalytic

environment, *i.e.* solvent, counter ions, salts etc.,[21] constituting the second coordination sphere.[22] To overcome this difficulty, combinatorial methods have been developed and implemented for the discovery of new, effective enantioselective catalysts.[23-26]

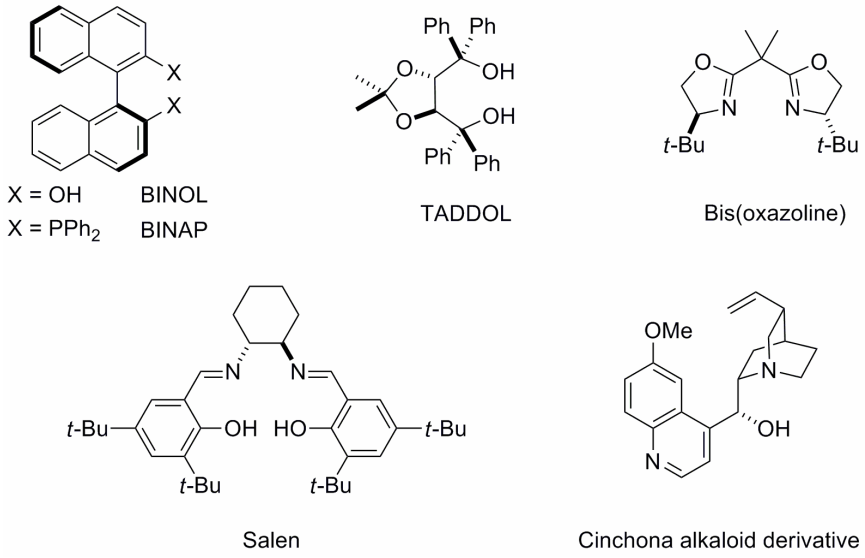

Scheme 6. Examples of privileged ligands.

1.4.2 Enzymatic Catalysis

Enzymes are models of energy-efficient, extremely selective and environmentally friendly chemical agents and they represent a permanent source of inspiration for designing synthetic catalysts. Unlike man-made catalysts, enzymes not only provide a chiral first coordination sphere, but their second coordination sphere is naturally evolved to maximize their efficiency inside organisms. Their catalytic site is deeply buried inside well-defined binding pockets and can be accessible through a narrow channel that contributes to the stereoselectivity of the reaction. These features, difficult to mimic in organometallic catalysis, are responsible for the high specificity and selectivity.[5]

Exploiting the natural chirality of biomolecules for enantioselective catalysis has depended for a long time on the discovery of recombinant DNA technology, which provided an efficient way to express and produce reasonable quantities of enzymes in the laboratory.[5] Biocatalysis has greatly expanded over the past decades and found a number of applications in industrial processes (one example is given in Scheme 7).[27] However, there are some practical issues associated with developing biocatalysts. Among these, the high substrate specificity, the availability of only one enantiomer, the lack of stability under particular reaction conditions and the extent of substrate / product inhibition are of particular

importance.[28] Nowadays, the ability to manipulate functions and structures of proteins through genetic engineering offers a means to optimize these features and to make enzymes more suitable for industrial use.[4,29,30] Recent advances regarding promiscuity in biocatalysis – the capacity of enzymes to catalyze transformations other than the ones they evolved for – suggest new applications in organic synthesis.[31,32]

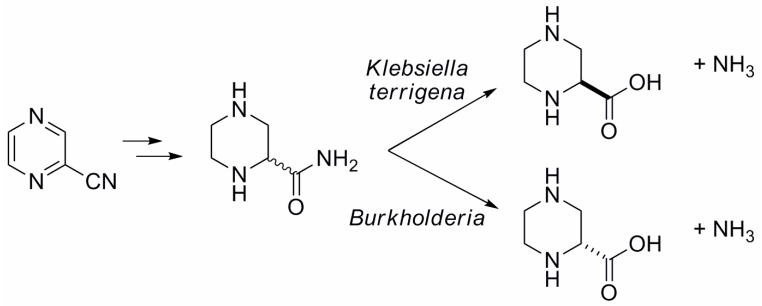

Scheme 7. Lonza process for the production of enantiomerically pure piperazine-2-carboxylic acids.

Biocatalytic reactions can be carried out either with isolated enzymes or with whole cell systems. Although the procedure employing the entire microorganism to perform a transformation is attractive as it avoids eventual co-factor regeneration and the use of special equipment for protein purification,[33] sometimes isolated enzymes are preferred, because they form fewer side products and there are no problems associated with membrane permeability and cell toxicity of the substrate.[34]

The following section of this chapter will describe some applications of homogeneous organometallic and enzymatic catalysis (only purified enzymes will be treated) in enantioselective reduction and oxidation reactions.

2 Enantioselective Catalytic Reduction and Oxidation Reactions

2.1 Transfer Hydrogenation of Carbonyl Bonds

2.1.1 Transition Metal-Mediated Catalytic Methods

Chiral alcohols are important intermediates in the synthesis of various high value-added chemicals.[35] The asymmetric reduction of carbonyl bonds is one of the most straightforward and energetically viable routes to access this class of compounds.

Although it appears as a simple transformation, the stereoselective reduction of ketones was for a long time a serious challenge for synthetic chemists. The chemical paths involved the use of stoichiometric reducing agents, like borane reagents,[36] BINAL-H[37] or the Corey-

Bakshi-Shibata method (CBS) using a chiral oxazaborolidine catalyst and a stoichiometric borane reagent.[38] The work of Noyori et al. on catalytic asymmetric reduction of simple and functionalized ketones initiated a new era in this field.[35] Ruthenium-BINAP-based systems for the hydrogenation of unsaturated compounds represent nowadays a tool of choice for the synthesis of enantiomerically enriched pharmaceuticals or their precursors (Scheme 8).[16] Because hydrogen is a clean and cheap resource, its use in industrial and research applications is very attractive.[39]

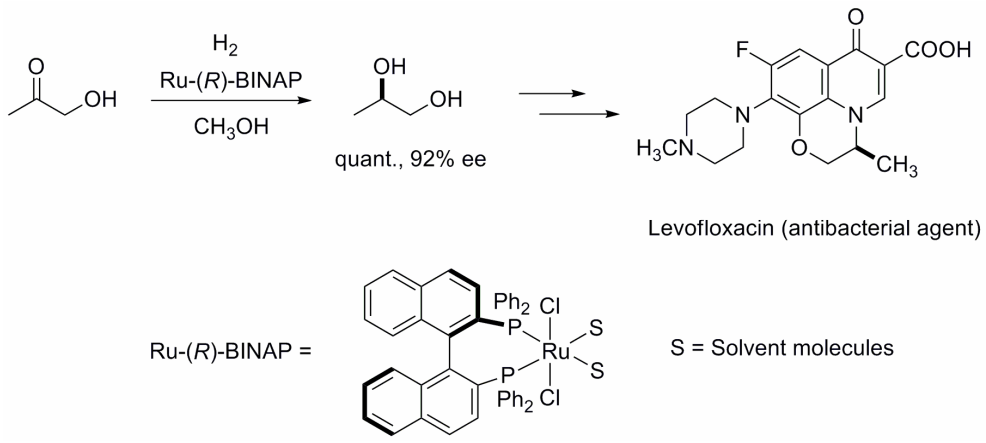

Scheme 8. Catalytic asymmetric hydrogenation of hydroxyacetone to (*R*)-1,2-propanediol, an intermediary in the industrial synthesis of the antibacterial levofloxacin.

Asymmetric hydrogen transfer reactions are a practical alternative to hydrogenation processes, in that they are easy to implement, they usually take place under mild conditions and they do not use hazardous hydrogen gas. They are particularly suitable for small- and medium-scale syntheses.

Transfer hydrogenation refers to the reduction of an unsaturated molecule using a hydrogen donor other than H_2. The first example of hydrogen transfer to the carbonyl group is the Meerwein-Ponndorf-Verley reduction discovered in 1925.[40-42] The past decade witnessed an extensive development of highly active and selective catalytic systems for the transfer hydrogenation of carbon-heteroatom unsaturated bonds.[43-45] Designed by Hashiguchi, Ikariya, Noyori et al., d^6 piano-stool ruthenium complexes in conjunction with aminosulfonamides such as TsDPEN (*N*-(*p*-toluenesulfony1)-1,2-diphenylethylenediamine **1**, Scheme 9) represent one of the most significant discoveries in this field.[46]

Metal complexes. A variety of bi-, tri- or tetradentate ligands bearing usually nitrogen, oxygen or phosphorous atoms have been developed for the successful reduction of various

carbonyl compounds with outstanding selectivities. An overview of some of the most effective ligands developed in the past years is presented in Scheme 9.[39,45,47] The most successful, in terms of activity as well as enantioselectivity, are the monotosylated diamines such as **1** and **2**,[46,48] the 1,2-aminoalcohols, such as **3a**, **3b** and **4**[43,49,50] and some phosphino-oxazoline derivatives such as **5**.[51,52] Recently, Reetz et al. described a selective catalyst with a very large scope, the BINOL-derived diphosphonite **8**.[53]

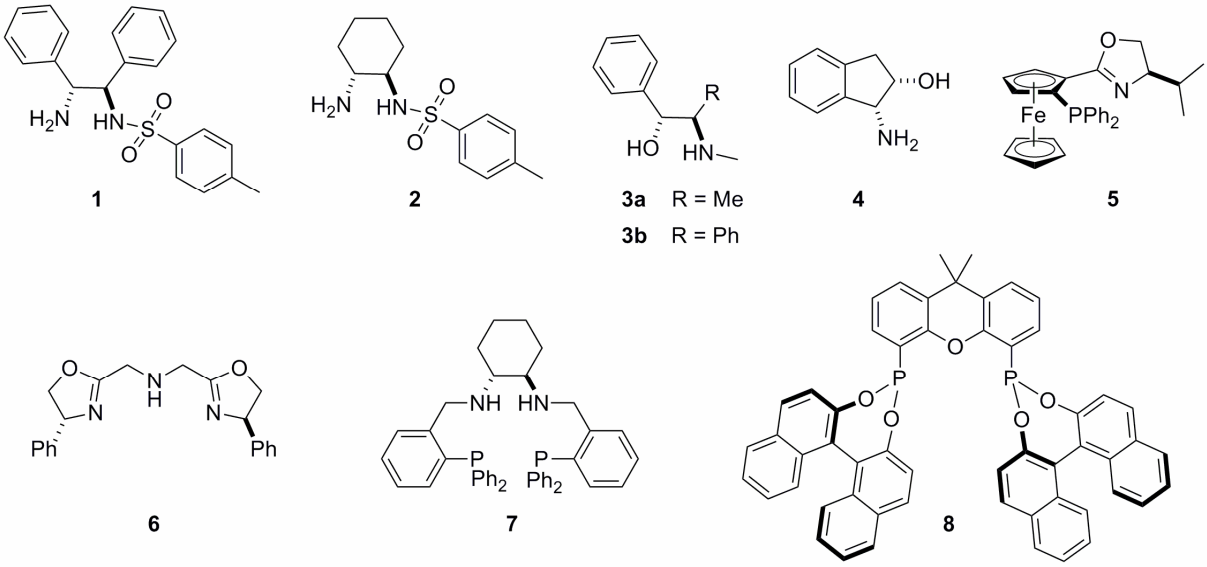

Scheme 9. Some of the most effective ligands for the enantioselective transfer hydrogenation of ketones.

The typical metal fragment which associates with the bidentate ligands (1,2-diaminoalcohols or monotosylated 1,2-diamines) is constituted of half-sandwich π-complexes, such as Ru-arene or Rh- / Ir-cyclopentadienyl moieties, possessing an additional anionic ligand, typically a halide (Scheme 10).

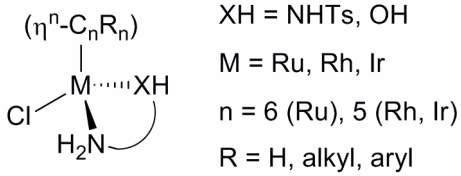

Scheme 10. Schematic representation of Ru^{II}, Rh^{III} and Ir^{III} complexes for asymmetric transfer hydrogenation.

Hydrogen source. Isopropanol (*i*-PrOH), formic acid / triethylamine azeotropic mixture (HCOOH / Et_3N) or aqueous sodium formate (HCOONa) are the most common hydrogen sources for the transfer hydrogenation. *i*-PrOH is the conventional hydrogen donor, since it is a cheap and easy to handle compound. Activation of the starting complex is achieved in the

presence of a base, like potassium hydroxide.[54,55] During the reaction, *i*-PrOH is transformed into acetone, which represents a possible substrate for the Ru catalyst. Therefore, the reduction of ketones by *i*-PrOH is reversible and governed by the oxidation potential of the relevant ketone / alcohol couple. Moreover, since the major enantiomer is more susceptible to the reverse reaction, the enantioselectivity decreases with increasing conversion. The reversibility of the reaction constitutes the major limitation of the reductions with *i*-PrOH.[43] Other hydrogen sources have been developed to overcome this problem. Using HCOOH / Et_3N or HCOONa in an open system allows an irreversible hydride transfer to the Ru complex, due to the formation and continuous elimination of gaseous CO_2.[56,57] However, some complexes tend to decompose faster upon contact with formic acid.[45]

Mechanism. Depending on the metal, ligand and hydrogen donor used, different mechanistic pathways can be envisaged for the hydrogen transfer from a catalyst to a carbonyl group (Scheme 11). "Direct hydrogen transfer" usually occurs with main group metals, while transition metal catalysts follow the "hydridic route", in which a mono- or a dihydride metal species is involved.[58-61] The monohydridic transfer can either occur via ketone coordination to the metal, or via an outer sphere variant. Still further, when no substrate-metal bonding is involved, the mechanism can be concerted or stepwise.

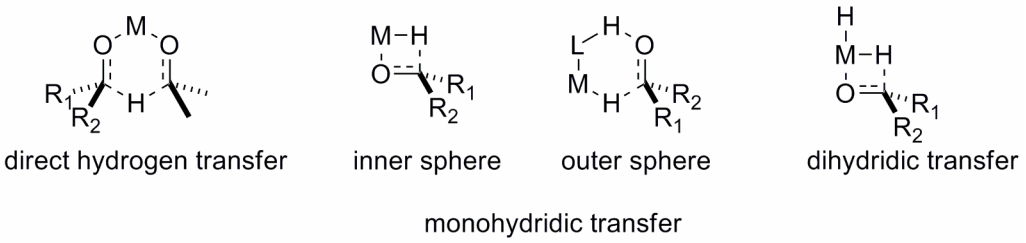

Scheme 11. Possible transition states for the mechanism of hydrogen transfer to a ketone.

The currently accepted mechanism for the Noyori-type transfer hydrogenation catalyzed by Ru-, Rh- or Ir-complexes is the outer sphere concerted hydride transfer and relies on metal-ligand cooperation.[54,60] Both the metal and the ligand participate to the bond breaking and forming process and the transition state does not involve direct coordination of the substrate to the metal. Ligands possessing an acidic group, namely primary or secondary amines upon complexation with the Lewis acidic metal, facilitate the hydride delivery to the carbonyl by forming an NH···O=C hydrogen bond in the transition state.

The full catalytic cycle is depicted in Scheme 12 for the highly effective [Ru(*p*-cymene)(*R*,*R*-TsDPEN)Cl] complex.[43,55,60] The true catalytic species is the 16e$^-$ Ru complex **B** formed

from the catalyst precursor **A** by elimination of HCl in the presence of a base. Deprotonation of the hydrogen donor leads to the 18e$^-$ Ru-hydride complex **C**. The hydride and the axial NH proton are transferred simultaneously from the 18e$^-$ Ru complex to the substrate via a six-membered ring transition state, to re-form the 16e$^-$ complex **B**.

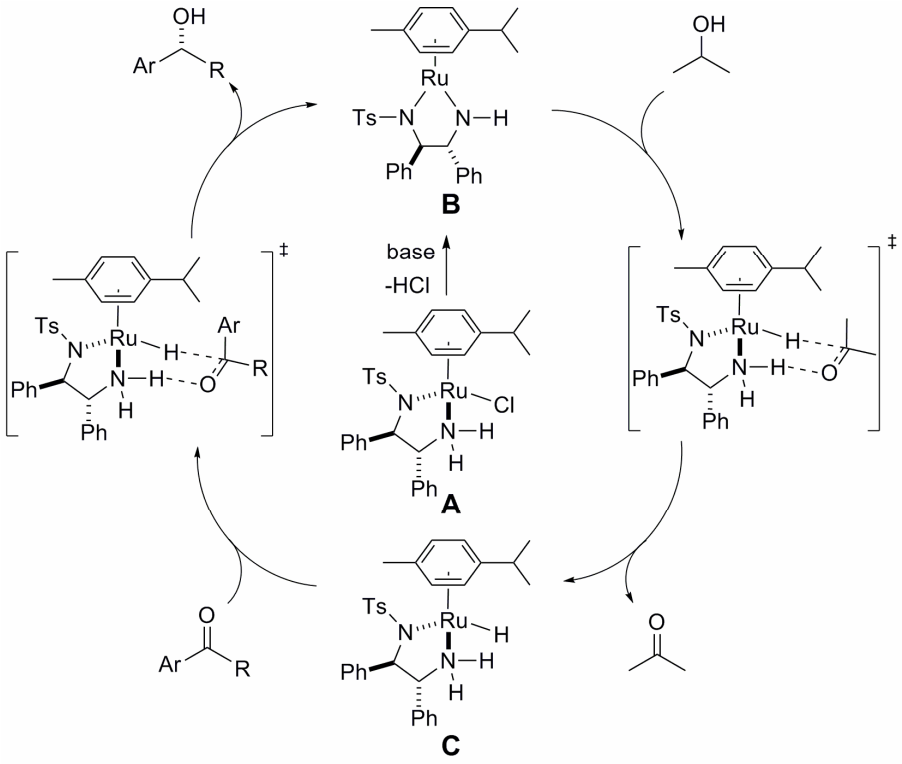

Scheme 12. Catalytic cycle for the transfer hydrogenation of an aromatic ketone using the [Ru(*p*-cymene)(*R,R*-TsDPEN)Cl] complex and *i*-PrOH as hydrogen donor.

Origin of enantioselection. The enantioselectivity of the reaction illustrated in Scheme 12 is a consequence of a judicious combination of steric and electronic factors.[60] The formation of the hydride complex from the planar 16e$^-$ species is sterically controlled by the enantiopure ligand to give one major diastereomer that is chiral at the Ru centre.[55] The conformation of the five-membered chelate ring containing the Ru atom is also defined by the ligand, with the bulky groups (phenyl groups in the case of TsDPEN) occupying equatorial positions.[55] The discrimination between the two prochiral faces of the ketone is a consequence of the interaction between the η^6-arene ligand at Ru and the aryl group of the ketone.[62] Computational investigations showed that the $C_{aromatic}H$-π attraction ($C(sp^3)H$-π attraction in the case of the η^n-C_nR_n ligands, $R \neq H$) at this level contributes to the stabilization of the more spatially congested transition state and thus is the major factor influencing the

enantioselectivity (Scheme 13).[60] Therefore, the outcome of the reaction can be modulated by carefully choosing the arene substituents. Polyalkylated capping arenes with increased π-donation power have a greater contribution to the $C_{aromatic}H$-π attraction and thus generally provide higher ee's than their unsubstituted counterparts.[45]

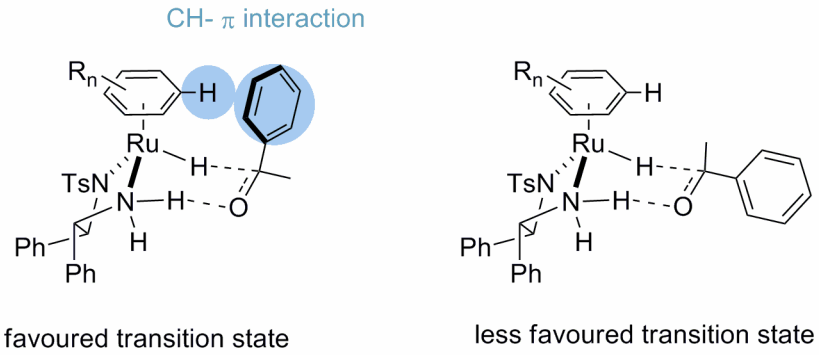

Scheme 13. Structures of the two possible transition states for the transfer hydrogenation of acetophenone. The chirality of (*R*,*R*)-TsDPEN determines the (*S*)-configuration at the Ru centre. The $C_{aromatic}H$-π interaction between the η^6-arene ligand and the aryl substituent of the ketone leads to a more stable transition state.

Water compatible systems. In the context of increasing concern about implementing environmentally benign processes, aqueous-phase transfer hydrogenation reactions have been developed recently.[47] Even though water-soluble ligands, bearing polar solubilizing groups like sulfonic acids, have been synthesised and successfully used in aqueous-phase hydrogen transfer reactions,[63] recent results show that the non-modified water-insoluble ligands are more active and more enantioselective.[47] In order to overcome substrate and catalyst solubility problems, surfactants can be added to the reaction mixture but, in most cases, ketone insolubility does not affect the reaction rate.[47] The reduction rates are considerably faster using HCOONa than the HCOOH / Et_3N azeotrope or *i*-PrOH.[64] Studies by the groups of Ogo and Xiao have shown that both the reaction rate and the enantioselectivity of aqueous transfer hydrogenation reactions critically depend on the pH.[65,66] The presence of two catalytic cycles has been suggested, each one favoured at a given pH.[66]

Asymmetric transfer hydrogenation of non-aromatic ketones. Phenyl alkyl ketones are the substrates of choice for the catalytic hydrogen transfer with d^6 piano-stool metal complexes and their reduction proceeds with good to excellent enantioselectivities.[43] In contrast, dialkyl ketones are challenging, as the postulated critical enantiodiscriminating $C_{aromatic}H$-π interaction between the η^6-arene ligand and the substrate's aryl group is absent for these substrates.[60,62] To circumvent this limitation, Woggon et al. tethered a ruthenium piano-stool

complex to a β-cyclodextrin, thus providing a pre-organized hydrophobic cavity for enantioselective reduction of purely aliphatic substrates (ee 42-95%).[67] Tethered ruthenium catalysts, in which the η^6-arene ring and the diamine ligand are connected, have also been used with some success (69% ee in the reduction of cyclohexyl methyl ketone).[68] Some alternative systems based on Ru-phosphino-oxazoline catalysts have been developed for the asymmetric transfer hydrogenation of selected dialkyl ketones.[52,69,70] Finally, Reetz et al. designed a general system for the reduction of aliphatic ketones, using Ru-diphosphonite ligands such as **8** (see Scheme 9).[53] However, the reduction of these substrates under transfer hydrogenation conditions remains a challenge for homogeneous catalysis.

Applications. Although transfer hydrogenation reactions occur with very high enantioselectivities, they cannot compete with the hydrogenation systems in terms of substrate scope and catalytic activity.[39] The reported TONs and TOFs for the piano-stool catalysts are moderate and limit their industrial application.[39] At the laboratory scale, this method is interesting as it avoids the use of gas and pressure equipment and it provides mild conditions for the reduction of ketones bearing sensitive functionalities. For example, the transfer hydrogenation of the multifunctionalized ketone **9** catalyzed by [Ru(mesitylene)(*R*,*R*-TsDPEN)Cl] gives the corresponding (*R*)-alcohol in 92% ee, an intermediate for the synthesis of a leukotriene antagonist (Scheme 14).[43]

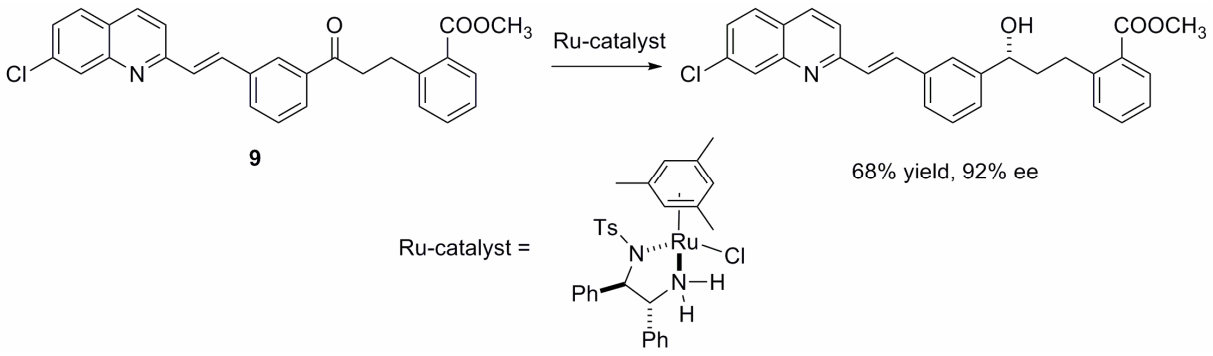

Scheme 14. Synthetic application of the Ru-catalyzed transfer hydrogenation reaction.

2.1.2 Biocatalytic Methods

The biocatalytic production of chiral alcohols can be performed following several synthetic pathways: oxidoreductases catalyze redox reactions (for example, the reduction of ketone bonds or oxidation of carbon-hydrogen bonds); hydrolases mediate the cleavage of carbon-oxygen single bonds in esters thus forming chiral alcohols through (dynamic) kinetic

resolution; and lyases catalyze the formation of carbon-carbon bonds (for example, by reacting two ketone substrates, hydroxy-ketones are available).[34]

The second coordination sphere of oxidoreductases such as alcohol dehydrogenases is exquisitely tailored to perform highly regio- and enantioselective transfer hydrogenations (Figure 3a).[71] In the context of asymmetric synthesis of optically active aliphatic alcohols, they represent some of the most versatile catalysts, thanks to optimization through directed evolution techniques.[72,73]

a) b)

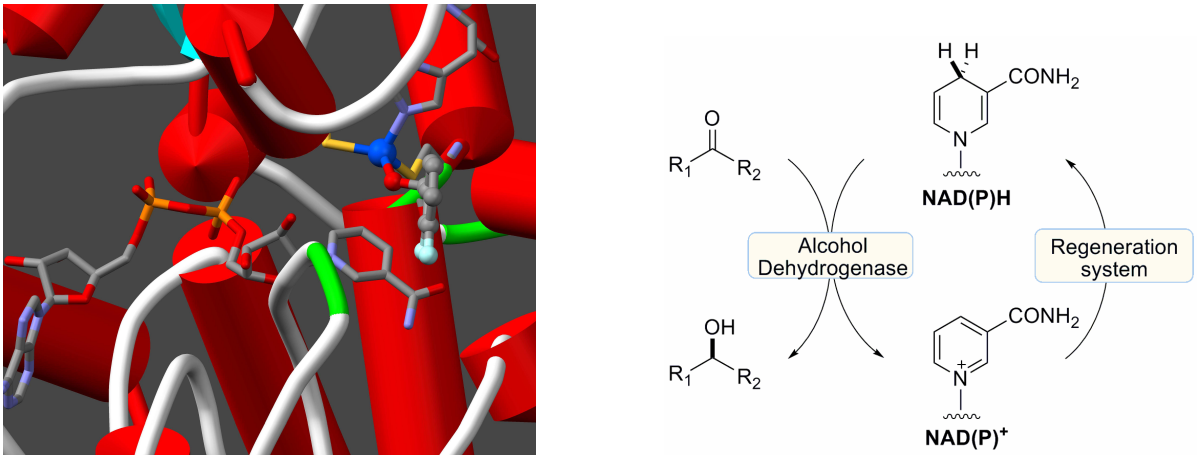

Figure 3. a) Structure of the active site of horse liver alcohol dehydrogenase complexed with NAD^+ and 2,3-difluorobenzylalcohol, PDB reference code 1MG0; the oxygen atom of the alcohol (red) is directly coordinated to the Zn^{2+} ion (blue), while the side chain interacts with the hydrophobic cavity of the protein; the amino acids directly coordinated to Zn are highlighted. b) General scheme for the asymmetric reduction of prochiral ketones using a NAD(P)H-dependent alcohol dehydrogenase and a co-factor regeneration system.

The majority of alcohol dehydrogenases are zinc metalloenzymes dependent on nicotinamide co-factors such as NADH or NADPH (Figure 3).[5] In horse liver dehydrogenase, for example, the Zn^{2+} ion is coordinated to three amino acid residues (C46, H67 and C174) and an additional water molecule. During catalysis, the relevant oxygen atom of the substrate displaces the latter, while its side chain binds in a hydrophobic pocket. The reduction occurs selectively via hydride ion transfer of one of the two diastereotopic hydrogen atoms in the 4-position of the nicotinamide ring to the substrate (Figure 3a).[5]

Given the high cost of nicotinamide co-factors, an important parameter of the reaction is their regeneration during catalysis (Figure 3b). Chemical, electrochemical, photochemical or enzymatic pathways have been reported.[34]

2.2 Sulfoxidation

2.2.1 Oxidation Systems Based on Transition Metals

2.2.1.1 Generalities

Oxidation reactions are powerful tools for the introduction or modification of functional groups and they offer an important methodology for the transformation of petroleum-based materials into higher oxidation state compounds. Their enormous potential in organic synthesis has lead to the extensive development of a variety of oxidative reactions. The difficulties associated with these methods include the high costs of the reagents, the formation of toxic waste, the highly reactive nature of many oxidants and, most importantly, the safety factor.[74] Thus, many efforts have been directed towards the creation of clean and safe oxidation procedures.[74-76]

Transition metal-catalyzed oxidation reactions can be achieved by applying a variety of oxidants and transition metals in combination with the appropriate ligands.[76] Depending on the oxidant – metal complex combination, different mechanistic pathways have been proposed, mostly relying either on metal-peroxo or on metal-oxo complexes (Scheme 15).[77] Early transition metal complexes in a high oxidation state, such as Ti(IV), V(V), Mo(VI) and W(VI), can facilitate the heterolysis of alkyl or hydrogen peroxides, by forming peroxo complexes. Oxidation reactions catalyzed by late (*e.g.* Ru, Os) or some first row transition metals (*e.g.* Fe, Mn, Cr) generally occur with the formation of high-valent metal-oxo or metal-dioxo species. Alkyl and hydrogen peroxides can also be applied as oxidants with Fe- or Mn-based systems, although catalyst inactivation can occur upon homolytic cleavage of the peroxide bond, leading to radical formation. This problem can be diminished in presence of an axial ligand, such as imidazole.

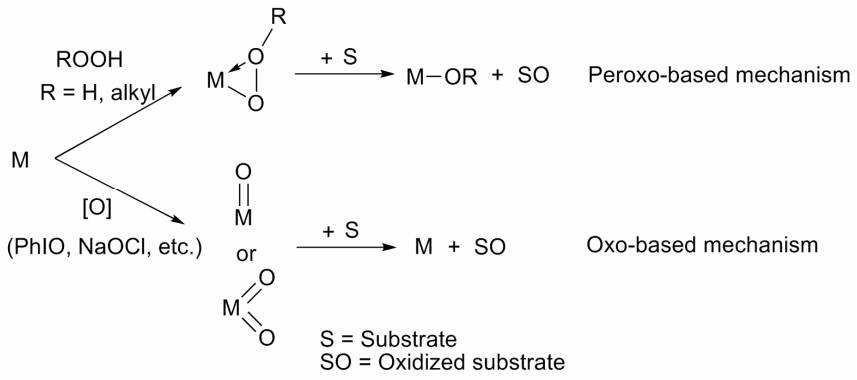

Scheme 15. Schematic representation of metal-oxo and metal-peroxo intermediates in oxidation reactions.

2.2.1.2 Manganese – Salen Complexes for Asymmetric Oxidation

Among the potential feedstocks for the chemical industry, alkanes are the most abundant and therefore the least expensive hydrocarbon resource. Unfortunately, very few selective methods are available for their functionalization.[78] In contrast, the selective oxidation of alkenes allows easy addition of heteroatoms and therefore is one of the most useful methods in organic synthesis.[79] Moreover, many simple alkenes are prochiral, thus providing an easy access route to the chiral world.

The first major breakthrough in asymmetric oxidation using synthetic catalysts was realized by Sharpless and Katsuki with the directed asymmetric epoxidation of allylic alcohols using titanium tartrate.[80] The substrate scope of asymmetric epoxidation was extended by Jacobsen and Katsuki using another catalytic system, based on metal-salen complexes and very effective for the epoxidation of conjugated alkenes (Scheme 16).[81-83] The advantage of these catalysts derives from the synthetic accessibility and versatility of the salen ligands.[84]

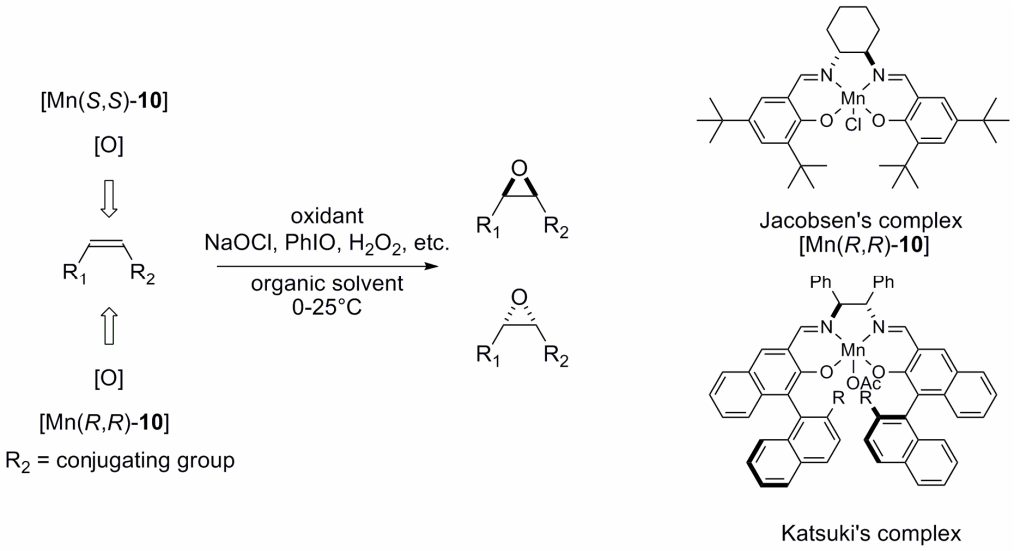

Scheme 16. Asymmetric epoxidation of alkene derivatives using chiral Mn-salen complexes introduced by Jacobsen and Katsuki.

Since their discovery, optically active metal-salen complexes bearing manganese,[83,85,86] chromium,[85] vanadium,[87] titanium,[88] ruthenium,[89] cobalt[90] and nickel[91] as metal centre have been successfully applied to asymmetric epoxidation,[83] sulfoxidation[87,92,93] or C-H oxidation reactions.[94-96] A variety of oxidants were succesfully employed, including alkyl hydroperoxides, peroxy acids, hypochlorite, iodosylbenzene, hydrogen peroxide, amine *N*-

oxides, periodate and oxone.[97] Among these systems, the manganese complexes for asymmetric alkene epoxidation using NaOCl or PhIO have been the most extensively studied.

The mechanism of the asymmetric epoxidation catalyzed by Mn-salen catalysts has generated much controversy over the years.[85] Mechanistic studies suggest that different oxygen-transfer species can be formed, depending on the oxidant used. With most oxidants, the Mn-oxo species (Mn^{V}=O) is believed to transfer oxygen to the substrate, via a concerted or a stepwise reaction pathway (Scheme 17a). Radicals and metallaoxetanes were proposed as intermediates for the stepwise mechanism. Nowadays, the scientific community seems to agree that the mechanism of this reaction can differ as a function of the oxidant or the substrate used.[85]

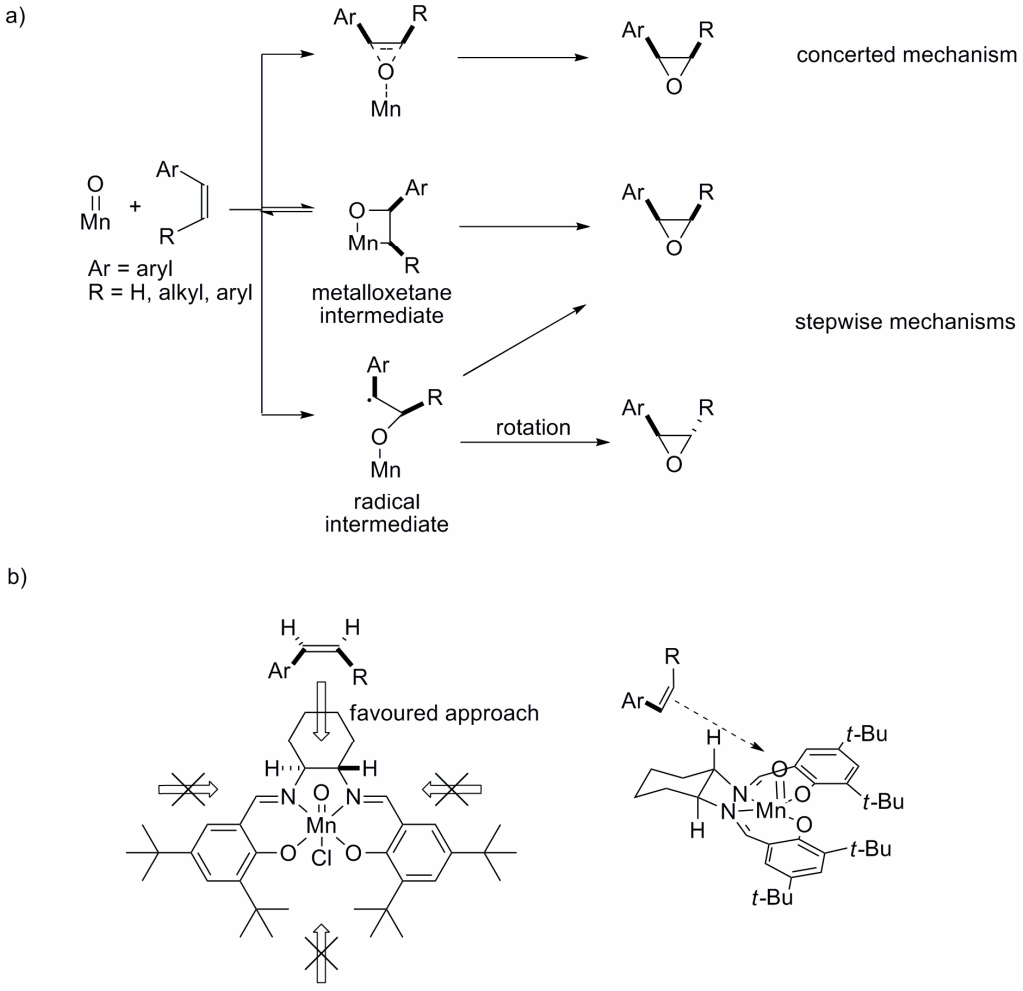

Scheme 17. a) Proposed concerted and stepwise mechanisms for the epoxidation of conjugated alkenes catalyzed by Mn-salen-oxo complexes; b) Enantioselection mechanism for alkene epoxidation using Jacobsen's catalyst.

In terms of enantioselection, the generally accepted oxo-transfer mechanism relies on a perpendicular ("side-on") approach of the substrate at the Mn-oxo species (the angle between the Mn-oxo bond and the new C-O bond is close to 90°). The bulky substituents on the salicylide moiety determine the trajectory of the approaching substrate from the side in which the stereochemical communication with the dissymmetric diimine bridge is maximized (Scheme 17b).[98,99]

2.2.2 Catalytic Sulfoxidation with Transition Metals

Oxidation of heteroatoms like nitrogen or sulfur is also of great importance in organic synthesis and several methods exist for such transformations.[100] As amines and sulfides are easily oxidized to form a number of different products, the development of chemoselective systems is highly desirable. This section will deal with the selective oxidation of sulfides to sulfoxides in an enantiospecific manner.

Upon oxidation by single oxygen transfer, sulfides are converted into sulfoxides. In the case of oxidation of unsymmetrical sulfides, the corresponding sulfoxides bear four different substituents at the sulfur atom: a lone electron pair, an oxygen atom and two different carbon ligands and are therefore chiral. Further oxidation can occur with formation of sulfone and thus an important aspect of organosulfur oxidation is to obtain high chemoselectivity for the formation of sulfoxide over sulfone (Equation 2). Although this characteristic depends on the oxidation system, the reactions generally proceed with good chemoselectivity, as the sulfide is more nucleophilic than the corresponding sulfoxide and hence reacts faster with the electrophilic reagent.[100]

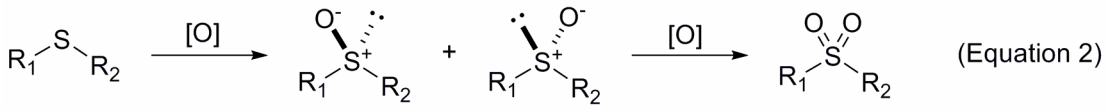

(Equation 2)

The importance of chiral sulfoxides as efficient chiral auxiliaries in asymmetric synthesis and their application in pharmaceutical research due to their biological activity are the reasons for increasing interest in the preparation of optically active sulfoxides over the past decades.[101-103] Among the biologically relevant sulfoxides, it is worth mentioning the gastric proton pump inhibitor omeprazole, an antiulcer agent, which was the world's highest selling drug in 1997. First commercialized in racemic form, it is now available as the enantiopure (*S*)-enantiomer esomeprazole, reported to have a superior activity (Scheme 18).[103]

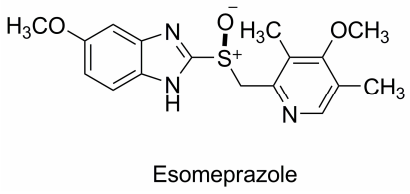

Esomeprazole

Scheme 18. Structure of esomeprazole, an antiulcer agent.

The methods to produce optically active sulfoxides are generally based on enantioselective oxidation of prochiral sulfides or on nucleophilic substitution on chiral sulfur derivatives.[102] Among these, the most efficient route to chiral sulfoxides is the asymmetric catalytic oxidation, using either enzymes or transition metal catalysts.[102-104] Although sulfide oxidation and alkene epoxidation are fundamentally different reaction classes, they can be effected with similar oxidation systems. As sulfides are very reactive substrates, a particular aspect to take into consideration is the uncatalyzed oxidation performed by powerful stoichiometric oxidants, which leads to racemic sulfoxides, thus lowering the overall ee.

An overview of the main homogeneous catalytic routes to the synthesis of optically active sulfoxides is presented in Scheme 19.

Systems based on titanium (Scheme 19a). The pioneering works of Kagan and Modena on enantioselective sulfoxidation were based on modifications of the Ti reagent introduced by Sharpless for the epoxidation of allylic alcohols.[105,106] Careful control of the amount of water in the system is necessary and is achieved by the addition of molecular sieves.[107] The asymmetric Ti-catalyzed sulfoxidation with organic hydroperoxides such as *tert*-butyl hydroperoxide (*t*-BuOOH) or cumyl hydroperoxide (cumylOOH) also works using chiral diols like BINOL (**12**).[108] Although good enantioselectivities can be obtained with the Ti-based systems, the yields of the corresponding sulfoxides are moderate and overoxidation to sulfone represents a non-negligible side-reaction. A highly enantioselective system based on dimeric Ti-salen complexes and hydrogen peroxide was reported by Katsuki et al.[88]

Systems based on manganese (Scheme 19b). The well established Mn-salen epoxidation catalysts are less effective for the homologous oxidation of aryl alkyl sulfides. In this case, NaOCl is too reactive for efficient enantiodifferentiation and moderate enantioselectivities are obtained using PhIO[92] or H_2O_2[93] as terminal oxidants. Among the rare efficient catalysts of this type is the Mn-salen **13**, bearing additional axial chirality, which is used in conjunction with PhIO to afford good enantioselectivities (up to 94% ee).[109] Although some chiral tetraphenyl porphyrin ligands showed good activities in catalytic sulfoxidations with PhIO, as

for Mn-porphyrin complexes the enantioselectivities obtained were only moderate (40-68% ee).[110]

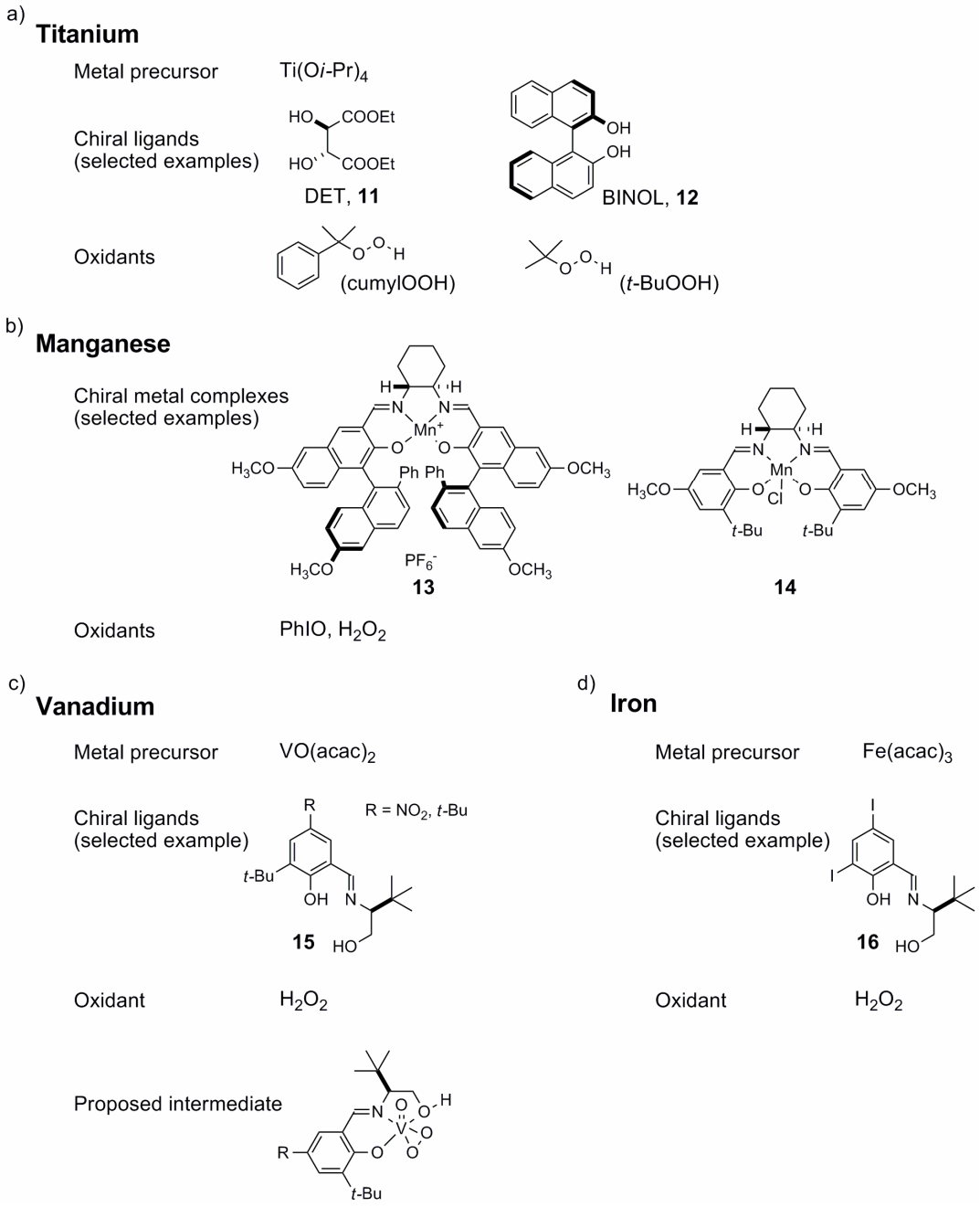

Scheme 19. Summary of the main transition metal-based asymmetric sulfoxidation systems.

Systems based on vanadium (Scheme 19c). The first asymmetric sulfoxidation with a vanadium catalyst was investigated by Fujita et al. using a chiral salen ligand and cumylOOH.[87] Later, remarkable activities and enantioselectivities were obtained by Bolm and Bienewald with V-oxo complexes formed *in situ* from $VO(acac)_2$ and tridentate O-N-O-type

Schiff bases such as **15** in the presence of aqueous H_2O_2.[111] The simple catalytic conditions that allow performing the reaction in the presence of air, at room temperature and using cheap H_2O_2 as oxidant have made this transformation particularly attractive, and since the initial discovery, several ligand modifications have been reported.[112] Although an unambiguous description of the reaction mechanism is still required, the reaction is believed to proceed through a V(V)-oxo-peroxo intermediate.[112]

Systems based on iron (Scheme 19d). While Fe-containing enzymatic systems have been extensively studied, asymmetric organometallic catalysts based on non-toxic and inexpensive Fe are relatively underrepresented in the field of enantioselective oxidations. Structurally complex porphyrin[113] and bipyridine[114] ligands have been reported, but they achieve only moderate ee's. In the spirit of the V-catalyzed sulfoxidation, Bolm et al. have developed a highly enantioselective system using a chiral Fe catalyst formed *in situ* from $Fe(acac)_3$ and O-N-O-type Schiff bases such as **16**. In the presence of a simple carboxylic acid and with H_2O_2 as terminal oxidant, the reaction proceeds with remarkable enantioselectivities (up to 96% ee) in moderate to good yields.[115,116] The use of a Fe-salan system with H_2O_2 (salan = fully reduced salen ligand) also gives good enantioselectivities with a wide range of substrates, including the challenging dialkyl sulfides.[117]

The structure of the substrate has a large influence on the outcome of these metal-catalyzed enantioselective sulfoxidations and the typical reactions have been usually optimized for model aryl methyl sulfides, bearing two substituents of very different size.[103] Except for the Ti-based methods, where the amount of water has to be carefully controlled, the presence of water is tolerated in the other systems, although the reactions are usually performed in organic solvent. A comparison between the main metal-catalyzed sulfoxidation reactions is presented in Table 1.[103]

Table 1. Comparison between the main homogeneous catalytic sulfoxidation systems.[a]

Entry	Catalyst	Oxidant	Solvent	Conditions
1	$Ti(O\textit{i}\text{-}Pr)_4$ / DET / H_2O	*t*-BuOOH or cumylOOH	CH_2Cl_2	-20°C
2	$Ti(O\textit{i}\text{-}Pr)_4$ / BINOL	*t*-BuOOH	CCl_4	0°C
3	Mn-salen	aqueous H_2O_2 or PhIO	MeCN	r.t.
4	$VO(acac)_2$ / **15**	aqueous H_2O_2	CH_2Cl_2	r.t.
5	$Fe(acac)_3$ / **16**	aqueous H_2O_2	CH_2Cl_2	r.t.

[a] r.t.= room temperature

2.2.3 Biocatalytic Sulfoxidation

Biocatalytic oxidations performed by redox enzymes (oxidoreductases) represent a cleaner alternative to the asymmetric oxidation with chiral chemical agents, as they make use of hydrogen peroxide or oxygen as stoichiometric oxidants. According to the oxidant they use and the reaction they catalyze, oxidoreductases are classified into four categories: dehydrogenases, oxidases, oxygenases (mono- or di-) and peroxidases.[118] Among these, various peroxidases and monooxygenases have been used as biocatalysts for sulfoxidation reactions.[100]

Unlike monooxygenases,[119] peroxidases do not require the use of expensive co-factors.[118] This class of enzymes catalyzes oxidative transformations using hydrogen- or alkyl peroxides. Based on the structure of their active site, they can be classified into: heme- (Fe-porphyrin complex), vanadium- or non-metal peroxidases. They have a variety of biological functions, from the synthesis of biomolecules to the detoxification of H_2O_2 and can accommodate a broad range of unnatural substrates in a diversity of reactions.[118]

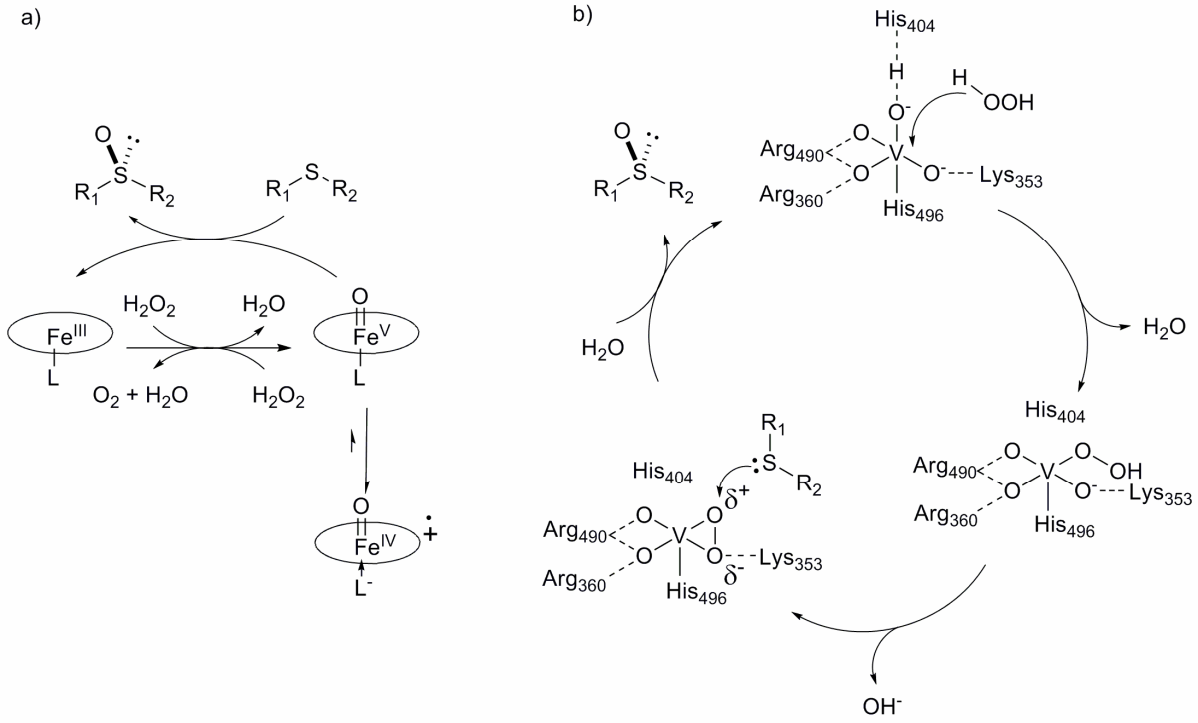

Scheme 20. Reaction scheme for sulfoxidations catalyzed by peroxidases: a) containing heme as prosthetic group; b) containing a vanadate ion in the active site.

One of the most versatile peroxidases is the heme-containing chloroperoxidase from *Caldariomyces fumago* (CPO), which has been shown to catalyze enantioselective sulfoxidation, epoxidation and C-H bond oxidation reactions.[118] However, a major limiting factor for the application of this heme-enzyme is its low stability under oxidizing conditions, due to oxidative destruction of the porphyrin ring.[120] Vanadium haloperoxidases are non-heme enzymes and thus are more stable, although their utility is limited due to a narrow substrate range.[120] Such V-containing enzymes have been explored as potential catalysts in the enantioselective oxidation of sulfides with up to 91% ee, but with moderate activities.[121] The two catalytic cycles for oxygen transfer catalyzed by heme- and V-containing peroxidases are depicted in Scheme 20.

3 Artificial Metalloenzymes for Enantioselective Transformations

3.1 Enzyme Engineering: Modification of Existing Enzymes

Natural evolution provided a large set of enzymes crucial for the survival and reproduction of organisms, not for applying in chemical processes. Although many complicated reactions can be efficiently performed by natural enzymes, their use is limited by a narrow range of applications in terms of enantiomer accessibility, substrate specificity, thermal stability and alternate activity.[28]

To address this issue, one strategy is to use enzymes from organisms living in extreme conditions (temperature, pressure, pH), adapt the formulation of the enzyme (by using surfactants or immobilization techniques) or change the reaction parameters.[30] For example, subtle modifications of the substrate and solvent engineering (pH control, use of ionic liquids) are simple methods to fine-tune the stereochemical outcome of an enantioselective enzymatic transformation.[122]

On the other hand, natural diversity cannot address all the desired reactions, and sometimes no natural enzymes with a desired activity or enantioselectivity are found. In this case, modifying existing biomolecules with similar activities or structures through enzyme engineering represents a viable alternative.

The remarkable evolutionary adaptability of enzymes has lead to the development of laboratory evolution methods as an attractive means for producing biocatalysts with the desired properties. There are two approaches for enzyme optimization: fine-tuning existing scaffolds by rational redesign[123] or creating random libraries of possible catalysts by

combinatorial methods[30,124,125] and then improving them by screening[30] or selection techniques (Scheme 21).[126] In the field of asymmetric catalysis, these techniques open new perspectives for the application of biocatalysis.

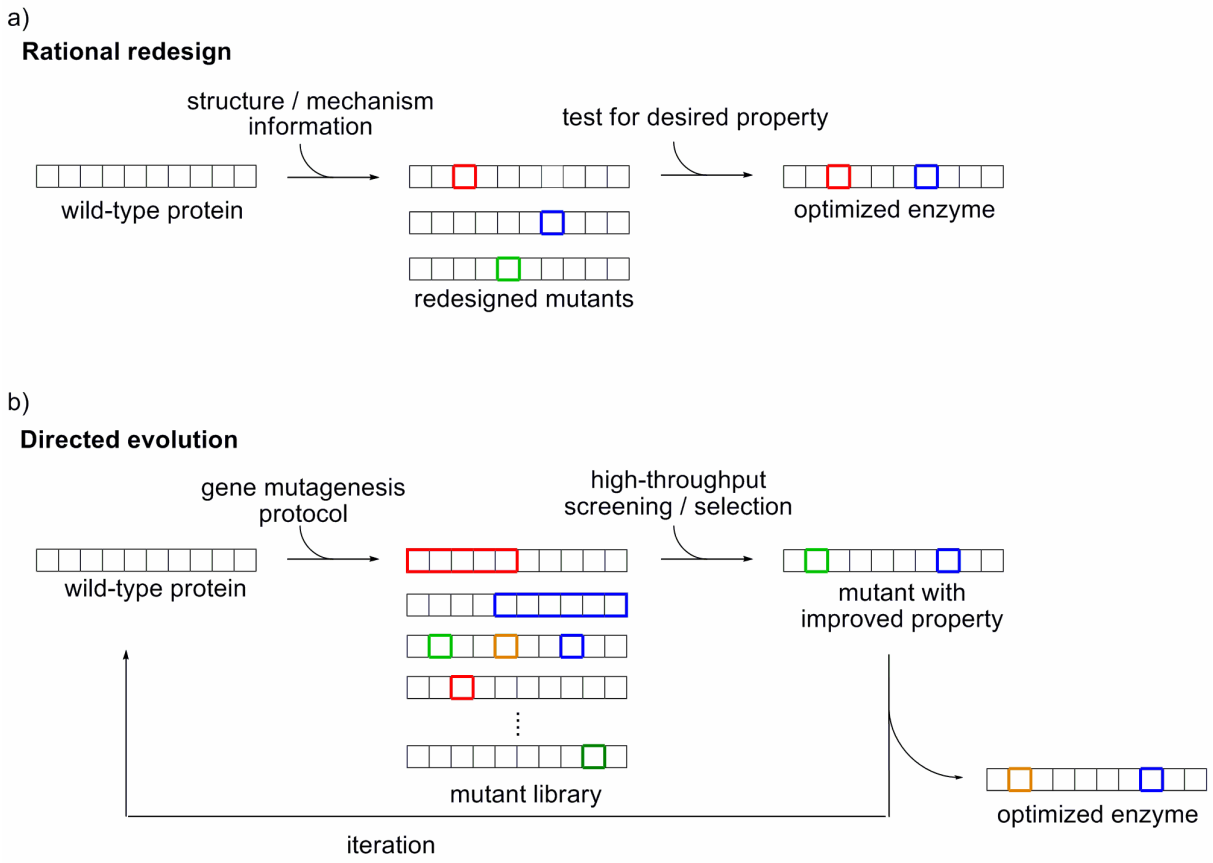

Scheme 21. Main techniques for the engineering of existing biocatalysts: a) rational redesign; b) directed evolution.

Choosing the best method for an enzyme engineering task depends on available structural and functional information, as well as on suitable selection techniques. A comparison between the two strategies is presented in Table 2.[29,127]

In terms of mutation target, rational methods focus on mutations close to the active site,[123] as their effect is easier to predict, while random mutagenesis can often find distant mutations with better activity and stability.[128] Considering enantioselectivity, a study of improved single mutants reveals that, even though distant mutations can have a beneficial effect, it is often more effective to focus on mutations near the catalytic site.[128]

Table 2. Comparison of rational redesign and directed evolution techniques.

	Rational redesign	Directed evolution
Protein structure	Required	Not required
Mechanism	Required	Not required
Gene mutagenesis protocol	Point mutations Saturation mutagenesis at pre-identified spots	Error-prone PCR Saturation mutagenesis Massive mutagenesis Gene shuffling Synthetic shuffling
Screening / selection techniques	Sensitive enzyme assay	High-throughput screening methods High-throughput selection methods

Reetz et al. were the first to demonstrate that directed evolution methods can be successfully applied to the creation of enantioselective enzymes, by evolving (*R*)- and (*S*)-selective lipases for hydrolytic kinetic resolution (Scheme 22).[129,130]

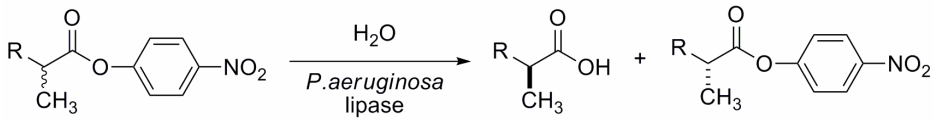

Scheme 22. Hydrolytic kinetic resolution using (*R*)- or (*S*)-selective lipases.

Genetic engineering offers the possibility of changing any position of the protein sequence to improve a specific property of an enzyme or even to create a completely new activity (catalytic promiscuity).[31,32] Still, the number of building blocks that can be genetically introduced into proteins remains limited. Although the 20 natural amino acids contain a variety of functional groups, proteins require a number of other chemical functionalities to carry out their functions. These are provided in nature through post-translational modifications or by the use of co-factors. In the hands of molecular biologists, this limitation can sometimes be overcome by the use of ingenious techniques for the incorporation of non-natural amino acids.[131] Yet, these techniques are mainly successful only for those building blocks that have a close structure to the natural ones.

Besides the genetic approach, chemical methods also represent a valuable tool for protein engineering.[132] Chemical modification of amino acid side chains allows incorporation of new functional groups into a biocatalyst, but such reactions are in general non-specific, thus

creating heterogeneous mixtures of proteins, with consequently varied, imprecise and uncontrolled properties.[5] However, some successful strategies have been developed, which exploit efficient and selective protein chemistry to alter natural catalytic activity or to introduce new enzymatic activity within a protein.[133]

3.2 Artificial Systems

The optimization of existing enzymatic systems is well-established and can cope with several problems associated with the application of biocatalysts in asymmetric synthesis. Nevertheless, there are still many problems for which natural systems cannot even offer a suitable starting point for evolution. Sometimes the existing enzymes are not necessarily appropriate for the desired transformation and other frameworks can be much better functional solutions. In this context, the creation of artificial enzymes represents another possible strategy to address uncommon chemical reactions using biomolecules.

3.2.1 Catalytic Antibodies

One of the first approaches to artificial systems was the creation of catalytic antibodies. An antibody is a large protein produced by the immune system against a foreign molecule (antigen). The affinity of an antibody for its antigen is in the range of 10^5 to 10^{12} M^{-1}. The ability of the immune system to produce receptors with such high affinity against any chemical ligand has been exploited to create a new class of catalytic proteins.

The method is based on Pauling's principle of enzymatic catalysis, which states that enzymes catalyze a chemical reaction by stabilizing its transition state better than the substrate.[134] Thus, the complementarity between the active site and the transition state should cause an acceleration of the reaction by forcing the substrates to resemble the transition state. The first catalytic antibodies were described independently by Lerner and Schultz.[135,136] The antigens they used, phosphonic esters, are known inhibitors of hydrolases and mimics for the transition state of hydrolytic reactions. Theoretically, if the antigen is carefully designed, one can perform any catalytic reaction using this method. In practice, the construction of stable transition state analogues is a difficult task. Efforts have been made in this field to apply catalytic antibodies to a larger range of chemical transformations: cationic cyclizations, Diels-Alder reactions or pro-drug activation *in vivo*.[137,138]

3.2.2 Artificial Metalloenzymes

Approximately half of all proteins contain a metal atom, either as an isolated ion or coordinated to an organic component.[139] The redox properties and high catalytic activities of the transition metals enable them to carry out even the most difficult transformations. The complex structures and functions of metalloenzymes have inspired chemists and biochemists in designing highly efficient and selective catalytic systems. Several types of interactions govern the reactions of a metal centre: the electronic properties of the metal itself, the first coordination sphere (*e.g.* coordination number and geometry, type of ligand), the secondary coordination sphere (*e.g.* hydrogen bonding interactions of the first coordination sphere with the close environment) and the long-range interactions (usually electrostatic in nature).[140]

Traditional homogeneous catalysis is based on the use of relatively small organic ligands surrounded by a uniform environment (solvent molecules) and thus is characterized mainly by the first two types of interaction. In contrast, in metalloenzymes, the metal atom is embedded in a highly organized protein framework, which provides exceptional control through second coordination sphere and long-range contacts. The creation of artificial metalloenzymes aims at combining the features of both homogeneous and enzymatic catalysis and represents a rather new approach in the field of asymmetric transformations. Their design is based on exploiting second coordination sphere interactions for tailoring the enantioselectivity of the reaction.

Three main approaches can be identified to date for the creation of enantioselective artificial metalloenzymes, based on the manner of incorporation of the metal fragment: the dative, the covalent, and the supramolecular anchoring strategy. The metal fragment can be either a small metal ion or a metal-containing native or non-native prosthetic group. Since several reviews summarizing the latest advances in the field of artificial metalloenzymes for enantioselective catalysis have been recently published,[141,142] only a brief description of these hybrid catalysts will be presented here.

Dative anchoring. Several natural metalloenzymes contain a metal ion directly bound to the protein, without the intermediate of an organic compound. Substitution of these metal ions with others having different properties and activities affords artificial metalloenzymes.[143-145] Metal ions can also be accommodated in specific binding sites of certain non-metal-containing proteins.[146,147] For example, Sheldon et al. exploited the structural similarity of the active sites of vanadium-dependent haloperoxidases and acid phosphatases to design a

semisynthetic peroxidase for enantioselective sulfoxidation (up to 66% ee was obtained upon sufoxidation of thioanisole using H_2O_2 as stoichiometric oxidant).[147]

Covalent anchoring. Covalent linkage is based on chemical modification of an amino acid residue and allows site-specific incorporation of a metal complex that does not display high affinity for the protein. This strategy involves specific modification of an accessible amino acid and has been successfully applied to native proteins or mutants containing one or two free cysteine residues.[148-150] Dual covalent anchoring of a Mn-salen complex into the heme-binding site of apo-myoglobin, combined with specific orientation of the metal-complex by a dative bond with a histidine residue proved to be a successful strategy for the design of artificial metalloenzymes for the sulfoxidation of thioanisole (up to 51% ee).[150]

Supramolecular anchoring. This non-covalent approach exploits the high affinity of a given protein (host) for a small organic molecule (guest). Chemical modification of the guest is necessary in order to attach the organometallic moiety and it shouldn't drastically affect the host-guest binding affinity. Ideally, the binding pocket of the protein should be deep enough to accommodate the derivatised prosthetic group (Scheme 23).

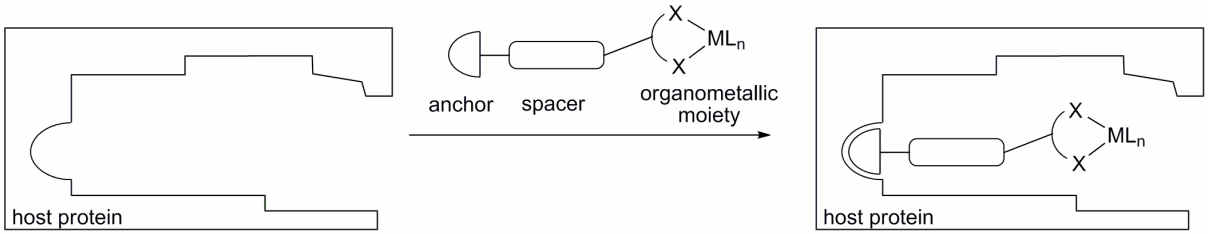

Scheme 23. Schematic representation of artificial metalloenzymes based on supramolecular anchoring of an active catalyst within a host protein.

One class of proteins that display high affinity towards a variety of hydrophobic guests are the serum albumins, which function as transport proteins in plasma. Their hydrophobicity has been utilised for the non-covalent incorporation of metal-containing co-factors that catalyze enantioselective reactions.[151,152] It is worthy of note that the hydrophobic pockets of bovine serum albumin (BSA) also constitute possible binding sites for hydrophobic substrates and therefore can provide asymmetric environments for the transition state.[153] In this context, Klibanov proposed the use of a hydrolytic enzyme with a single well-defined hydrophobic pocket (α-chymotrypsin) instead of BSA, as chiral mediator in enantioselective sulfoxidations.[154]

Heme-containing proteins are another class of proteins that possess a hydrophobic cavity capable of non-covalent interactions with metal-complexes. Supramolecular incorporation of metal-salen complexes into the active site of apo-myoglobin affords semisynthetic metalloenzymes that catalyze enantioselective sulfoxidations.[155,156]

Since the supramolecular approach is based on high affinity between the protein and the co-factor bearing the metal fragment, the choice of the guest-host couple is very important for its success. When it comes to high association constants, the system that naturally comes to mind is biotin-avidin, which has one of the highest non-covalent interactions known in nature (K_a ~10^{15} M^{-1}).[157] As early as 1978, Whitesides and Wilson converted avidin into an enantioselective homogeneous catalyst by incorporating a biotinylated achiral rhodium-diphosphine complex into the biotin-binding pocket.[158] This was the first example of an artificial metalloenzyme. Later, Chan et al. extended the concept to the use of chiral ligands.[159] Since 2003, Thomas Ward's group in Neuchâtel has focused on the development of artificial metalloenzymes based on the biotin-(strept)avidin technology (hereafter, (strept)avidin refers either to avidin or to streptavidin). A detailed description of the system is presented in the next section.

At the interface between organometallic catalysis and enzyme chemistry, the hybrid catalysts represent a complementary approach to asymmetric transformations and may allow quick development of a broad reaction range in environmentally benign media. In terms of activity, reaction and substrate range, and operating conditions, they take advantage of the performance of the organometallic component. In contrast, the enantioselection path is determined by the biomolecular scaffold, which controls second coordination sphere interactions. The attractive feature of such systems is their optimization potential, which combines chemical and genetic methods to screen diversity space.

4 Biotin-Streptavidin System

The choice of an appropriate guest-host couple is a crucial step when designing a new hybrid catalytic system. Supramolecular anchoring appears more interesting than covalent or dative strategies, since it allows separate variation, followed by straightforward combination of the chemical and the genetic counterparts. Moreover, no chemical modification step is required after the incorporation of the catalyst precursor, thus ensuring the integrity of the organometallic species.[160]

A robust protein scaffold and a very strong affinity between the protein and the organometallic host are essential. In this context, the use of the biotin-(strept)avidin system presents the following advantages:[161]

Guest ⊂ host binding. The affinity constant of either avidin or streptavidin for biotin is one of the highest known in nature ($K_a = 1.7 \cdot 10^{15}$ M^{-1} for avidin and $K_a = 2.5 \cdot 10^{13}$ M^{-1} for streptavidin).[157] This strong binding ensures the immediate and complete formation of the protein – metal complex hybrid catalyst. Furthermore, derivatization of the biotin side chain to introduce the catalytic functionalities does not cause dramatic change in the affinity constant.[162]

Stability. Streptavidin has an exceptional stability towards heat (the biotin-containing tetramer is stable at 110 °C for several minutes)[163], extreme pH conditions (denaturation requires 6 M guanidinium chloride at pH 1.5),[164] high concentrations of organic solvent (50% ethanol) and the presence of surfactants (such as sodium dodecyl sulphate, SDS).[165] Therefore, the use of a large panel of reaction conditions can be envisaged.

Protein expression. Both avidin, naturally available from egg white[164] and streptavidin, secreted by *Streptomyces* bacteria,[157] are available as recombinant proteins. Avidin has proven difficult to produce in bacteria, but reasonable yields can be obtained in eukaryotic production systems like *Pichia pastoris*.[166] In contrast, streptavidin can be expressed from *E. coli* culture at relatively high yields (in our lab the production yields reach typically 200 $mg \cdot L^{-1}$).[167] Both proteins are easily purified by affinity chromatography using immobilized 2-iminobiotin.

Structural and functional information. The exceptional affinity and stability properties described above are the reasons for the particular attention that avidin and streptavidin have received from the scientific community. The biotin-(strept)avidin system is the basis for a great number of practical applications and is an interesting model system to study the affinity between a macromolecule and a small ligand.[168,169] Therefore, it is not surprising that the structural and functional characteristics of these two proteins have been extensively studied.[170] The crystal structures of a number of (strept)avidin variants have been determined and biotin binding is well defined, thus allowing rational tailoring of the artificial metalloenzymes.

Despite an amino acid similarity of only 41% (amino acid identity 30%),[171] the secondary, tertiary, and quaternary structures of avidin and streptavidin are almost identical to each other.[172,173] They fold in an eight-stranded antiparallel β-barrel and their quaternary structure

is composed of four identical barrels. Each subunit has a single biotin-binding site placed near one end of the barrel and containing two main motifs: the hydrophilic contact residues that form hydrogen bonds with biotin (Figure 4a) and the hydrophobic pocket created by several aromatic residues (Figure 4b). The binding site residues provide a precise fit to biotin, so that in the unoccupied binding site, the position of the solvent molecules is similar to the shape of the biotin molecule. After biotin-binding, the flexible loop between the strands β3 and β4 (loop L3,4) becomes ordered, locking the biotin in the binding site (Figure 4a). A critical hydrophobic interaction is provided by a tryptophan residue supplied by a neighbouring subunit (Figure 4b) and therefore the two proteins are considered as a dimer of functional dimers.

It is worthy noting that the deep hydrophobic cavity of (strept)avidin can also bind, albeit with significantly reduced affinity, a variety of ligands, including HABA, ANS and different oligopeptides,[164,168,169,174] suggesting the possibility of second coordination sphere interactions with a wide range of functionalities attached to the biotinylated moiety.

a) b)

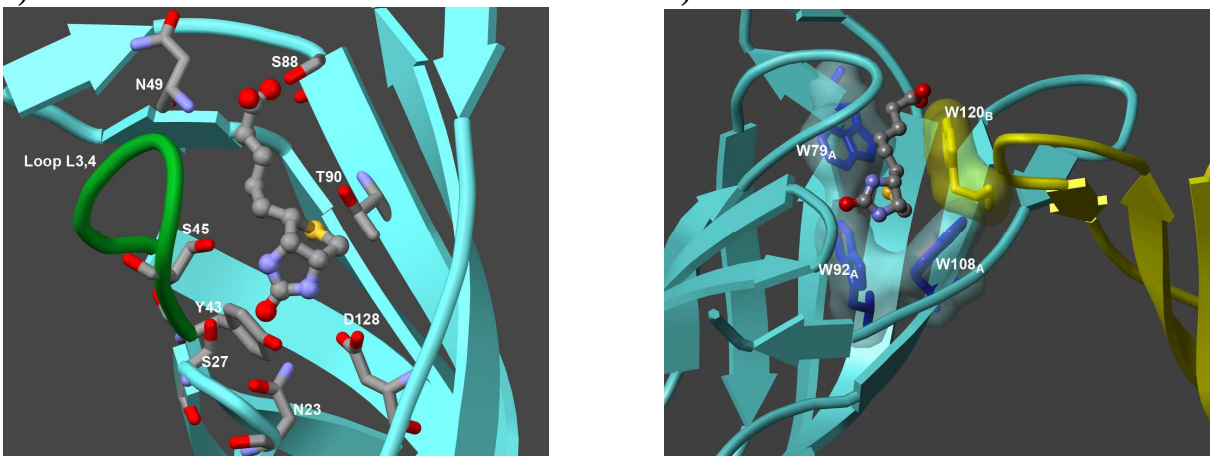

Figure 4. Biotin binding pocket of streptavidin (PDB reference code 1STP).[172] a) Hydrogen bonding net stabilizing the urea moiety (N23, S27, Y43, S45, D128), the sulfur atom (T90) and the carboxylic acid of the valeric side chain (N49 and S88) of biotin; the L3,4 loop (residues 45-52) is highlighted in green; b) Hydrophobic interactions with tryptophane residues: W79, W92 and W108 from monomer A (blue) and W120 from the adjacent monomer B (yellow).

Considering the above features, the biotin-(strept)avidin couple appears as an ideal starting point for the development of hybrid catalysts. Three decades after Whitesides' work, the great potential of chemogenetic optimization made possible the development of very selective catalytic systems. This approach, implemented thus far in our laboratory for hydrogenation

reactions, is based on generating chemical and genetic libraries to explore diversity space.[175] A chemogenetic optimization procedure[133] implemented for the hydrogenation of α-acetamidoacrylic and α-acetamidocinnamic acids using streptavidin in conjunction with biotinylated rhodium diphosphine complexes allowed rapid generation of (*R*)- and (*S*)-selective as well as substrate specific metalloenzymes (up to 96% ee (*R*)).[175,176] Higher activities and selectivities are obtained when streptavidin is used instead of avidin.

Chemical optimization of the system can be achieved by modifying the localization of the catalytic moiety inside the protein upon introduction of a spacer between the biotin anchor and the diphosphine ligand. The nature of the biotinylated ligand determines the general activity and selectivity trends. The critical second coordination sphere interactions determine the selective coordination of the prochiral face to the catalytic moiety, as well as substrate differentiation, and can be fine-tuned by introducing point mutations in the host protein. The general principle is summarized in Scheme 24.[175,177]

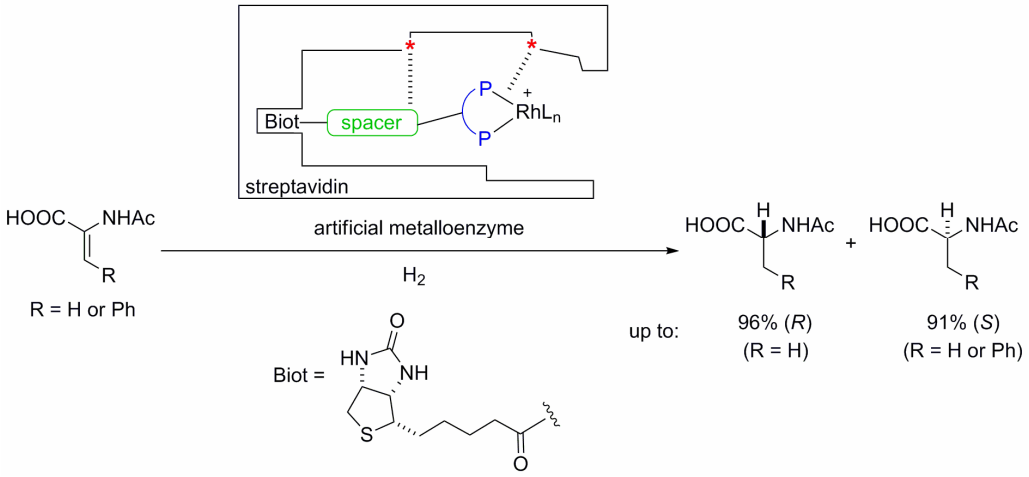

Scheme 24. Artificial metalloenzymes based on the biotin-streptavidin system for enantioselective hydrogenation reactions. Introduction of a spacer (green) and variation of the diphosphine ligand (blue) allow chemical optimization; introduction of point mutations (red) leads to genetic optimization of the host protein.

In contrast to the rational design used by the Ward group, another approach to generate selective artificial metalloenzymes for hydrogenation reactions has been implemented by the group of Manfred Reetz, who first proposed the application of directed evolution methods to hybrid catalysts based on biotin-streptavidin.[178] Due to problems associated with the protein expression system and the air sensitivity of the metal complexes, screening the artificial enzymes has proven more difficult than screening classical enzymatic systems.[124] However,

Reetz et al. demonstrated the possibility of breeding a better catalyst over several evolutionary cycles.

The creation of such artificial metalloenzymes opens new horizons in the field of enzyme application. The real challenge is to generate novel activities that are impossible to obtain using classical enzymatic systems. Encouraged by the results on hydrogenation reaction, the research in Thomas Ward's group has focused on more difficult reactions, including transfer hydrogenation of ketone derivatives,[179-181] oxidation of secondary alcohols[182] and, more recently, allylic alkylation.[183]

5 Scope of this Thesis

As described above, the artificial metalloenzymes based on the biotin-streptavidin technology offer new perspectives for protein engineering by combining chemical and genetic modifications to create new activities and to fine-tune the selectivity. The objective of this thesis is the development of efficient hybrid catalysts for challenging reduction and oxidation reactions. Hence, the work is divided into two distinct parts, dealing with two different reactions: the transfer hydrogenation of carbonyl compounds and sulfoxidation.

The first part relies on the discovery of a selective artificial transfer hydrogenase based on biotin-streptavidin during a previous PhD project in Thomas Ward's laboratory (PhD thesis of Dr. Christophe Letondor).[179] The goal of the following studies is the implementation of a robust protocol for the chemogenetic optimization of such enzymes and a closer investigation of the catalytic system. Furthermore, we aim to exploit the influence of the second coordination sphere to create artificial keto-reductases for the reduction of difficult substrates, such as dialkyl ketones.

Creating artificial metalloenzymes for oxidation reactions represents the second challenge of this thesis. From a panel of possible enantioselective oxidations, we selected the sulfoxidation reaction as a starting point. Our initial studies focus on the implementation of a sulfoxidation system that is compatible with the presence of water and protein. Further research is centered on the incorporation of a catalytically active metal ion (vanadyl) into the binding pocket of streptavidin. In this way, streptavidin can be transformed into a metalloenzyme without the use of the biotin co-factor.

Chapter 2 Results and Discussion

1 Transfer Hydrogenation of Carbonyl Compounds

The starting point of this work is constituted by previous studies conducted in our laboratories by Dr. Christophe Letondor.[184] His efforts allowed the identification of active and selective artificial metalloenzymes for the transfer hydrogenation of acetophenone derivatives based on the biotin-streptavidin technology. Moreover, they suggested that both chemical and genetic methodologies can be implemented for the optimization of the system. For a better comprehension of the following results, a short description of the catalytic system discovered by Dr. Letondor will be presented in Section 1.1.[179] The results presented in Section 1.2 were obtained in collaboration with Dr. Letondor and therefore have already been largely discussed elsewhere.[180,184] Only a brief account of the outcome of this first optimization protocol will be provided.

1.1 The Catalytic System

The Noyori-type asymmetric transfer hydrogenation of ketones was chosen as a model reaction, considering the nature of the critical non-covalent interactions within the transition state (see Chapter 1, Section 2.1.1). In this context, it was reasoned that the second coordination sphere contacts between the host protein and the substrate may lead to good selectivities. Most importantly, recent examples in the field of chemo-enzymatic catalysis demonstrated the compatibility between d^6 piano-stool metal complexes and enzymatic systems at elevated temperatures, thus suggesting that biotinylated piano-stool complexes may perform their task in the presence of streptavidin acting as a host protein.[8]

Derivatisation of an achiral aminosulfonamide ligand with a biotin anchor, followed by complex formation with ruthenium afforded the stable and water compatible catalyst precursors [η^6-(arene)Ru(**Biot-*q*-L**)Cl], which were combined with wild-type streptavidin (abbreviated hereafter WT Sav) to afford artificial metalloenzymes for transfer hydrogenation reactions ([η^6-(arene)Ru(**Biot-*q*-L**)Cl] $\subset$ WT Sav; arene = *p*-cymene, benzene; *q* = *ortho*-, *meta*- or *para*-position for the biotin anchor, Scheme 1a). Studies of the hydrogen source, pH and buffer system, temperature, reaction time and organic co-solvent revealed the best conditions for the reduction of the model substrate acetophenone **1** (Scheme 1b and Table 1, entry 1). Acetophenone derivatives **2** and **3** afforded even higher conversions and selectivities (Table 1, entries 2-3). In the absence of Sav, these complexes catalyzed the aqueous transfer hydrogenation of acetophenone to yield racemic 1-phenylethanol in quantitative yield.

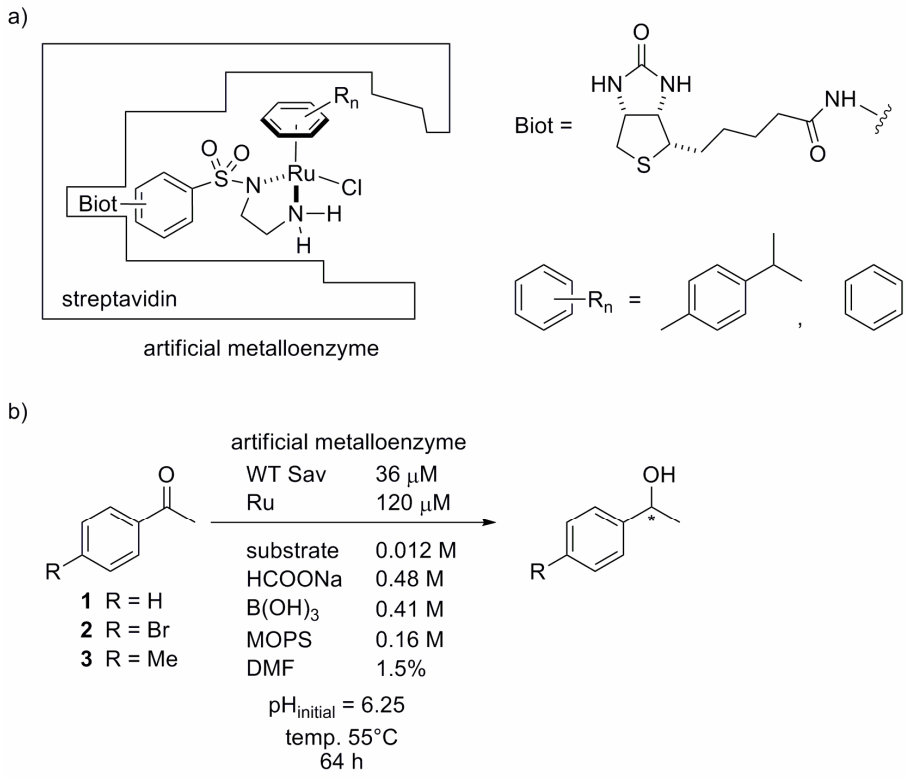

Scheme 1. a) Schematic representation of artificial metalloenzymes based on biotin-streptavidin for transfer hydrogenation reactions ([η^6-(arene)Ru(**Biot-*q*-L**)Cl] ⊂ WT Sav, arene = *p*-cymene or benzene, *q* = *ortho*-, *meta*- or *para*-); b) Reaction conditions for the enantioselective reduction of acetophenone derivatives.

Table 1. Best results obtained after the optimization of the reaction conditions for the transfer hydrogenation of acetophenone derivatives with [η^6-(arene)Ru(**Biot-*p*-L**)Cl] ⊂ Sav.

Entry	η^6-(arene)	Protein	Substrate	Conv. (%)	ee (%)
1	*p*-cymene	WT Sav	**1**	82	68 (*R*)
2	*p*-cymene	WT Sav	**2**	93	87 (*R*)
3	*p*-cymene	WT Sav	**3**	86	91 (*R*)
4	benzene	WT Sav	**1**	54	48 (*S*)
5	*p*-cymene	P64G Sav	**1**	90	85 (*R*)
6	*p*-cymene	P64G Sav	**3**	92	94 (*R*)
7	*p*-cymene	S112G Sav	**1**	90	28 (*R*)

The nature of the capping arene was found to play a crucial role in determining both the activity and the selectivity of [η^6-(arene)Ru(**Biot-*p*-L**)Cl] ⊂ WT Sav. Most unexpectedly, substitution of the η^6-(*p*-cymene)- by an η^6-(benzene)-cap produced the opposite enantiomer of 1-phenylethanol, under otherwise identical reaction conditions (Table 1, entries 1 and 4).

60

This initial finding suggested an important interaction between the protein and the ruthenium complex.

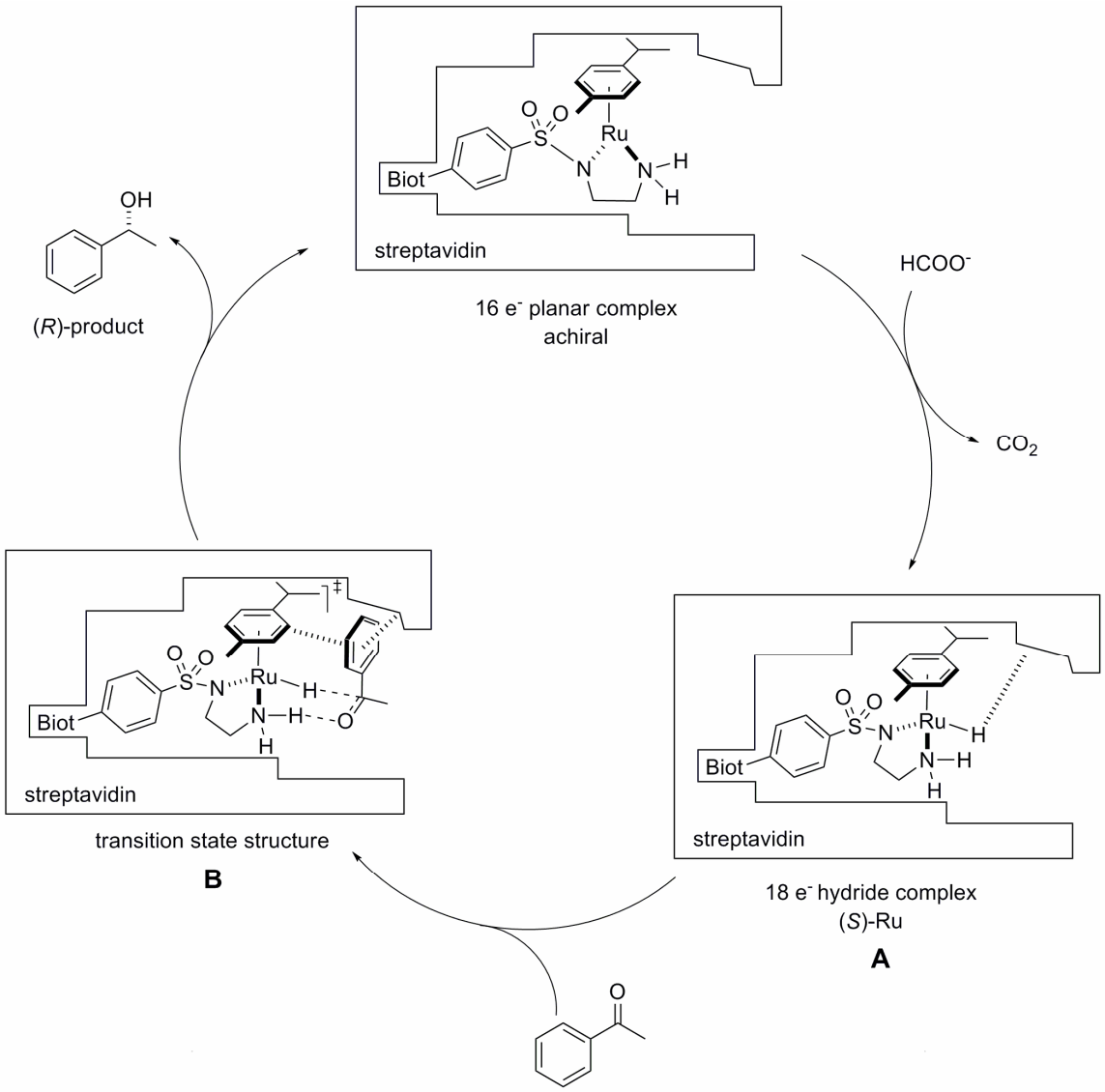

Scheme 2. Suggested weak contacts critical for the observed enantioselectivity in the reduction of acetophenone catalyzed by [η^6-(*p*-cymene)Ru(**Biot-*p*-L**)H] ⊂ WT Sav. The absolute configuration at Ru may be determined by second coordination sphere contacts between the biotinylated catalyst and streptavidin (**A**); the preferential delivery of one prochiral face of the substrate may be biased by second coordination sphere interactions between the substrate and streptavidin (**B**).

To rationalize this observation, two complementary enantioselection mechanisms can be envisaged. First, the absolute configuration at Ru in the hydride piano-stool complex may be controlled by second coordination sphere interactions with Sav. This differs from classical Noyori-type catalysts where the Ru-configuration is determined by the chirality of the

chelating ligand scaffold.[55] Second, additional contacts between the substrate and the protein may compete (matched or mismatched) with interactions between the substrate and the η^6-capping arene to favour the approach of one prochiral face of the substrate. These two possible enantiodiscriminating events are outlined in Scheme 2 for the (*R*)-selective [η^6-(*p*-cymene)Ru(**Biot-*p*-L**)Cl] ⊂ WT Sav combination.

Introduction of point mutations within the host protein showed that the protein with the most remote site of mutation (P64G Sav) significantly increased enantioselectivity, while the closest lying mutation (S112G Sav) afforded the greatest variation in enantioselectivity as well as the highest conversions (Table 1, entries 5-7).

1.2 First Round of Evolution: Exploring the Active Site

With the aim of broadening the substrate scope and gaining mechanistic insight into the new system, a library of chemically and genetically modified catalyst variants was produced and screened for activity and selectivity for the reduction of prochiral ketones. As no high-throughput methodology was implemented, we focused on minimal modifications of the active site, likely to dramatically affect the reaction outcome: the position of the biotin-anchor, the capping arene and the metal, as well as the residues predicted to lie close to the active site.[180]

1.2.1 Screening Strategy

In order to limit the number of screening experiments, we opted for a representational search strategy (positional scanning)[23] to optimize the activity and selectivity of the artificial metalloenzymes. Three variables were expected to have an important effect on the reaction outcome: chemical diversity (catalyst structure), genetic diversity (protein environment), and substrate (Scheme 3).

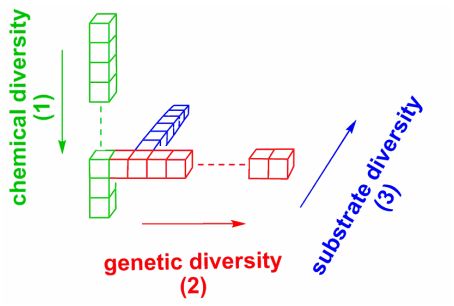

Scheme 3. Screening strategy based on positional scanning for the chemogenetic optimization of the artificial transfer hydrogenases.

Successive optimization rounds were carried out by modifying a single parameter at a time (Scheme 4).

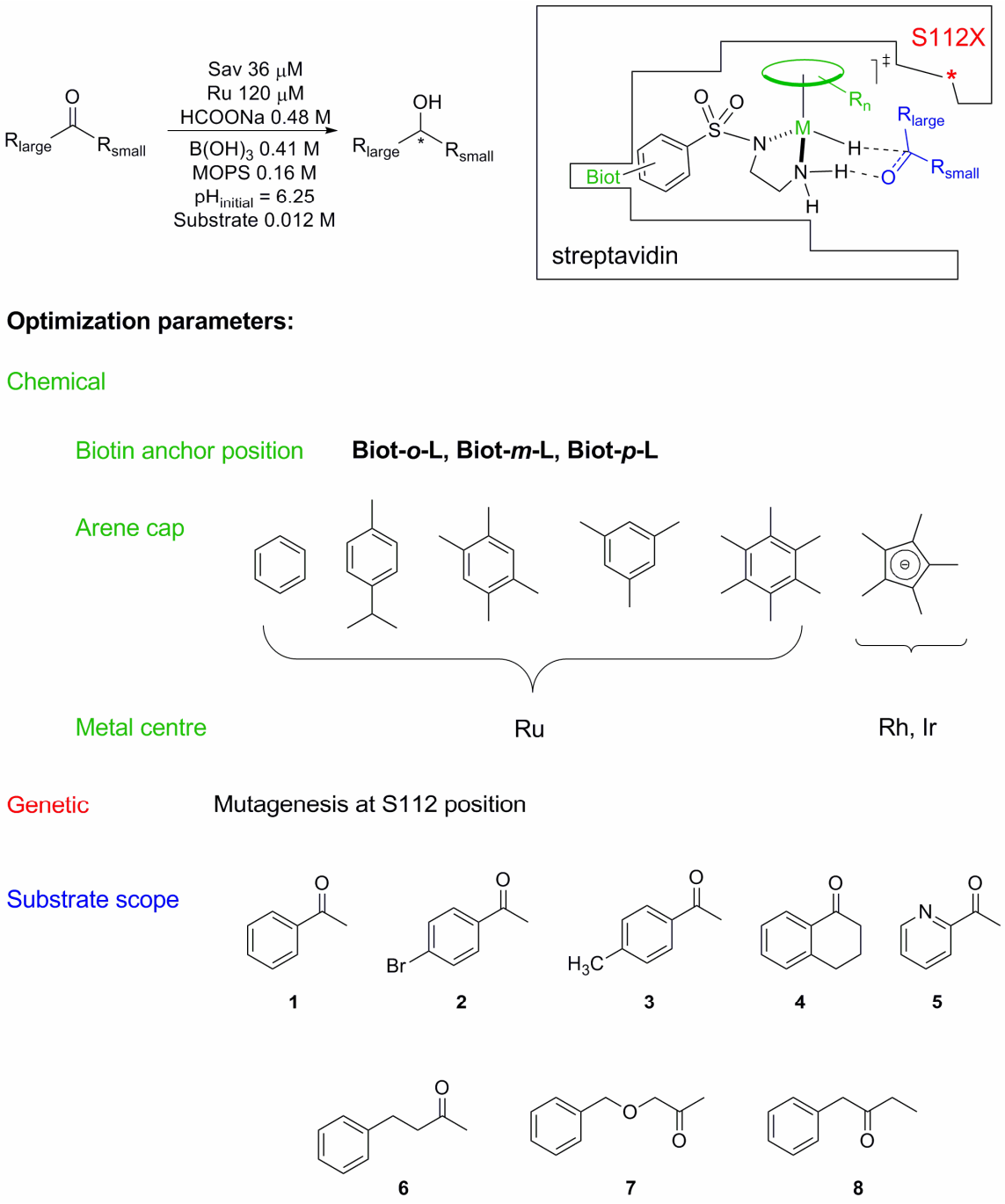

Scheme 4. Chemical, genetic and substrate diversity used for the chemogenetic optimization of enantioselective artificial transfer hydrogenases.

The influence of the biotinylated catalyst structure on the asymmetric transfer hydrogenation for the three acetophenone derivatives **1-3** was evaluated first. Then, changes

of the host protein through targeted mutations were explored by screening with the most promising organometallic scaffolds. Finally, the scope of the reaction was assessed using the best catalyst ⊂ protein combinations. While this approach did not take into account the possible cooperativity effects between the different factors (metal complex, protein and substrate), it allowed the identification of selective catalysts using a modest screening effort.

1.2.2 Insight into the Active Site: Construction of the First Model

To minimize the number of experiments required for efficient optimization, we focused on modifications close to the active site, assuming that these have more influence on cataysis than distant ones.[123,128] In the absence of crystallographic information on the exact location of the catalytic centre, docking studies were performed, in collaboration with Dr. Sylwester Mazurek at the University of Ljubljana, to obtain a qualitative model of the hybrid catalyst.

The most stable docked structure of the ruthenium hydride catalyst [η^6-(*p*-cymene)Ru(**Biot-*p*-L**)H] ⊂ WT Sav reveals that the C_α atoms of serine S112 and S122 lie closest to the ruthenium moiety. However, the S112 side chain points towards the piano-stool fragment while the S122 side chain is directed away from the complex.

1.2.3 Chemical Optimization

The biotinylated metal complex was modified by varying the capping arene, the position of the biotin anchor and the metal centre. A total of twenty-one catalyst precursors was generated by combining the three different ligands (*ortho*-, *meta*- and *para*-biotinylated sulfonamides **Biot-*q*-L**H) with seven d^6 piano-stool fragments containing five arene caps and three different metals (η^5-(C_5Me_5)RhCl, η^5-(C_5Me_5)IrCl and η^6-(arene)RuCl, arene = *p*-cymene, benzene, durene, mesitylene, hexamethylbenzene, Scheme 4).

Screening of these catalysts in the presence of WT Sav and P64G Sav allowed rapid identification of the most promising metal complexes for the reduction of acetophenone derivatives **1-3**: [η^6-(*p*-cymene)Ru(**Biot-*p*-L**)Cl], [η^6-(benzene)Ru(**Biot-*p*-L**)Cl], [η^6-(durene)Ru(**Biot-*p*-L**)Cl], [η^6-(C_5Me_5)Ir(**Biot-*p*-L**)Cl] and [η^6-(C_5Me_5)Rh(**Biot-*p*-L**)Cl]. The two Sav isoforms used in the screening displayed similar trends. It is worthy noting that only the *para*-anchored ligands afforded significant levels of conversion, suggesting that the *meta*- and *ortho*-anchoring localize the ruthenium centre in a position that is not easily accessible for the substrate.

1.2.4 Genetic Optimization

The preliminary results obtained with the S112G Sav mutant, which showed the most pronounced changes in conversion and selectivity (see Table 1, entry 7), encouraged the selection of position S112 for genetic optimization through saturation mutagenesis. This choice was further motivated by the docking studies, which suggested close contacts between the S112 amino acid side chain and the ruthenium moiety. Thus, the five biotinylated ruthenium complexes were screened in conjunction with the twenty streptavidin isoforms, S112X Sav.

Table 2. Selected results for the chemogenetic optimization of the artificial transfer hydrogenases for the reduction of the acetophenone derivatives **1-3**.

Entry	Protein	Complex	Substrate	Conv. (%)	ee (%)
1	S112Y Sav	[η^6-(*p*-cymene)Ru(**Biot-*p*-L**)Cl]	**1**	95	90 (*R*)
2	S112Y Sav	[η^6-(durene)Ru(**Biot-*p*-L**)Cl]	**2**	88	92 (*R*)
3	S112T Sav	[η^6-(benzene)Ru(**Biot-*p*-L**)Cl]	**2**	90	55 (*S*)
4	S112D Sav	[η^6-(*p*-cymene)Ru(**Biot-*p*-L**)Cl]	**1**	0	-
5	S112A Sav	[η^6-(*p*-cymene)Ru(**Biot-*p*-L**)Cl]	**3**	98	91 (*R*)
6	S112A Sav	[η^6-(benzene)Ru(**Biot-*p*-L**)Cl]	**3**	74	41 (*R*)
7	S112K Sav	[η^6-(*p*-cymene)Ru(**Biot-*p*-L**)Cl]	**1**	50	20 (*S*)
8	S112K Sav	[η^6-(benzene)Ru(**Biot-*p*-L**)Cl]	**1**	37	55 (*S*)
9	S112R Sav	[η^6-(benzene)Ru(Biot-*p*-L)Cl]	**3**	23	62 (*S*)

General trends emerge from this second optimization step:

- The nature of the capping arene by-and-large determines the preferred enantiomer: (*R*)-reduction products are obtained with η^6-(*p*-cymene)- and η^6-(durene)-bearing complexes and (*S*)-reduction products are obtained with the η^6-(benzene)-bearing complex (Table 2, entries 1-3 and Figure 1a). The overall performance of the rhodium- and iridium-containing metalloenzymes is modest and depends very much on the host protein (Figure 1a).
- Sav mutants bearing a potentially coordinating amino acid side chain at position S112 (cysteine, methionine, aspartic or glutamic acid, histidine) inhibit the catalytic

performance of the artificial transfer hydrogenases (Table 2, entry 4). This confirms the initial hypothesis that S112 is close to the organometallic fragment.

- Introduction of cationic residues (lysine, arginine) at position S112 favours (*S*)-reduction products, while hydrophobic residues (tyrosine, phenylalanine, valine, alanine) at position S112 favour (*R*)-reduction products (Figure 1b).

The (*R*)-and (*S*)-selective proteins and metal complexes can act either in a matched or mismatched fashion to afford good levels of selectivity for (*R*)-reduction products or moderate (*S*)-selectivities (Table 2, entries 5-9).

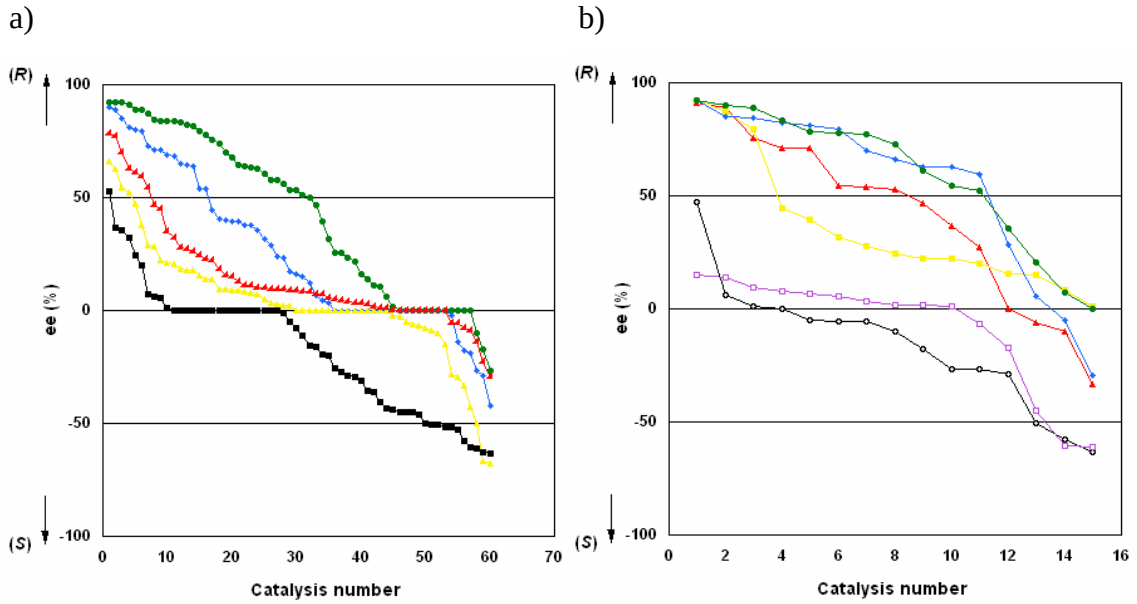

Figure 1. Summary of the enantioselectivity trends of the chemogenetically optimized artificial metalloenzymes, arranged from the highest to the lowest ee value, according to: a) the nature of the complex, irrespective of the protein and substrate used: [η^6-(*p*-cymene)Ru(**Biot-*p*-L**)Cl] (●), [η^6-(benzene)Ru(**Biot-*p*-L**)Cl] (■), [η^6-(durene)Ru(**Biot-*p*-L**)Cl] (♦), [η^6-(C_5Me_5)Ir(**Biot-*p*-L**)Cl] (▲) and [η^6-(C_5Me_5)Rh(**Biot-*p*-L**)Cl] (◄); b) the Sav isoform, irrespective of the Ru complex and substrate used: S112Y (●), S112F (♦), S112V (▲), S112A (■), S112R (□) and S112K (○).

1.2.5 Substrate Scope

Having identified the most efficient hybrid catalysts, we proceeded to test substrates **4-8**, bearing bulky (**4**), coordinating (**5**) or dialkyl groups (**6-8**, Scheme 4). The five substrates were tested in the presence of the (*R*)-selective [η^6-(*p*-cymene)Ru(**Biot-*p*-L**)Cl] and of the (*S*)-selective [η^6-(benzene)Ru(**Biot-*p*-L**)Cl] catalysts. These were combined with ten representative S112X Sav isoforms (X = A, G and L: aliphatic residues with increasing bulk; F and W: aromatic residues with increasing bulk; S and T: polar residues; E: coordinating

anionic residue; R: cationic residue; N: neutral amidic residue) and the best results are summarized in Table 3.

The selectivity and conversion trends are similar to those obtained for the acetophenone derivatives **1-3**. Only modest activities and enantioselectivities are obtained with the non-aromatic ketones (Table 3, entries 1-4). High (*R*)-selectivities are obtained for α-tetralone (Table 3, entry 5). Interestingly, the (*S*)-selective trend of the artificial enzymes bearing cationic residues at position 112 (S112K and S112R) is particularly pronounced for 2-acetylpyridine **5**, suggesting that the presence of a positive charge at this position is beneficial for this substrate (Table 3, entries 6-7). We speculated that the presence of a hydrogen bond between the cationic residue and the pyridine moiety played a key role in this context.

Table 3. Selected results for the transfer hydrogenation of substrates **4-8** with the most selective combinations [η^6-(arene)Ru(**Biot-*p*-L**)Cl] ⊂ Sav isoform.

Entry	Protein	Complex	Substrate	Conv. (%)	ee (%)
1	S112A Sav	[η^6-(*p*-cymene)Ru(**Biot-*p*-L**)Cl]	**6**	98	48 (*R*)
2	S112A Sav	[η^6-(*p*-cymene)Ru(**Biot-*p*-L**)Cl]	**7**	97	69 (*R*)
3	S112G Sav	[η^6-(benzene)Ru(**Biot-*p*-L**)Cl]	**7**	73	45 (*S*)
4	S112A Sav	[η^6-(*p*-cymene)Ru(**Biot-*p*-L**)Cl]	**8**	71	30 (*R*)
5	S112F Sav	[η^6-(*p*-cymene)Ru(**Biot-*p*-L**)Cl]	**4**	70	96 (*R*)
6	S112R Sav	[η^6-(benzene)Ru(**Biot-*p*-L**)Cl]	**5**	93	69 (*S*)
7	S112K Sav	[η^6-(benzene)Ru(**Biot-*p*-L**)Cl]	**5**	97	70 (*S*)

1.3 Second Round of Evolution: X-Ray Guided Designed Evolution

1.3.1 From Model to Reality: First X-Ray Structure of a Streptavidin-Based Artificial Metalloenzyme

With the aim of gaining structural and functional insight into the artificial transfer hydrogenases, a significant effort was invested into crystallizing the most promising combinations of metal complex and Sav isoform. The crystal structure of the (*S*)-selective [η^6-(benzene)Ru(**Biot-*p*-L**)Cl] ⊂ S112K Sav was determined by Dr. Marc Creus in collaboration with Dr. Isolde LeTrong and Prof. Ronald Stenkamp from the University of Washington. The refined model (1.58 Å resolution, PDB reference code 2QCB) provides a

fascinating insight into the organization of the active site and the close contacts between the Ru complex and amino acid residues in several loop regions.[181]

It is important to note that the occupancy of the Ru site is only 20%, probably due either to conformational flexibility inside the host protein, to Ru decomplexation during crystallization or to steric clash in the case of simultaneous occupation of two adjacent binding sites by the Ru complex. Indeed, the metal moiety is located near a subunit-subunit interface and lies too close to the neighbouring biotinylated complex (Ru⋯⋯Ru distance 4.44 Å), thus hindering the occupancy of the adjacent biotin binding site (Figure 2a). This short contact suggests that substituting the capping η^6-benzene by a bulkier η^6-*p*-cymene may force the latter biotinylated complex to adopt a different position and / or configuration at the metal to avoid steric hindrance. It is also noteworthy that incorporation of the bulky [η^6-(benzene)Ru(**Biot-*p*-L**)Cl] within S112K Sav does not lead to a major structural reorganization of the host protein (Figure 2b). Compared to WT Sav, a root mean square (RMS) of 0.276 Å is computed for all 121 C_α atoms present.

a) b)

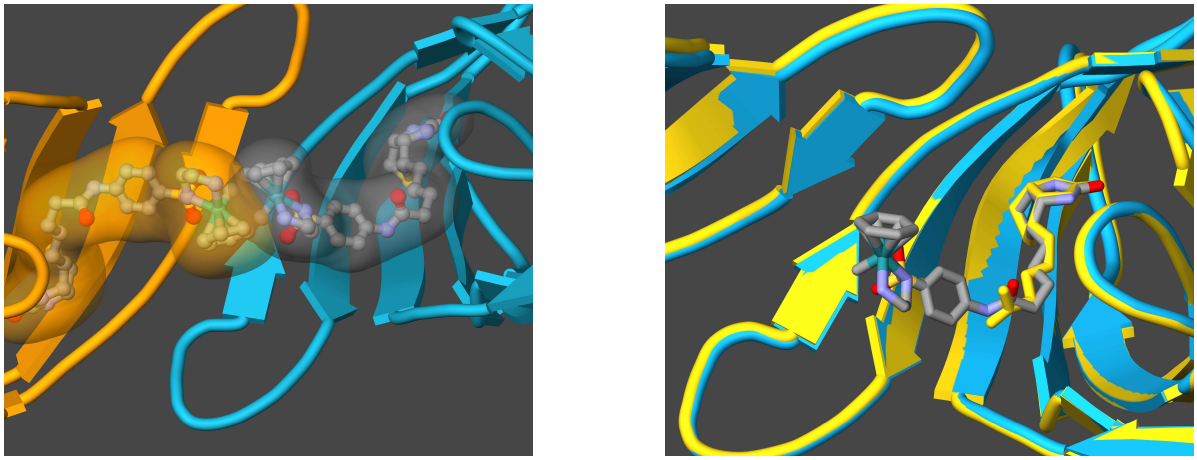

Figure 2. a) Short contact between the two biotinylated complexes [η^6-(benzene)Ru(**Biot-*p*-L**)Cl] from adjacent monomers A and B of S112K Sav. b) Superimposition of the structure of [η^6-(benzene)Ru(**Biot-*p*-L**)Cl] ⊂ S112K Sav (blue schematic representation) with the structure of biotin ⊂ core WT Sav (PDB reference code 1STP, yellow schematic representation, biotin: yellow stick). Only monomers A and B are displayed for clarity. This view emphasizes the minimal structural reorganization of the host protein required to accommodate the biotinylated catalyst.

Most interestingly, despite the use of a racemic Ru piano-stool complex for crystallization, only the (*S*)-enantiomer of [η^6-(benzene)Ru(**Biot-*p*-L**)Cl] was localized in the crystal structure (Figures 2 and 3). In homogeneous systems, the (*S*)-Ru configuration of the chloride

complex is predicted to afford (*S*)-reduction products of acetophenone derivatives. The [η^6-(benzene)Ru(**Biot-*p*-L**)Cl] ⊂ S112K Sav was the most (*S*)-selective hybrid catalyst identified during the first screening round (see Figure 1b). This observation further supports our hypothesis that second coordination sphere interactions enforce a preferential configuration at ruthenium (see Scheme 2).

The structure also confirms the docking results suggesting that the S112 position lies in the immediate vicinity of the Ru atom. Several additional short contacts between the biotinylated catalyst and amino acid side chains can be identified (Figure 3). These include residues of the L7,8 loop (110-120) of both Sav monomers A and B as well as G48 (part of L3,4 loop) and H87 (part of L5,6 loop) of the monomer A in which the biotinylated catalyst [η^6-(benzene)Ru(**Biot-*p*-L**)Cl] is located. Position 121 is of particular interest, as the K121 residues of both monomers A and B can interact both with the η^6-arene ($K121_B$) and with the expected trajectory of the incoming substrate ($K121_A$). Other residues in the L7,8 loop of monomer A might also influence the approach of the substrate (*i.e.* N118, A119, W120).

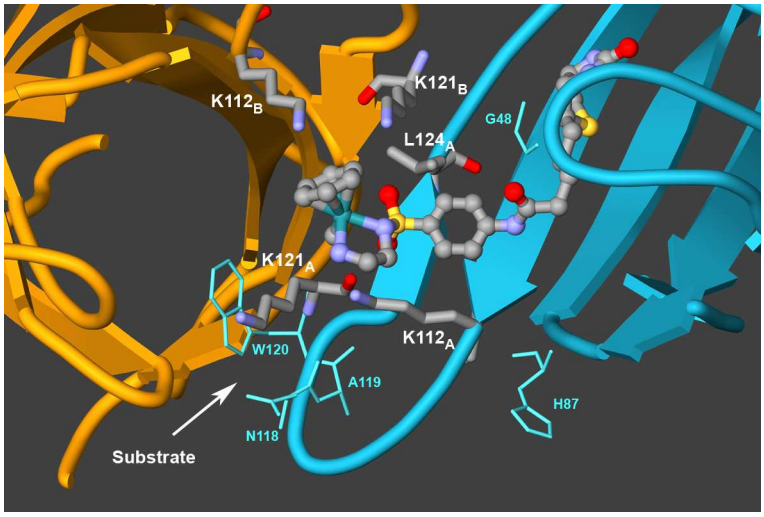

Figure 3. Close up view of the structure of [η^6-(benzene)Ru(**Biot-*p*-L**)Cl] ⊂ S112K Sav determined by X-ray crystallography (only one dimer of the tetramer depicted for clarity: monomer A – blue and monomer B – orange). Only monomer A is occupied by the biotinylated Ru complex. Residues K112, K121 and L124 of monomer A and K112, K121 of monomer B, close-lying to the Ru atom, are highlighted (stick). Residues G48 and H87 (C_α-Ru distances < 12 Å), as well as N118, A119 and W120 (possibly interfering in the trajectory of the substrate) of monomer A are also highlighted as light blue lines. A possible trajectory of the incoming prochiral substrate is also indicated by an arrow. It should be noted that the occupancy of the metal moiety is only 20%.

Detailed inspection of the structure reveals that the side chain of residue L124 displays a short contact with the SO_2 moiety that links the piano-stool complex to the biotin anchor (Figure 3, $H_3C_{Leu}\cdots OSORR'_{Ligand}$ distance 3.53Å) and thus may influence the position of the biotinylated complex inside the hydrophobic pocket.

1.3.2 New Challenge: Reduction of Dialkyl Ketones

Even though the X-ray structure provides some important knowledge about the positioning of the biotinylated moiety inside the host protein, it does not offer any precise information about the enantioselection mechanism. In this context, further evolution of the artificial metalloenzymes cannot rely exclusively on rational redesign, but requires the use of random mutagenesis and screening experiments to perfect those elements which cannot be predicted. Starting from the previously identified (*R*)- and (*S*)-selective variants and from the close-lying residues identified from the X-ray structure, we implemented a designed evolution methodology[185] for the optimization of the artificial transfer hydrogenases. Given the difficulty of predicting the effect of a particular amino acid residue on the reaction outcome, saturation mutagenesis was performed at the selected positions.

During the first chemogenetic optimization step, highly (*R*)-selective combinations were identified for the reduction of aromatic ketones. In contrast, only moderate (*S*)-selectivities were obtained for these substrates, while the dialkyl ketones were reduced with modest activities and enantioselectivities (ee's up to 69% (*R*) and 45% (*S*)). Consequently, we reasoned that it would be interesting to further evolve the hybrid catalyst to create selective systems for the reduction of dialkyl ketones. Moreover, by carefully choosing the mutation sites, the modest (*S*)-selectivity of the artificial enzymes might be improved.

Dialkyl ketones are challenging for the homogeneous transfer hydrogenation catalysis, as the postulated critical enantiodiscriminating $C_{aromatic}H–\pi$ interaction between the η^6-arene ligand and the aryl group of the ketone is absent for such substrates.[60,62] In contrast, in enzymatic systems like alcohol dehydrogenases, enantiodiscrimination is controlled by second coordination sphere interactions between the substrate and the enzyme, leading to highly enantioselective reduction of aliphatic ketones (see Chapter 1, Sections 2.1.1 and 2.1.2). Considering the streptavidin-based transfer hydrogenases, we hypothesized that the second coordination sphere contacts between the host protein and the substrate may lead to good selectivities, even for these challenging substrates. However, the first results suggest that

the 112 position has little influence on determining the orientation of the approaching dialkyl substrates **6-8**.

In this context, identification of residue K121 as possibly interacting both with the η^6-arene ($K121_B$) and with the incoming substrate ($K121_A$) was of particular interest. We targeted residues K121 and L124 for saturation mutagenesis, speculating that the first could steer the delivery of the substrate, while the second could alter the position of the metal complex within the binding pocket (through the $H_3C_{Leu}\cdots OSORR'_{Ligand}$ interaction), thus influencing the enantioselectivity of the reaction.

Saturation mutagenesis at K121 and L124 positions was performed starting in the genetic backgrounds of S112A Sav and S112K Sav ((*R*)-, respectively (*S*)-selective mutants), as well as that of WT Sav. Although it was not the most (*R*)-selective mutant identified during the first chemogenetic optimization step (see Figure 1b), S112A Sav was chosen since this Sav isoform displayed a good level of protein expression, far better than either S112F or S112Y Sav. The promising (*S*)-selectivity trends and the crystallographic information dictated the choice of the S112K Sav mutant.

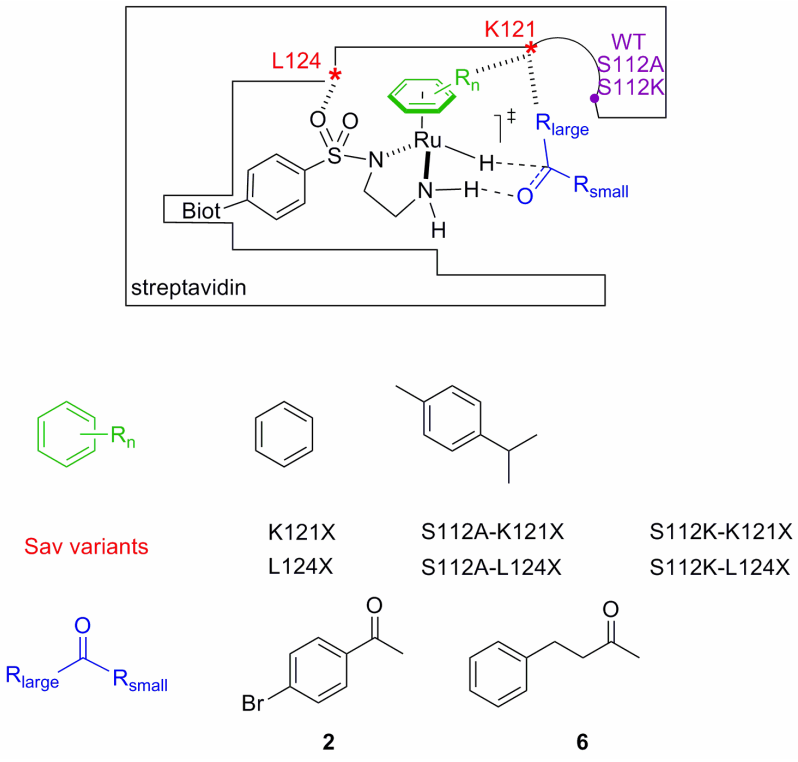

Scheme 5. Parameters optimized during the designed evolution protocol: η^6-arene = *p*-cymene, benzene; Sav mutant = K121X, L124X, S112A-K121X, S112A-L124X, S112K-K121X, S112K-L124X; substrate = *p*-bromoacetophenone **2,** 4-phenyl-2-butanone **6**.

A total of 114 new Sav mutants (K121X; L124X; S112A-K121X; S112A-L124X; S112K-K121X and S112K-L124X) were produced by the molecular biology team of our laboratory (Miss Alessia Sardo, Dr. Anita Ivanova and Dr. Marc Creus) and tested in combination with the [η^6-(*p*-cymene)Ru(**Biot-*p*-L**)Cl] and [η^6-(benzene)Ru(**Biot-*p*-L**)Cl] complexes. The activated *para*-bromoacetophenone **2** and the challenging 4-phenyl-2-butanone **6** were chosen as model aromatic, respectively aliphatic substrates (Scheme 5).

1.3.3 Extraction-Immobilization Protocol: Quick Screening Strategy

To accelerate the optimization process, a quick screening protocol had to be implemented. The first round of screening for the chemogenetic optimization required the use of milligram quantities (3-4 mg per catalytic experiment) of the twenty purified Sav mutants to perform the catalytic experiments. Since the set up for the production and purification of Sav in our laboratory lasts nearly three weeks for the production of one mutant (including purification and lyophilisation), an alternative technique for testing the 114 new Sav mutants was necessary.

1.3.3.1 Catalysis with Streptavidin-Containing Crude Cell Extracts

In the absence of colony selection techniques, the quickest way to test the performance of the Sav mutants is screening for catalysis in crude cell extracts after Sav production in small volume *E. coli* cell cultures. After extraction of the substrate and of the product using an organic solvent, the conversions and ee's can be determined by chiral HPLC analysis of the organic phase. The problems associated with this method are the low levels of Sav production in the small culture volumes, as well as the presence of a variety of potential catalyst inhibitors in the cell extract (for example, anionic DNA constitutes a possible ligand for the Ru complex).

In a first approach, the use of crude cell extracts containing the S112Y Sav mutant was tested in the reduction of acetophenone **1**. After protein expression and production in a 50 mL *E. coli* culture, the cell pellet containing ~ 1 mg Sav (determined by titration with biotin-4-fluorescein)[186] was treated with DNA-ase, re-suspended in ~ 800 μL of water and tested for catalysis. Following this procedure, the concentration of the artificial metalloenzyme inside the reaction mixture is roughly three times more dilute than in the standard experiment. Using pure S112Y Sav under these conditions affords much lower conversion and ee than the standard experiment with concentrated protein (Table 4, entries 1-2). Moreover, as

anticipated, the presence of the cellular extract completely inhibits the catalytic activity of the organometallic complex (Table 4, entries 3-4).

These results suggest that, in contrast to enzyme optimization via evolutionary techniques – where screening can often be performed with either colonies or crude cell extracts –, the presence of an exogenous metal sets very stringent protein purity requirements to ensure reproducible activity of the artificial metalloenzymes. Indeed, to the best of our knowledge, all experiments in the area of artificial metalloenzymes have thus far been performed with protein purified to homogeneity. This lengthy purification step is a significant bottleneck for artificial metalloenzyme optimization.

Table 4. Comparison of the results afforded by purified S112Y Sav with the results obtained using crude cellular extracts containing S112Y Sav for the reduction of acetophenone **1** using [η^6-(*p*-cymene)Ru(**Biot-*p*-L**)Cl].

Entry	Protein	[Sav] (μM)	Conv. (%)	ee (%)
1	pure	36	95	90 (*R*)
2	pure	14.3	59	60 (*R*)
3	cell extract	14.3	0	-
4	pure + cell extract	14.3	0	-

1.3.3.2 Immobilization Technique: Rapid Protein Extraction and Purification

To overcome this limitation, we reasoned that the tetrameric nature of Sav could be exploited to purify the host protein by immobilization using commercially available iminobiotin- or biotin-sepharose. Thanks to the very high and selective affinity of biotin (and, to a lesser extent, iminobiotin) for Sav, we speculated that the immobilization step could be performed directly on the crude *E. coli* cellular extract. The change in the affinity of Sav for iminobiotin with the variation of pH (the binding strength decreases as the pH decreases) can be exploited to release pure protein after immobilization (Scheme 6a).[187] When biotin-sepharose is used, sacrifying one biotin-binding site for immobilization purposes leaves up to three biotin binding sites to incorporate the biotinylated piano-stool and to perform catalysis (Scheme 6b).

The performances of the two purification techniques for the reduction of *para*-methylacetophenone **3** were compared using the most selective artificial metalloenzyme identified to date, [η^6-(*p*-cymene)Ru(**Biot-*p*-L**)Cl] $\subset$ P64G Sav (Table 5). The results suggested that both methods can be used for the rapid purification and testing of Sav-

containing crude cell extracts, although with some loss with respect to conversion and selectivity. However, some disadvantages can be associated with the iminobiotin-sepharose extraction and purification protocol:

- the affinity of Sav for iminobiotin is lower than the affinity for biotin; this feature is especially important as the concentration of the protein in the cell extract can be very low in some cases;
- careful adjusting of the pH is necessary after the elution step at pH 2.9 ($pH_{initial}$ = 6.25 for optimal results in catalysis – see Section 1.1). This step is associated with an increase in the total volume of catalysis and thus with a decrease in Sav concentration.

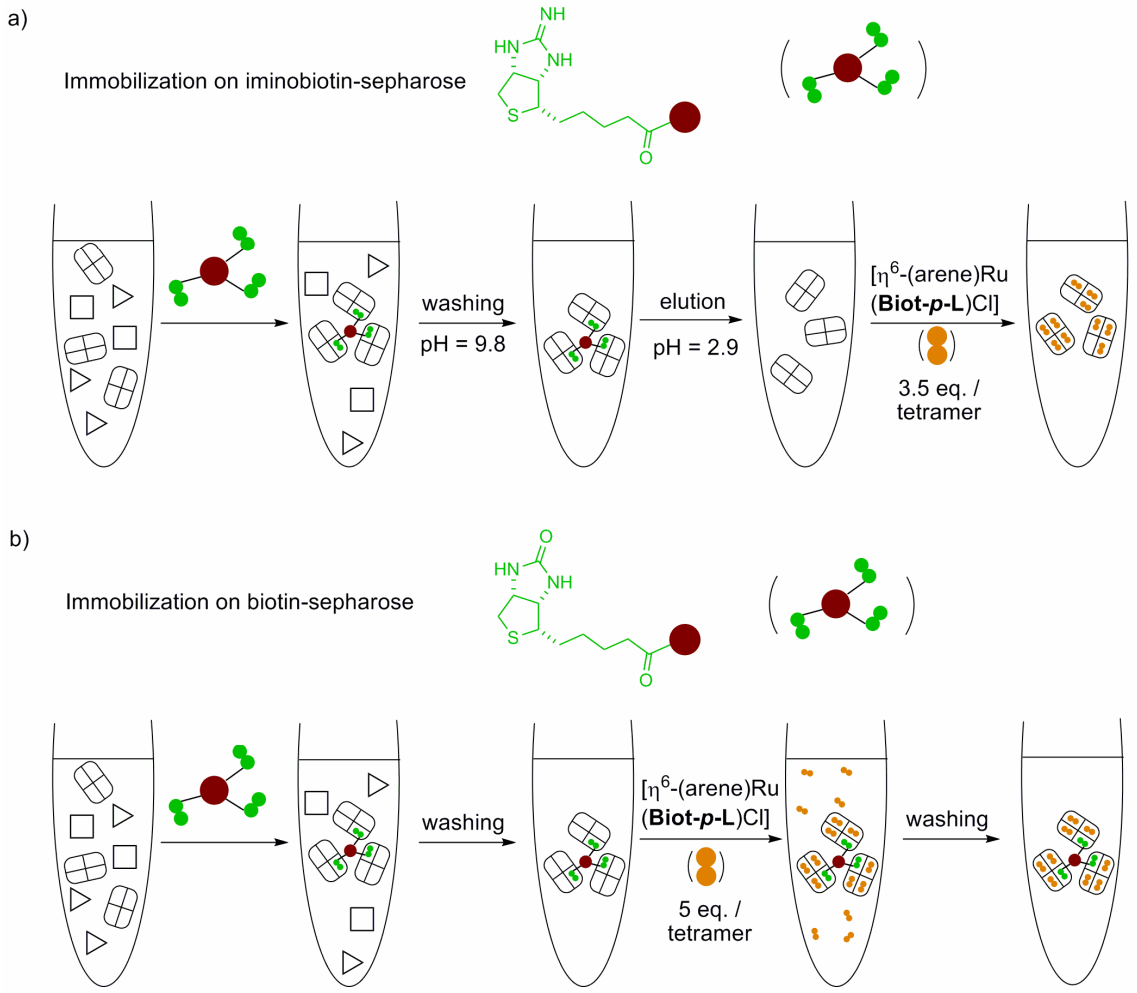

Scheme 6. Rapid techniques for the extraction and purification of streptavidin from crude cell extracts. a) Immobilization on iminobiotin-sepharose, followed by washing (pH = 9.8) and elution (pH = 2.9) steps affords pure Sav; b) Using biotin-sepharose affords the immobilized artificial metalloenzyme after several washing cycles.

In contrast, immobilization on biotin-sepharose appeared to be a more robust system and was selected for further use for the screening of the 114 Sav mutants. Guanidinium chloride (1 M solution) and the $HCOONa{\cdot}B(OH)_3$ mixture (the hydrogen source for catalysis) were used as washing solutions for the first and the second washing steps, respectively.

Table 5. Comparison of the iminobiotin- and biotin-sepharose extraction and purification techniques of streptavidin from crude cell extracts. The catalysis were performed using [η^6-(*p*-cymene)Ru(**Biot-*p*-L**)Cl] ⊂ P64G Sav for the reduction of *para*-methylacetophenone **3**. The washing steps in the case of biotin-sepharose immobilization were realized using H_2O / DMF = 100 / 2.

Entry	Purification technique	Protein	Conv. (%)	ee (%)
1	-	pure	92	94 (*R*)
2	biotin	pure	92	93 (*R*)
3	iminobiotin	pure	90	87 (*R*)
4	biotin	cell extract	76	73 (*R*)
5	iminobiotin	cell extract	57	82 (*R*)

Following a growth of 50 mL *E. coli* cell culture in a 250 mL baffled flask, the cell pellet was collected by centrifugation, frozen at –25°C, thawed and re-suspended in 1.5 mL of water. The amount of Sav in the crude cell extract was estimated by fluorimetric titration using biotin-fluorescein as a probe[186] (the titrations were performed in our laboratory by Mr. Thibaud Rossel and Miss Alessia Sardo using a 96-well plate microreader). To a suspension of biotin-sepharose in water, a solution containing a two-fold excess of tetrameric Sav with respect to the capacity of the biotin-sepharose beads was added. Centrifugation followed by three washing cycles with 1 M guanidinium chloride and one washing step with water afforded immobilized Sav, which was re-suspended in water and thoroughly degassed with dinitrogen. Addition of five equivalents (*vs.* immobilized tetrameric Sav) of biotinylated catalyst [η^6-(arene)Ru(**Biot-*p*-L**)Cl] (arene = benzene or *p*-cymene) and three washing cycles with the $HCOONa{\cdot}B(OH)_3$ mixture yielded yellow suspensions, which were charged with the $HCOONa{\cdot}B(OH)_3{\cdot}$MOPS mixture and with the appropriate substrate and heated at 55°C for 64 hours under an inert atmosphere.

Catalysis results comparing purified Sav and Sav from crude cellular extracts immobilized via the protocol outlined above are presented in Table 6. The technique was tested with the three Sav isoforms selected for the designed evolution (WT, S112A and S112K), using the

two Ru complexes and the aromatic substrate **2**. From these initial results, it appears that, although the purification-immobilization with biotin-sepharose leads to a noticeable erosion of both of the activity and the selectivity, this straightforward protocol significantly speeds up the screening process to afford valuable trends. We thus set out to exploit the immobilization-purification strategy to perform a round of directed evolution.

Table 6. Comparison of the results obtained for the transfer hydrogenation of *p*-bromoacetophenone **2** using biotin-sepharose immobilized- and purified homogeneous artificial metalloenzymes [η^6-(arene)Ru(**Biot-*p*-L**)Cl] $\subset$ Sav.

Entry	η^6-(arene)	Sav isoform	Pure non-immobilized Sav		Immobilized Sav (from cellular extract)	
			Conv. (%)	ee (%)	Conv. (%)	ee (%)
1	*p*-cymene	WT Sav	93	87 (*R*)	81	65 (*R*)
2	benzene	WT Sav	43	57 (*S*)	31	39 (*S*)
3	*p*-cymene	S112A Sav	78	87 (*R*)	57	64 (*R*)
4	benzene	S112K Sav	25	44 (*S*)	21	38 (*S*)

1.3.4 Screening and Trends of the Immobilized Artificial Metalloenzymes

The catalytic experiments of this screening round were performed with the help of Mr. Thibaud Rossel. Using the immobilization strategy, semi-quantitative trends were rapidly obtained for the reduction of 4-phenyl-2-butanone **6** as well as for *p*-bromoacetophenone **2**. The enantioselectivity trends for the two substrates are displayed in Figure 4 in a fingerprint format, associating red with (*R*)- and blue with (*S*)-enantioselectivity. This type of display allows a rapid identification of the most selective combinations, as well as a comparison between the different variables influencing the enantioselectivity outcome. A refined comparison between these elements is also presented in Figure 6a-d.

The trends identified in this screen can be classified according to the following parameters:

Substrate: aromatic *vs.* dialkyl ketone. In general, the two substrates behave similarly in terms of enantioselectivity. It is noteworthy that the enantioselectivity obtained for the dialkyl product is greater or opposite to the ee of the aromatic product for more than half of the artificial metalloenzymes, reaching a $|\Delta ee|$ (difference in enantioselectivity) of up to 65%

(Figure 5 and Table 7, entries 1 and 2). This suggests that protein-substrate interactions, reminiscent of keto-reductases are intimately involved in the enantioselection mechanism, as the classical $C_{aromatic}H$-π interaction cannot be invoked for dialkyl substrates.

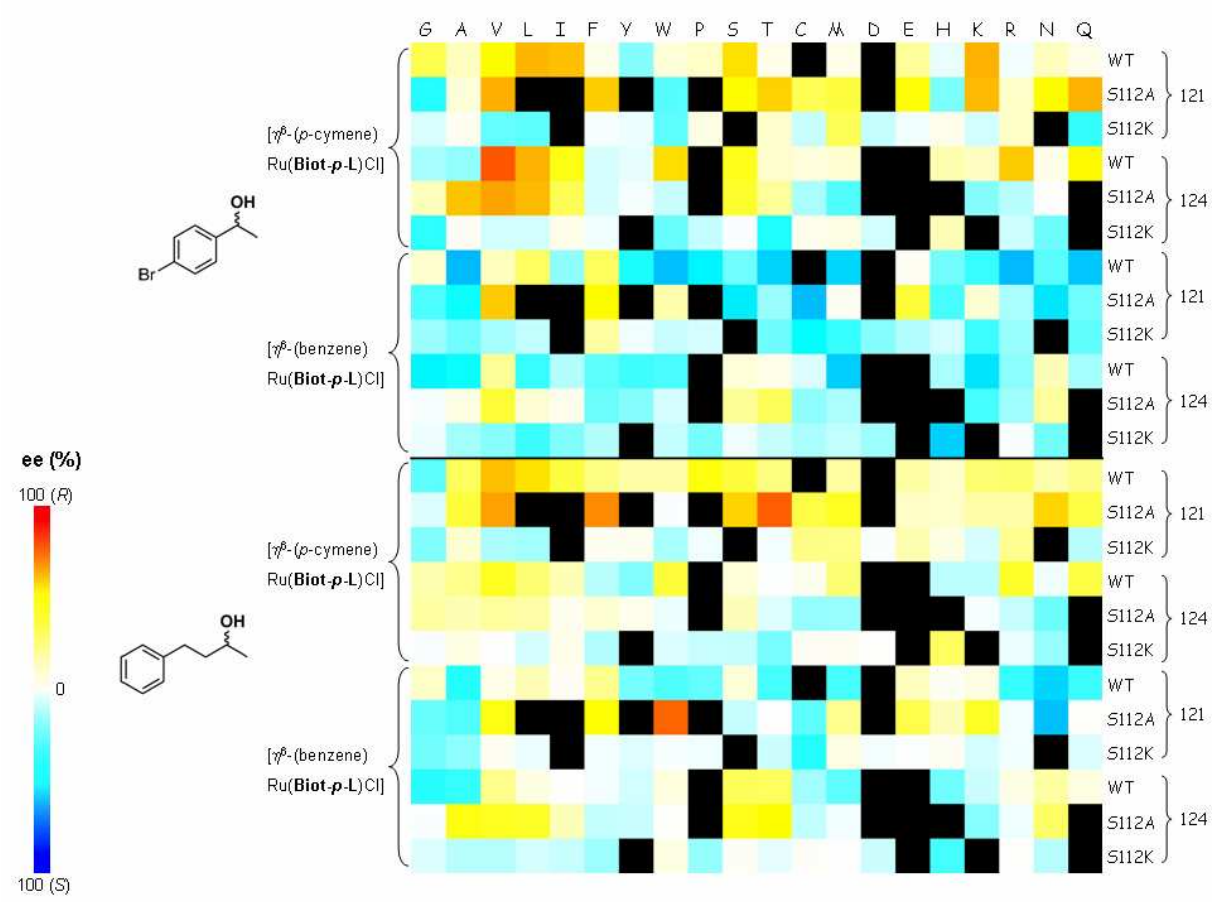

Figure 4. Fingerprint display of the results for the designed optimization of the reduction of ketones **2** and **6** in the presence of biotin-sepharose-immobilized artificial metalloenzymes [η^6-(arene)Ru(**Biot-*p*-L**)Cl] ⊂ Sav mutant (K121X, S112A-K121X, S112K-K121X, L124X, S112A-L124X, S112K-L124X). Catalytic runs that could not be performed (insufficient soluble protein expression) are represented by black squares.

As expected, in most of the experiments, the activated *p*-bromoacetophenone **2** affords much better conversions than the aliphatic substrate **6**. The challenging dialkyl ketone gives comparable (*R*)-selectivity to the acetophenone derivative **2**, albeit using different biotinylated catalyst ⊂ protein combinations (ee's up to 83 % (*R*) for **2** and 82% (*R*) for **6**, Table 7, entries 3 and 4). In contrast, with some rare exceptions (Table 7, entry 5), only modest (*S*)-selectivities are obtained with substrate **6** (Figure 6a).

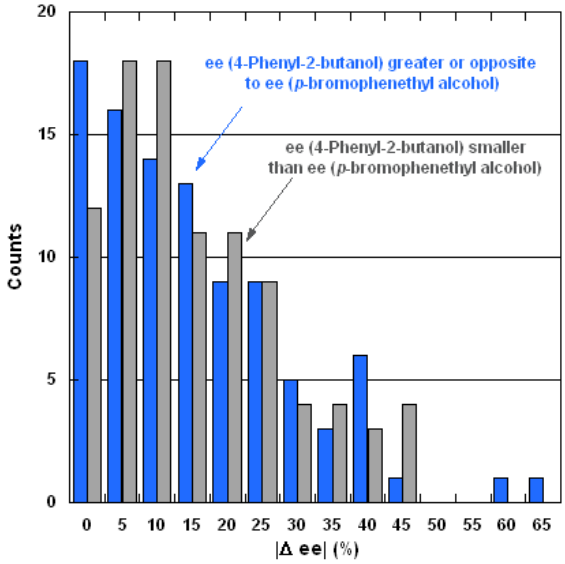

Figure 5. Difference in enantiomeric excess ($|\Delta ee|$) between the aromatic and the aliphatic reduction products, calculated for all the immobilized Sav isoforms.

Capping arene: η^6-*p*-cymene *vs.* η^6-benzene (Figure 6b)**.** As in the previous screening round (Section 1.2), the enantioselectivity of the reaction is mainly dictated by the chemical moiety. However, while good (*R*)-selectivities can be obtained with [η^6-(*p*-cymene)Ru(**Biot-*p*-L**)Cl], the best (*S*)-selectivities afforded by [η^6-(benzene)Ru(**Biot-*p*-L**)Cl] remain moderate using the immobilized Sav isoforms. Nonetheless, some selective combinations are identified. The opposite tendencies of the two complexes are best illustrated in the presence of S112A-K121N Sav for the reduction of both substrates (Table 7, entries 5-7).

Interestingly, some notable deviations from the (*S*)-trend of [η^6-(benzene)Ru(**Biot-*p*-L**)Cl] are observed in the case of metalloenzymes bearing the S112A mutation ([η^6-(benzene)Ru(**Biot-*p*-L**)Cl] ⊂ S112A-K121W Sav 80% ee (*R*), Table 7, entry 2).

Nature of the S112X residue: WT, S112A, S112K (Figure 6c). Artificial metalloenzymes incorporating the S112A mutation bring more diversity than the WT- and S112K-derived isoforms. Some of the best (*R*)- and (*S*)-selectivities for both the aromatic and the aliphatic substrates are obtained with catalyst variants bearing the S112A mutation (Table 7, entries 4-5 and 9-12).

Overall, the S112K double mutants are least selective, suggesting that a small side chain (alanine or serine) at position 112 may increase the influence of beneficial K121X or L124X mutations. The best S112K double mutant is [η^6-(*p*-cymene)Ru(**Biot-p-L**)Cl] ⊂ S112K-L124H Sav which affords 59% ee (*S*) for the reduction of substrate **2** (Table 7, entry 13).

Thus, within this round of designed evolution, the S112K mutation can be regarded as an evolutionary dead-end.

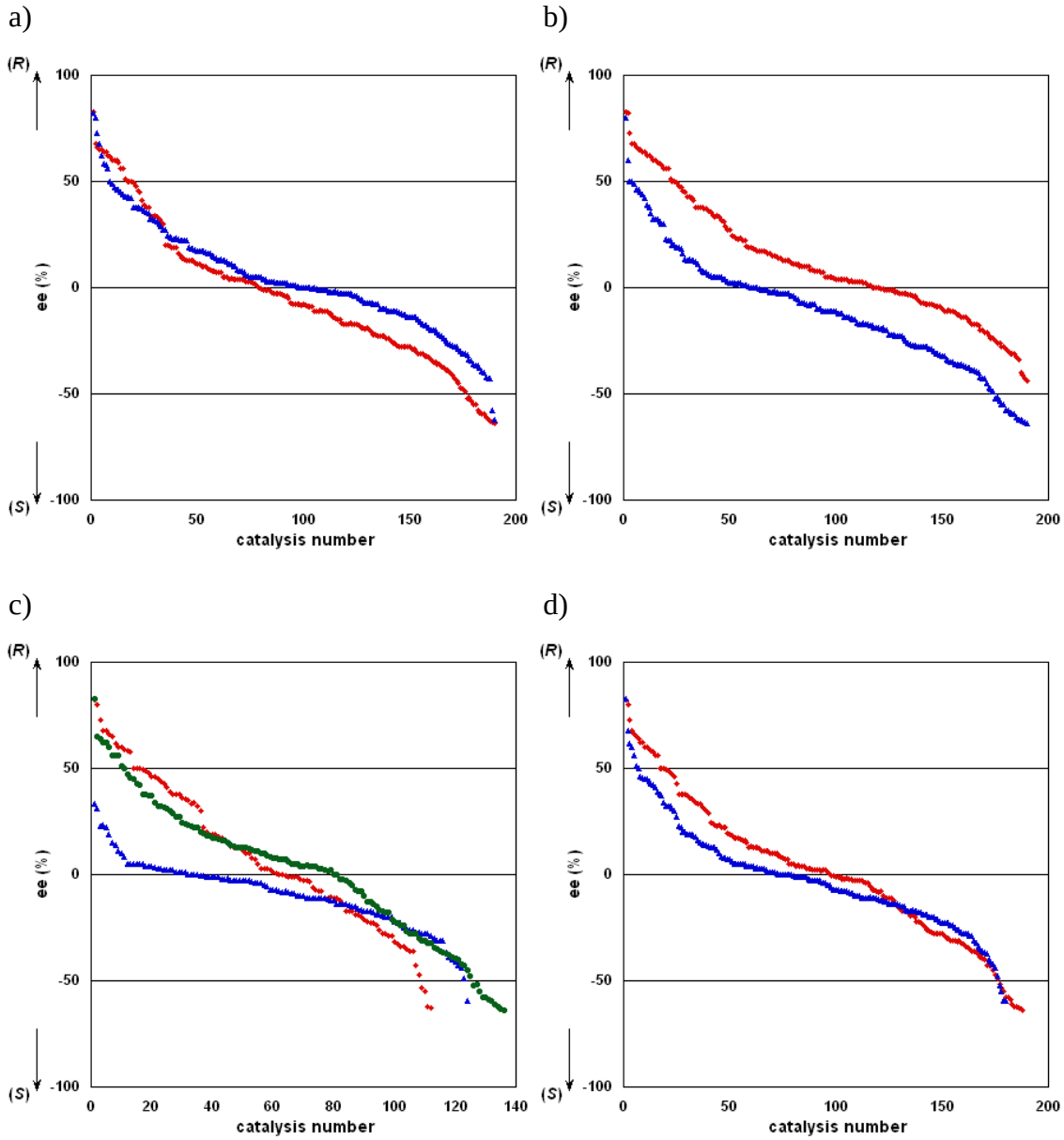

Figure 6. Enantioselectivity trends of the immobilized artificial transfer hydrogenases. The results are arranged from the highest to the lowest ee value, according to: a) the nature of the substrate: **2** (♦) and **6** (▲); b) the nature of the capping arene: *p*-cymene (♦) and benzene (▲); c) the nature of the S112X residue: S112A (♦), S112K (▲) and S112 (●); d) the position of the site of mutation: K121X (♦) and L124X (▲).

Position of the site of mutation: K121X *vs.* L124X (Figure 6d)**.** In terms of the site of mutation, saturation mutagenesis at position K121 is more effective and creates more diversity than the mutations in position L124. It is tempting to speculate that this effect may be due to the influence of the K121X side chains both on the piano-stool moiety ($K121X_A$)

and on the trajectory of the incoming prochiral substrate ($K121X_B$, see Figure 3). In the case of the dialkyl substrate, this latter contact may be crucial, as it provides a second coordination sphere interaction with the substrate, reminiscent of natural enzymes. Saturation mutagenesis at this position affords the best ee's for the aliphatic ketone (Table 7, entries 4-5 and 9-10, ee's up to 82% (*R*) and 62% (*S*) using immobilized catalysts).

A noteworthy exception however is the conservative mutation L124V, which gives the best (*R)*-selectivity for the reduction of substrate **2** with [η^6-(*p*-cymene)Ru(**Biot-*p*-L**)Cl] ⊂ L124V Sav (83% ee (*R*), Table 7, entry 3). In comparison, the best single mutant at position 121 is [η^6-(benzene)Ru(**Biot-*p*-L**)Cl] ⊂ K121R (also a conservative mutation) and affords 64% ee (*S*) for the reduction of **2** (Table 7, entry 14).

Table 7. Selected results for the designed optimization of the reduction of ketones **2** and **6** in the presence of biotin-sepharose-immobilized artificial metalloenzymes [η^6-(arene)Ru(**Biot-*p*-L**)Cl] ⊂ Sav mutant.

Entry	η^6-(arene)	Sav isoform	Substrate	Conv. (%)	ee (%)
1	benzene	S112A-K121W	**2**	89	16 (*R*)
2	benzene	S112A-K121W	**6**	86	80 (*R*)
3	*p*-cymene	L124V	**2**	90	83 (*R*)
4	*p*-cymene	S112A-K121T	**6**	84	82 (*R*)
5	benzene	S112A-K121N	**6**	95	62 (*S*)
6	*p*-cymene	S112A-K121N	**6**	81	58 (*R*)
7	benzene	S112A-K121N	**2**	99	55 (*S*)
8	*p*-cymene	S112A-K121N	**2**	63	50 (*R*)
9	*p*-cymene	S112A-K121F	**6**	96	73 (*R*)
10	*p*-cymene	S112A-K121V	**6**	92	68 (*R*)
11	*p*-cymene	S112A-K121V	**2**	73	66 (*R*)
12	benzene	S112A-K121C	**2**	63	63 (*S*)
13	benzene	S112K-L124H	**2**	64	59 (*S*)
14	benzene	K121R	**2**	96	64 (*S*)

1.3.5 Evaluation of Homogeneous Purified Sav Isoforms on Representative Substrates

The best results using the immobilized hybrid catalysts were subsequently reproduced using the purified Sav mutant in a homogeneous phase and, as expected, some increase in ee and conversion could be observed in almost all cases (Table 8, entries 1-7).

An interesting behaviour could be seen in the case of some proteins bearing mutations in position 121, which afforded opposite enantioselectivities when pure protein was used instead of the immobilized form. The most striking examples are the Sav mutants bearing the K121G mutation (Table 8, entries 8-9), which invert the enantioselectivity in combination with [η^6-(*p*-cymene)Ru(**Biot-*p*-L**)Cl]. It is tempting to speculate that the presence of the sepharose perturbs the spatial arrangement of the bulky [η^6-(*p*-cymene)Ru(**Biot-*p*-L**)Cl] within these mutants. These results also implicate the residue 121 in the enantioselection process.

Table 8. Selected results for the designed optimization of the reduction of ketones **2** and **6** in the presence of immobilized- and purified artificial metalloenzymes [η^6-(arene)Ru(**Biot-*p*-L**)Cl] ⊂ Sav mutant.

Entry	η^6-(arene)	Sav isoform	Substrate	ee (conv.) (%)	
				Immobilized Sav (from cell extract)	Pure non-immobilized Sav
1	*p*-cymene	L124V	**2**	83 (90)	91 (96)
2	benzene	S112A-K121N	**2**	-55 (99)	-75 (98)
3	benzene	S112K-L124H	**2**	-59 (64)	-65 (94)
4	benzene	K121R	**2**	-64 (96)	-68 (95)
5	*p*-cymene	S112A-K121T	**6**	82 (84)	88 (99)
6	benzene	S112A-K121W	**6**	80 (86)	84 (99)
7	benzene	S112A-K121N	**6**	-62 (95)	-72 (100)
8	*p*-cymene	S112A-K121G	**2**	-43 (97)	38 (66)
9	*p*-cymene	K121G	**6**	-31 (73)	23 (20)
10	*p*-cymene	S112K-K121C	**2**	-11 (91)	41 (68)

The reconstructed evolutionary path of the best (*R*)- and (*S*)-selective hybrid catalysts for the reduction of 4-phenyl-2-butanone **6** is sketched in Figure 7. It is interesting to note that the most selective artificial enzymes identified for this dialkyl ketone substrate ([η^6-(*p*-

cymene)Ru(**Biot-*p*-L**)Cl] ⊂ S112A-K121T Sav and ([η^6-(benzene)Ru(**Biot-*p*-L**)Cl] ⊂ S112A-K121N Sav) are reached by an evolutionary path involving a combination of two poorly adapted mutations that would not normally be selected individually. Screening for enantioselectivity likely optimizes second coordination sphere interactions between substrate and protein, exerting an evolutionary pressure toward substrate specialization.

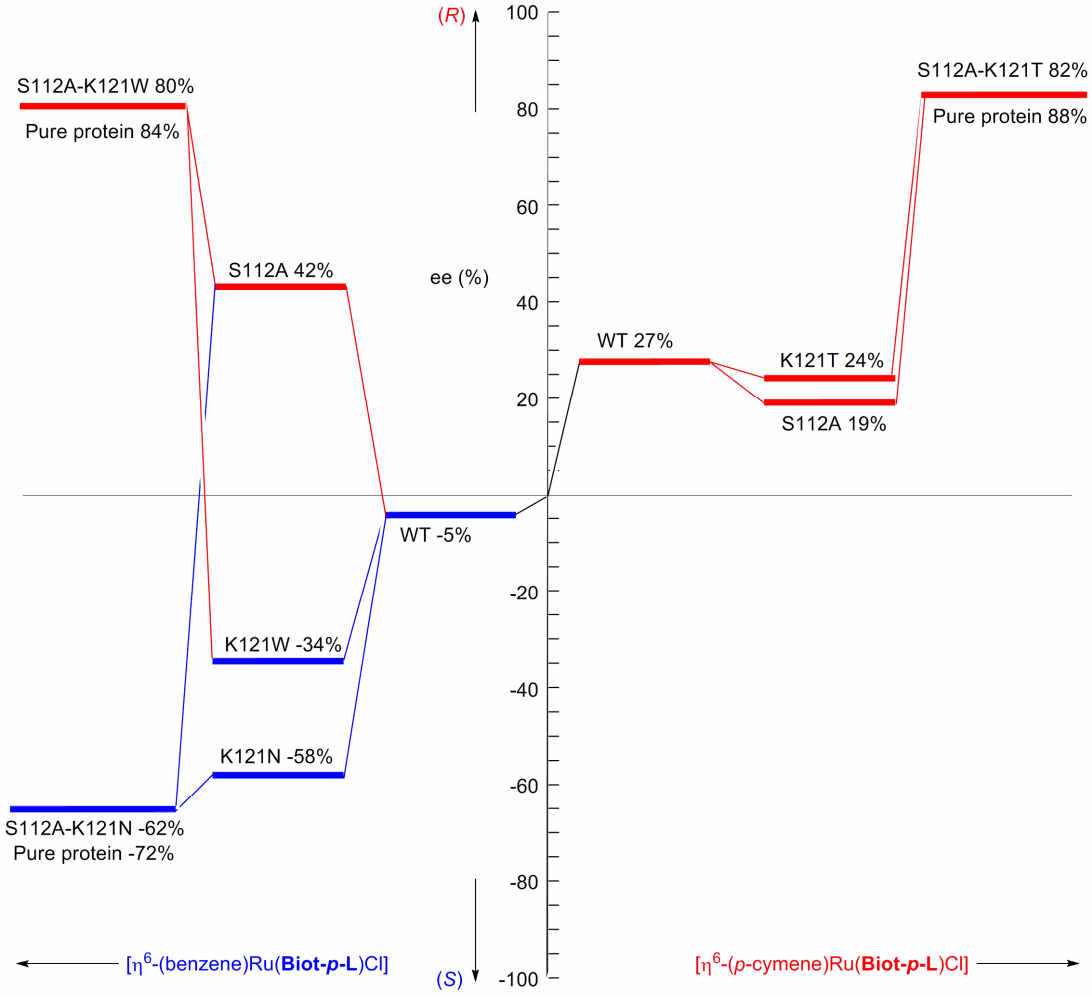

Figure 7. Reconstructed evolutionary path of the best (*R*)- and (*S*)-selective immobilized hybrid catalysts for the reduction of 4-phenyl-2-butanone **6**. Only the mutations present in the best double mutants are listed. The results obtained with the best purified double mutants are also shown.

The most efficient protein–Ru complexes were subsequently evaluated with the representative substrates **2-8**. Using the [η^6-(*p*-cymene)Ru(**Biot-*p*-L**)Cl] ⊂ S112A-K121T Sav combination, the aliphatic ketones **7** and **8** were reduced with good enantioselectivities (ee's up to 90% (*R*) for substrate **7** and 46% (*R*) for substrate **8**, Table 9, entries 1-2). A very surprising result was obtained for substrate **8** with the (*S*)-selective artificial enzyme [η^6-

(benzene)Ru(**Biot-*p*-L**)Cl] ⊂ S112A-K121N Sav, which afforded an unexpectedly high (*R*)-selectivity in this case (Table 9, entry 3). As expected, the deactivated *p*-methylacetophenone **3** afforded the highest ee with the best artificial metalloenzyme identified for the aromatic substrates, [η^6-(*p*-cymene)Ru(**Biot-*p*-L**)Cl] ⊂ L124V Sav (Table 9, entry 4).

Furthermore, using [η^6-(benzene)Ru(**Biot-*p*-L**)Cl] ⊂ S112A-K121N Sav, which is the most (*S*)-selective combination identified during the second round of screening with *p*-bromoacetophenone **2**, the aromatic ketones α-tetralone **4** and 2-acetylpyridine **5** were both reduced with 92% (*S*) (Table 9, entries 5-6). The designed evolution protocol allows the (*S*)-selectivity for the reduction of aromatic substrates to be increased from 70% to 92% for substrate **5**.

Interestingly, while methyl alkyl and methyl aryl ketones afford good levels of conversion and selectivity, ketones **4** and **8**, bearing a longer alkyl group give comparatively modest conversions (Table 9, entries 2 and 6-7), suggesting that such artificial metalloenzymes will have to be further evolved to display high substrate specificity. This specific behaviour is similar to yeast alcohol dehydrogenase, which in general only accepts aldehydes and methyl ketones as substrates.

Table 9. Selected results for the transfer hydrogenation of representative ketones **2-8** with purified homogeneous (*R*)- and (*S*)-selective artificial metalloenzymes [η^6-(arene)Ru(**Biot-*p*-L**)Cl] ⊂ Sav mutant, identified during the designed optimization step.

Entry	η^6-(arene)	Sav isoform	Substrate	Conv. (%)	ee (%)
1	*p*-cymene	S112A-K121T	**7**	100	90 (*R*)
2	*p*-cymene	S112A-K121T	**8**	50	46 (*R*)
3	benzene	S112A-K121N	**8**	63	80 (*R*)
4	*p*-cymene	L124V	**3**	97	96 (*R*)
5	benzene	S112A-K121N	**5**	100	92 (*S*)
6	benzene	S112A-K121N	**4**	54	92 (*S*)
7	*p*-cymene	L124V	**4**	20	87 (*R*)

In an attempt to further optimize these results, we combined the best Sav isoforms identified during the designed evolution step (S112A-K121T and L124 Sav) with the P64G mutation, previously identified as drastically improving the (*R*)-selectivity (Section 1.1 and Table 10, entries 1-2). While no triple mutant P64G-S112A-K121T Sav could be produced,

the double mutant P64G-L124V Sav afforded high production levels and could be easily purified in milligram quantities. Its evaluation in combination with [η^6-(*p*-cymene)Ru(**Biot-*p*-L**)Cl] for the transfer hydrogenation of aromatic substrates afforded the highest levels of selectivity obtained with the artificial metalloenzymes (Table 10, entries 5-6).

Table 10. Comparison of the results obtained with purified homogeneous Sav isoforms bearing P64G and / or L124V simple or double mutation for the transfer hydrogenation reaction.

Entry	η^6-(arene)	Sav isoform	Substrate	Conv. (%)	ee (%)
1	*p*-cymene	P64G	**2**	97	89 (*R*)
2	*p*-cymene	P64G	**3**	92	94 (*R*)
3	*p*-cymene	L124V	**2**	96	91 (*R*)
4	*p*-cymene	L124V	**3**	97	96 (*R*)
5	*p*-cymene	P64G-L124V	**2**	96	94 (*R*)
6	*p*-cymene	P64G-L124V	**3**	98	98 (*R*)

1.4 Concluding Remarks

In summary, identification of (*R*)- and (*S*)-selective artificial metalloenzymes by a chemogenetic optimization procedure and the information provided by the structural characterization of [η^6-(benzene)Ru(**Biot-*p*-L**)Cl] ⊂ S112K Sav has allowed us to implement a designed evolution protocol for the optimization of artificial transfer hydrogenases. The method is based on the combination between rational and combinatorial modifications, *i.e.* the mutation sites can be identified from the X-ray structure and the most efficient residues are selected after screening of the enzyme variants obtained by saturation mutagenesis.

A straightforward optimization step, performed on crude cellular extracts, allowed the discovery of [η^6-(*p*-cymene)Ru(**Biot-*p*-L**)Cl] ⊂ S112A-K121T Sav for the enantioselective reduction of dialkyl ketones. While a single point mutation is sufficient to generate selective catalysts for the aromatic ketones (>90% ee), double mutants obtained by the designed evolution protocol are required to identify hybrid catalysts for the reduction of dialkyl substrates (up to 90% (*R*)).

2 Sulfoxidation

2.1 Hybrid Catalysts Based on the Biotin-Streptavidin System

Among the metal catalysts for sulfide oxidations, titanium-based complexes are the most famous and have found the most applications in industry.[103] However, these systems require careful control of the amount of water in the reaction and thus are difficult to use for the construction of artificial metalloenzymes.

Salen-based complexes form another class of catalysts that has received considerable attention in the context of catalytic oxidation. Although their application in asymmetric sulfoxidation is limited, manganese- and chromium-salen derivatives are water compatible and have already been used in the context of artificial metalloenzymes as mimics of heme, the native co-factor of myoglobin.[150,156]

Inspired by these systems, we envisaged the creation of streptavidin-based artificial metalloenzymes for sulfoxidation reactions using achiral biotinylated Mn-salen complexes. Our choice was also motivated by the proposed mechanism of the oxidation reactions catalyzed by Mn- or Cr-complexes, which does not require binding of the substrate to the metal (see Chapter 1, Section 2.2.1.2). Hence, the chiral environment provided by the protein could have a determinant influence on the transition state.

For this purpose, four biotinylated Schiff base tetradentate ligands have been synthesised in collaboration with Miss Déborah Mathis (diploma student at the University of Neuchâtel) and their Mn complexes formed *in situ* were tested for activity in the sulfoxidation of thioanisole.

2.1.1 Biotinylated Salen Ligands

The biotinylated ligands were designed to offer a large structural diversity to maximize the possible interactions upon incorporation into Sav. The ligand type (aromatic or aliphatic imines), the biotin anchor position (on the diimine backbone or on the 2-hydroxybenzaldehyde moiety), and the spacer between the biotin and the coordinating moiety were varied and the four achiral salen ligands **Sal-1** – **Sal-4** were synthesized (Scheme 7).

The ligands were prepared by condensation of the appropriate diamine with the corresponding 2-hydroxybenzaldehydes. 3,5-Di-*tert*-butyl-2-hydroxybenzaldehyde was used to form the symmetric diimines **Sal-1**, **Sal-3** and **Sal-4** and the biotin anchor was attached to the diamine component before (**Sal-1**) or after Schiff base formation (**Sal-3**, **Sal-4**). The non-

symmetric diimine **Sal-2** was obtained in modest yield mixing ethylenediamine, 3,5-di-*tert*-butyl-2-hydroxybenzaldehyde and the aldehyde bearing the biotin anchor. The complete description of these syntheses can be found in Chapter 4, Section 4.

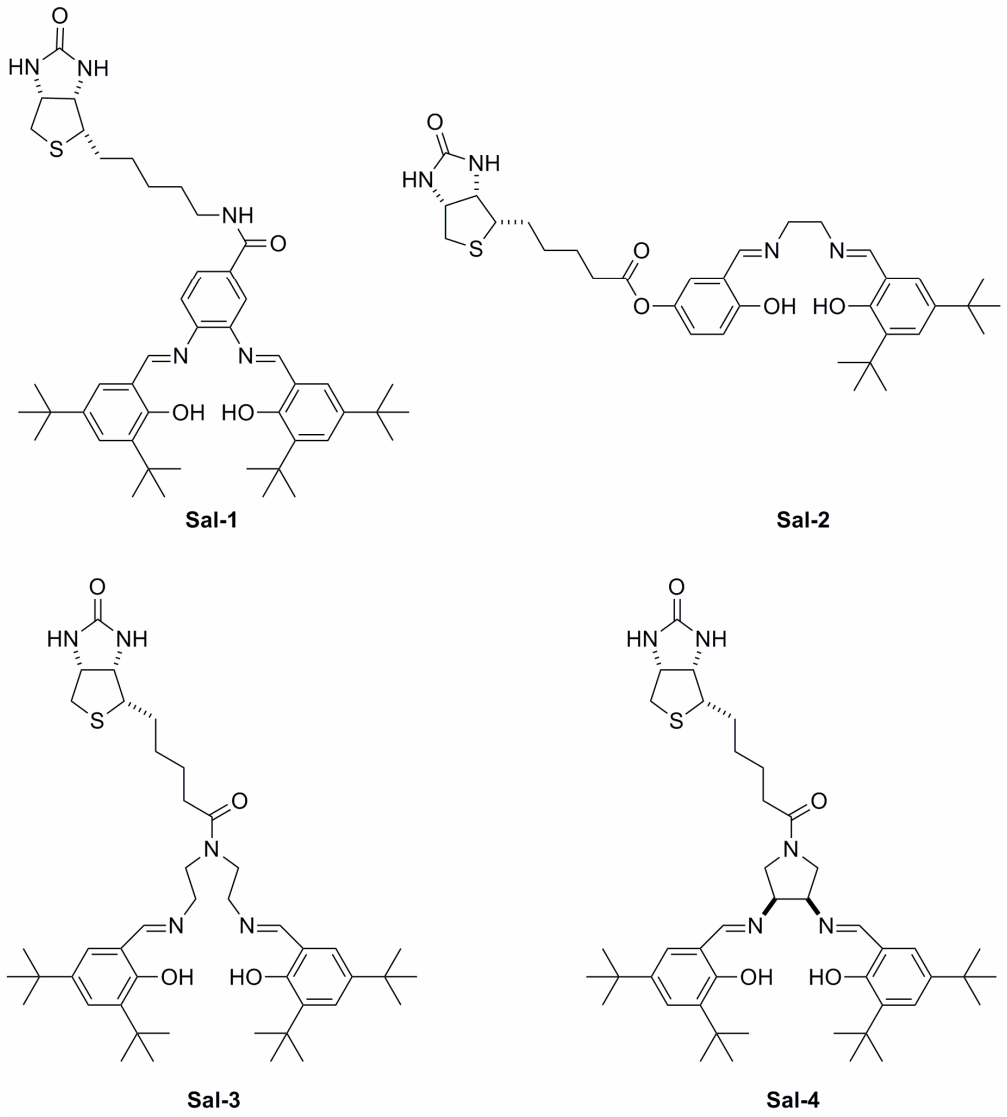

Scheme 7. Biotinylated salen ligands **Sal-1** – **Sal-4** used in this study.

2.1.2 Activity of the Manganese-Salen Complexes

The Mn complexes of **Sal-1** – **Sal-4**, abbreviated hereafter **Sal-X**, were evaluated for the sulfoxidation of thioanisole **9** (Scheme 8). Except for Mn-**Sal-4**, synthesised by treatment with manganese acetate, $Mn(OAc)_2 \cdot 4H_2O$, followed by ligand exchange with NaCl (replacement of acetate by the chloride ion) and purification on silica gel, the other Mn complexes were prepared *in situ* by reaction with $Mn(OAc)_2 \cdot 4H_2O$.

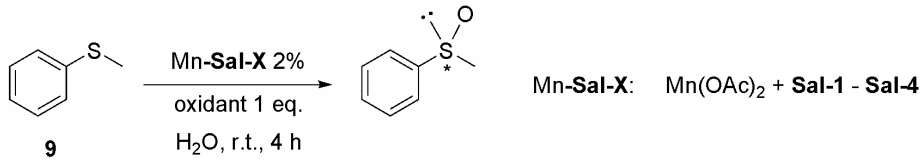

Scheme 8. Sulfoxidation of thioanisole **9** catalyzed by Mn-**Sal-1** – Mn-**Sal-4**.

Several oxidants have been reported to perform the oxidation of sulfides catalyzed by Mn-salen complexes. One of the problems associated with the reaction is the uncatalyzed oxidation (background reaction) leading to racemic sulfoxides. Therefore, before performing the activity tests for the new complexes, we evaluated the extent of the background reaction for the sulfoxidation of thioanisole **9** in water. While NaOCl, $NaIO_4$ and $PhI(OAc)_2$ were found to be very powerful oxidants in the absence of catalyst (Table 11, entries 1-3), PhIO was not suitable for oxidation in water because of its lack of solubility (Table 11, entry 4). Hydrogen peroxide (H_2O_2) was therefore chosen as the most appropriate reagent for future experiments (Table 11, entry 5).

Table 11. Extent of the background reaction using different oxidants and activity of the Mn-**Sal-X** complexes for the sulfoxidation of thioanisole.[a]

Entry	Catalyst	Oxidant	Solvent	Conv. (%)
1	-	NaOCl	H_2O	89
2	-	$NaIO_4$	H_2O	84
3[b]	-	$PhI(OAc)_2$	H_2O	80
4[b]	-	PhIO	H_2O	10
5	-	H_2O_2	H_2O	10
6[c]	Mn-**Sal-1**	H_2O_2	H_2O	44
7[c]	Mn-**Sal-2**	H_2O_2	H_2O	38
8[c]	Mn-**Sal-3**	H_2O_2	H_2O	19
9	Mn-**Sal-4**	H_2O_2	H_2O	10
10	Mn-**Sal-4**	H_2O_2	H_2O / EtOH 1 / 1	50

[a] Reaction conditions: 1-1.5% DMF in H_2O; thioanisole **9** 0.01 M; Mn 2% (if required); oxidant 1 eq.; room temperature; 4 h.
[b] 1% DMF and 4% MeOH in H_2O
[c] Thioanisole 0.005 M.

In combination with H_2O_2, the Mn-**Sal-X** complexes showed modest activities (Table 11, entries 6-9). Since these compounds were poorly soluble in water, the experiments were

repeated in a H_2O / EtOH 1 / 1 mixture, thus yielding reasonable activities (Table 11, entry 10). Reasoning that incorporation into Sav would solve the problem of solubility, we proceeded to testing these catalysts in the presence of host protein.

2.1.3 Sulfoxidation Tests in the Presence of Streptavidin

The four biotinylated Mn complexes were tested in the presence of several Sav isoforms and the best results are listed in Table 12. The choice of the Sav mutants was based exclusively on their availability in the laboratory.

A slight decrease in conversion was obtained with the catalysts in the presence of Sav, except for Mn-**Sal-4**, which was more active when incorporated into Sav. It is known that addition of coordinating ligands such as imidazole or pyridines in the axial position of the metal-complex can be beneficial for the Mn-catalyzed reactions with H_2O_2.[188,189] However, the activities of the biotinylated catalysts remained low, even upon addition of such ligands to the reaction mixture (Table 12, entries 7-8). Very modest enantioselectivities were obtained (maximum 13% ee (*R*), Table 12, entry 2).

Table 12. Selected results obtained for the sulfoxidation of thioanisole with Mn-**Sal-X** in presence of Sav.[a]

Entry	Sav mutant	Complex	Additive	Conv. (%)	ee (%)
1	S112D Sav	Mn-**Sal-1**	-	30	1 (*S*)
2	S112D Sav	Mn-**Sal-2**	-	32	13 (*R*)
3	S112D Sav	Mn-**Sal-3**	-	3	0
4	S112D Sav	Mn-**Sal-4**	-	25	5 (*S*)
5[b]	WT Sav	Mn-**Sal-4**	-	21	6 (*R*)
6[b]	S112G Sav	Mn-**Sal-4**	-	34	11 (*S*)
7	S112D Sav	Mn-**Sal-2**	pyridine-*N*-oxide	36	13 (*R*)
8	S112D Sav	Mn-**Sal-2**	*N*-methylimidazole	35	11 (*R*)

[a] Reaction conditions: 1.5% DMF in H_2O; Sav 0.00003 M; Mn-**Sal-X** 0.0001 M; thioanisole **9** 0.005 M; H_2O_2 0.005 M; additive 0.0002 M; room temperature; 4 h.
[b] Thioanisole 0.01 M; H_2O_2 0.01 M.

In this context, we reasoned that the Mn-based complexes are maybe not very appropriate for creating Sav-based artificial metalloenzymes, as their activity under the required reaction conditions is very modest. In our search for active catalysts for sulfoxidation in water, we turned our attention towards other metal-based oxidation systems.

2.2 Incorporation of the Vanadyl Ion into Streptavidin

2.2.1 Preliminary Tests: Vanadium-Salen Complexes

Vanadium-salen systems have been shown to catalyze sulfoxidation reactions in the presence of cumyl hydroperoxide.[87] In addition, sulfoxidations with vanadium complexes have been reported using tridentate Schiff base ligands with H_2O_2, suggesting that the catalytic system is active in the presence of water.[111] Moreover, the peroxidase activity of vanadium-containing enzymes has been studied in detail, showing that vanadium bound to ligands with O- and N-donors can catalyze oxygen transfer in water using peroxides as stoichiometric oxidants.[190]

In the light of these examples, we considered the creation of artificial metalloenzymes using the biotinylated **Sal-X** ligands in conjunction with vanadium. Several Sav mutants were employed in this preliminary test. To our satisfaction, oxidation of thioanisole **9** with the salophen derivative V-**Sal-1** in the presence of S112D Sav and *tert*-butyl hydroperoxide (*t*-BuOOH) as stoichiometric oxidant afforded methyl-phenylsulfoxide in 26% ee (*R*) (Table 13, entry 1). The four biotinylated V complexes, formed *in situ* by mixing the appropriate biotinylated ligand with vanadyl acetylacetonate, $VO(acac)_2$, in organic solvent, afforded similar results in the presence of S112D, S112V or S112T Sav mutants (Scheme 9 and Table 13, entries 1-6).

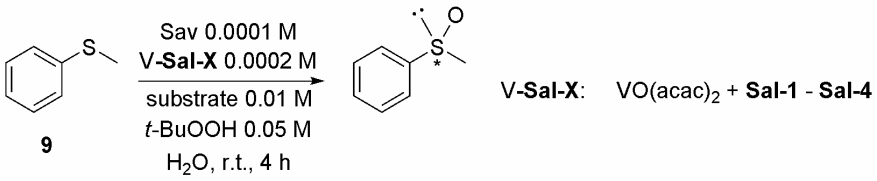

Scheme 9. Sulfoxidation of thioanisole **9** in the presence of Sav, V-**Sal-X** and *t*-BuOOH.

It is interesting to note that, irrespectively of the Sav mutant or of the biotinylated ligand used, the (*R*) enantiomer is always obtained (Table 13, entries 1-6). Moreover, the variation in ee is very small (within experimental error). This result is quite surprising, since previous results obtained in hydrogenation[175] and transfer hydrogenation reactions (Section 1 of this chapter) have shown that chemical diversity is associated with diversity in selectivity. Consequently, we envisaged the possibility that the V complexes dissociate in the presence of streptavidin, to form the same catalytic species in all the cases.

To test this hypothesis, we investigated the sulfoxidation of thioanisole with $VO(acac)_2$ incorporated into Sav in the absence of biotinylated ligand, using *t*-BuOOH as the

stoichiometric oxidant. Indeed, the reaction proceeded in an enantioselective manner (Table 13, entries 7-8). Comparable results were obtained when $VOSO_4$ was used, in which the vanadium moiety is devoid of chelating organic ligands (Table 13, entry 9). Hence, we hypothesized that the species interacting with Sav is an aqueous form of the vanadyl ion, $[VO]^{2+}$. WT Sav afforded similar results (Table 13, entry 10). In the absence of protein, the racemic sulfoxide was obtained with reasonable conversion (Table 13, entry 11).

Table 13. Selected results obtained for the sulfoxidation of thioanisole in the presence of Sav mutant, **V-Sal-X** and *t*-BuOOH.[a]

Entry	V complex	Sav mutant	Conv. (%)	ee (%)
1	V-**Sal-1**	S112D Sav	80	26 (*R*)
2	V-**Sal-1**	S112V Sav	98	34 (*R*)
3	V-**Sal-2**	S112D Sav	98	29 (*R*)
4	V-**Sal-3**	S112V Sav	100	32 (*R*)
5	V-**Sal-4**	S112D Sav	91	35 (*R*)
6	V-**Sal-4**	S112T Sav	91	31 (*R*)
7	$VO(acac)_2$	S112D Sav	99	34 (*R*)
8	$VO(acac)_2$	S112V Sav	100	35 (*R*)
9	$VOSO_4$	S112V Sav	100	40 (*R*)
10	$VOSO_4$	WT Sav	98	36 (*R*)
11	$VOSO_4$	-	88	-

[a] Reaction conditions: 1% DMF and 1.3% EtOH in H_2O; Sav 0.0001 M, V 0.0002 M, thioanisole 0.01 M, *t*-BuOOH 0.05 M, room temperature, 4 h.

2.2.2 Vanadyl Ion as Biotin Mimic

Two possibilities could be envisaged for the association of the vanadyl ion to streptavidin: non-specific binding to coordinating residues at the surface of the protein (*e.g.* glutamic or aspartic acid) or specific incorporation into a suitable binding site.

In this context, we reasoned that such a small polar coordination compound could be incorporated with reasonable affinity inside the biotin binding pocket of streptavidin. Indeed, besides biotin, the deep cavity of Sav can bind, albeit with significantly reduced affinity, a variety of ligands, including HABA, ANS, different oligopeptides etc.[164,168,169,174] In apo-streptavidin (Sav devoid of biotin), several water molecules occupy the binding site and their positioning is very similar to the shape of the biotin molecule. This network of water

molecules is displaced upon biotin binding.[172,173] Therefore, we envisaged that a hydrated vanadyl ion could interact with the biotin-binding residues via hydrogen bonds (Scheme 10). Another option for specific vanadyl binding to streptavidin would be interactions with coordinating residues *via* first coordination sphere contacts.

In terms of enantioselection, binding of the catalytically active vanadyl ion to the biotin-binding pocket of streptavidin could provide an asymmetric environment for the approach of the substrate during the sulfoxidation process. In addition, the presence of hydrophobic residues may favour substrate accumulation within the cavity, resulting in increased turnover rates for the catalyzed reaction (Scheme 10).

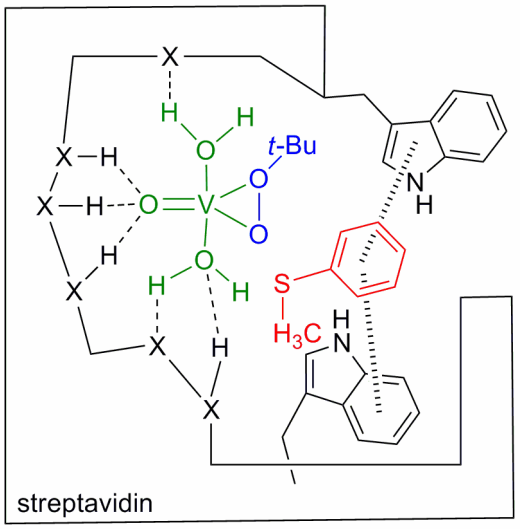

Scheme 10. Schematic representation of possible interactions during the sulfoxidation of thioanisole catalyzed by vanadyl incorporated into streptavidin.

Having discovered a promising system for the enantioselective oxidation of sulfides, we proceeded with a systematic study to identify the best conditions and to optimize the selectivity of this new artificial metalloenzyme.

2.2.3 Optimization of the Reaction Conditions

With the aim of identifying suitable reaction conditions, thioanisole **9** was selected as a model substrate for the enantioselective sulfoxidation using a V precursor in conjunction with Sav. The influence of several parameters (pH, V source, oxidant, V / Sav ratio) on the selectivity and activity of the catalyst was tested. The reactions were performed at 0.01 M substrate concentration for 4 h – in most of the cases no further conversion was observed after this time – and the occurrence of minimal background reaction – non-catalytic oxidation performed by

t-BuOOH – was checked. Very little overoxidation to the corresponding sulfone could be detected by HPLC (< 2%).

2.2.3.1 pH and Buffer System

The reaction of the vanadyl ion, $[VO]^{2+}$, with hydroperoxides is known to be pH-dependent.[191] Low pH is usually required for the oxidation to take place. When $VOSO_4$ in the presence of WT Sav was used with *t*-BuOOH for the sulfoxidation of thioanisole, high activities were obtained at acidic to neutral pH (pH range 3-7), while a decrease in selectivity was observed above pH 3 (Figure 8). At this pH, the major species present in an aqueous 0.0001 M vanadyl solution is $[VO(H_2O)_5]^{2+}$.[190] In this first screen, a small excess of Sav binding sites *vs.* V was employed (1.2 *vs.* 1).

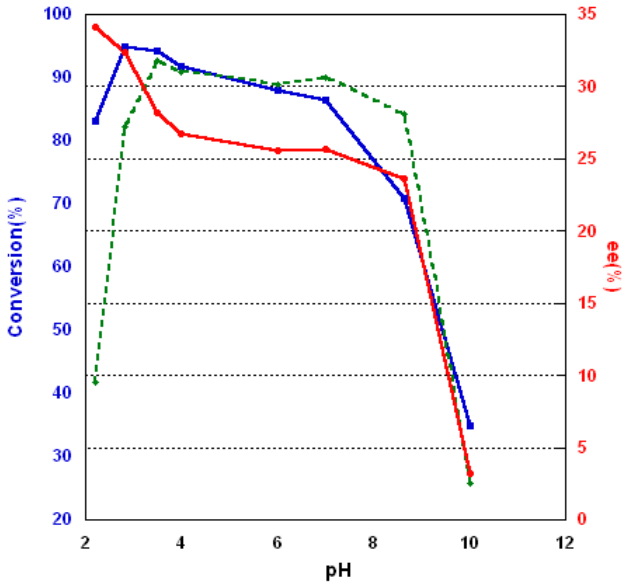

Figure 8. pH-dependence profile of the activity (■) and of the selectivity (●) obtained for the sulfoxidation of thioanisole with $VOSO_4$ in conjunction with WT Sav. For comparison, the activity of free $VOSO_4$ (♦) is represented by the dotted line. Reaction conditions: 2.3% EtOH; WT Sav 0.00003 M, $VOSO_4$ 0.0001 M, thioanisole 0.01 M, *t*-BuOOH 0.05 M; room temperature; 4 h; pH of the solutions adjusted with HCl or NaOH.

Next, we studied the influence of the buffer on the activity and the selectivity of the asymmetric sulfoxidation reaction. Different buffer systems around pH 3 were tested, and the best result was obtained using HCl / KCl buffer (buffering range 1.0-2.2)[192] at 0.05 M and pH 2.2 (Table 14).

Table 14. Influence of the buffer system on the activity and selectivity for the sulfoxidation of thioanisole by $VOSO_4$ in conjunction with WT Sav.[a]

Entry	Buffer system	pH	Conv. (%)	ee (%)
1	HCl / KCl	2.2	77	33 (*R*)
2	Citric acid / Sodium citrate	3	4	0
3	Glycine / HCl	3	90	28 (*R*)
4	Phtalic acid / Potassium phthalate	3	84	7 (*R*)
5	Formic acid / Sodium formate	3	92	26 (*R*)
6	Acetic acid / Sodium acetate	3.5	94	27 (*R*)
7	HCl / KCl[b]	2.2	82	35 (*R*)

[a] Reaction conditions: 2.3% EtOH in 0.1 M buffer; WT Sav 0.00003 M; $VOSO_4$ 0.0001 M; thioanisole 0.01 M; *t*-BuOOH 0.05 M; room temperature; 4 h.
[b] Buffer at 0.05 M.

2.2.3.2 Vanadium / Streptavidin Ratio

To gain some insight into the stoichiometry of vanadyl-binding to streptavidin, we studied the variation of the enantioselectivity as a function of the V / WT Sav binding site ratio. Increasing the number of V equivalents *vs.* Sav binding sites leads to a decrease in the ee value (Figure 9). Interestingly, the ee is not constant when an excess of binding sites *vs.* V is used (V / WT Sav binding sites ratio < 1), suggesting that not all the V-catalyst is incorporated into the Sav binding sites under these conditions.

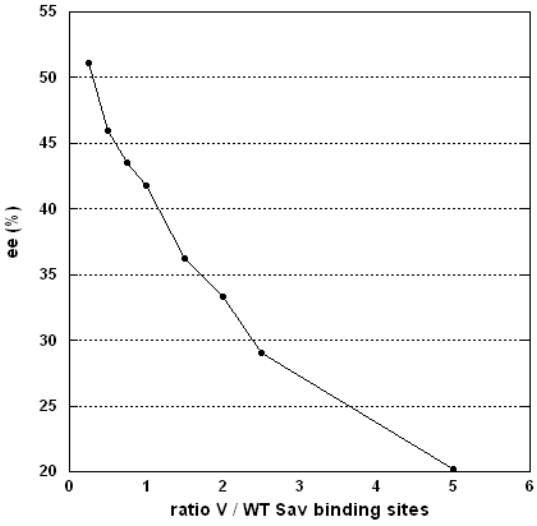

Figure 9. Variation of the selectivity for the sulfoxidation of thioanisole in function of the V / WT Sav binding sites ratio. Reaction conditions: 2.3% EtOH in HCl / KCl 0.05 M buffer at pH 2.2; WT Sav variable concentration; $VOSO_4$ 0.0002 M, thioanisole 0.01 M, *t*-BuOOH 0.05 M; room temperature; 4 h.

Moreover, variation of the catalyst loading from 1% to 3%, while keeping the V / WT Sav binding sites ratio constant at 0.5 / 1 also affords a modest variation in ee (Table 15).

Table 15. Influence of the catalyst concentration on the activity and selectivity for the sulfoxidation of thioanisole by $VOSO_4$ in conjunction with WT Sav.[a]

Entry	V (mole %)	Conv. (%)	ee (%)
1	1 %	91	41 (*R*)
2	2 %	94	46 (*R*)
3	3 %	98	51 (*R*)

[a] Reaction conditions: 2.3% EtOH in HCl / KCl 0.05 M buffer at pH 2.2; $VOSO_4$ / WT Sav monomer ratio 0.5 / 1; thioanisole 0.01 M; *t*-BuOOH 0.05 M; room temperature; 4 h.

These results suggest that the enantioselectivity strongly depends on the concentration of both vanadium and streptavidin in the reaction mixture. Unlike in the case of biotin, the lower affinity of the vanadyl ion for Sav probably leads to partial formation of the artificial enzyme. At higher concentrations of the two species, the equilibrium is displaced towards vanadyl incorporation into Sav, thus leading to higher ee's.

2.2.3.3 Vanadium- and Oxygen Source

The influence of the V form on the reaction outcome was tested using four vanadyl precursors, bearing different ligands and the V atom in different oxidation states. $V^{IV}O(acac)_2$, $V^{IV}OSO_4$, $V^{V}O(O\textit{i}\text{-Pr})_3$ and $Na_3V^{V}O_4$ were used as catalyst precursors. The results obtained were similar (Table 16 entries 1-4), confirming our initial hypothesis that the catalytic species is the same, irrespective of the V precursor. Based on this observation and considering the speciation of vanadyl ions in acidic media,[190] we suggest that the V species interacting with Sav is the pentahydrated vanadyl ion, $[VO(H_2O)_5]^{2+}$.

During the reaction, the oxidant binds to vanadium, forming a V-peroxo complex.[77,193] The importance of the nature of the hydroperoxide in the selectivity of an asymmetric reaction has been pointed out and the results may be associated with the steric effect of the alkyl or aryl groups.[194] We reasoned that changing the oxidant might change the interaction of the peroxo complex with the protein or the substrate, thus influencing the selectivity. We observe a drop in both conversion and ee when changing the oxidant to hydrogen peroxide (HOOH), while cumyl hydroperoxide (cumylOOH) gives a slight inversion of selectivity for the oxidation of thioanisole (Table 16 entries 5-6).

Table 16. Influence of the vanadium source and of the oxidant on the activity and selectivity of the V-containing Sav in the sulfoxidation reaction of thioanisole.[a]

Entry	Vanadium source	Oxydant	Conv. (%)	ee (%)
1	$VOSO_4$	*t*-BuOOH	94	46 (*R*)
2	$VO(acac)_2$	*t*-BuOOH	99	46 (*R*)
3	$VO(Oi\text{-}Pr)_3$	*t*-BuOOH	99	46 (*R*)
4	Na_3VO_4	*t*-BuOOH	92	46 (*R*)
5	$VOSO_4$	HOOH[b]	39	0
6	$VOSO_4$	cumylOOH[b]	82	15 (*S*)

[a] Reaction conditions: 2.3% EtOH in HCl / KCl 0.05 M buffer at pH 2.2; WT Sav 0.0001 M; V 0.0002 M; thioanisole 0.01 M; *t*-BuOOH 0.05 M; room temperature; 4 h.
[b] Oxidant 0.01 M (to suppress the background reaction).

2.2.4 Scope of the Artificial Peroxidases

Under the previously optimized conditions using 2 mol % V and 1 mol % tetrameric WT Sav, the sulfoxidation of thioanisole **9** afforded the corresponding sulfoxide in 94% conversion and 46% ee (*R*) (Table 17, entry 1). In the absence of V, very little conversion was observed, while the activity of the Sav-free catalyst was only modest (Table 17, entries 2-3).

To investigate the substrate scope of the new artificial metalloenzyme (abbreviated hereafter $[VO]^{2+} \subset$ WT Sav), we tested prochiral sulfides **10**-**15** (Scheme 11), which are typical substrates for homogeneous sulfoxidation reactions.[117] Dialkyl sulfides **14** and **15** are particularly interesting, as the classic methods are usually limited to alkyl aryl sulfides.[117]

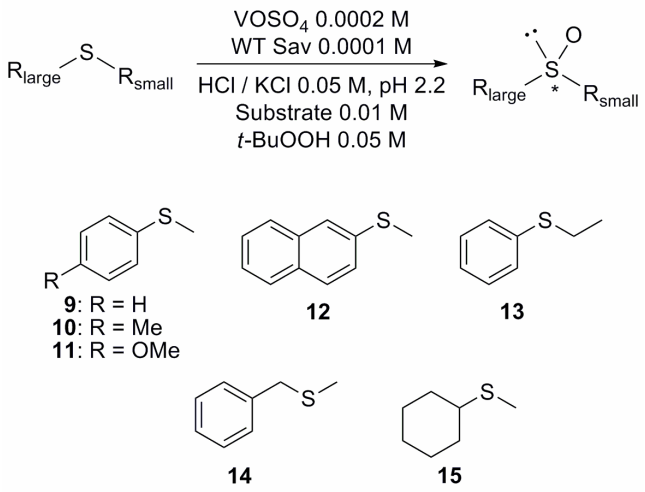

Scheme 11. Enantioselective sulfoxidation of prochiral sulfides **9**-**15** with the V-dependent artificial peroxidase.

For the aromatic sulfides, the sulfoxidation proceeds with high enantioselectivities (Table 17, entries 4-7). It is interesting to note that increasing the steric bulk of the aromatic moiety of the sulfide leads to an increase in selectivity: up to 93% ee for the sulfoxidation of methyl-2-naphthylsulfide **12**. However, the limited solubility of the substrate hampers complete conversion. Oxidation of dialkyl sulfides produces the corresponding sulfoxides with reasonable enantioselectivity (up to 86 % ee, Table 17, entries 8-9). For all substrates, very little overoxidation to the corresponding sulfone could be detected by HPLC (< 2%).

Table 17. Conversions and selectivities obtained in the $[VO]^{2+} \subset$ WT Sav-catalyzed sulfoxidation of substrates **9-15**.[a]

Entry	Catalyst	Substrate	Conv. (%)	ee (%)
1	$[VO]^{2+} \subset$ WT Sav	**9**	94	46 (*R*)
2	$[VO]^{2+}$	**9**	55	0
3	WT Sav	**9**	7	4 (*R*)
4	$[VO]^{2+} \subset$ WT Sav	**10**	96	87 (*R*)
5	$[VO]^{2+} \subset$ WT Sav	**11**	100	90 (*R*)
6	$[VO]^{2+} \subset$ WT Sav	**12**	53	93 (*R*)
7	$[VO]^{2+} \subset$ WT Sav	**13**	96	90 (*R*)
8	$[VO]^{2+} \subset$ WT Sav	**14**	100	73 (*R*)
9	$[VO]^{2+} \subset$ WT Sav	**15**	61	86 (*R*)

[a] Reaction conditions: 2.3% EtOH in HCl / KCl 0.05 M buffer at pH 2.2; WT Sav 0.0001 M; $VOSO_4$ 0.0002 M; substrate 0.01 M; *t*-BuOOH 0.05 M; room temperature; 4 h.

2.2.5 Exploring the Catalytic System

In the context of creation of catalytic activity from a non-catalytic protein, incorporation of the vanadyl ion into WT Sav appeared as an attractive idea for the development of new metalloenzymes. However, several questions arose regarding this system. Among these, our most important concern was: how does $[VO(H_2O)_5]^{2+}$ interact with Sav (first or second coordination sphere contacts are possible) and how specific is this interaction?

First, we proceeded to verify the initial hypothesis regarding the incorporation of the vanadyl ion into the biotin-binding pocket. Upon addition to the reaction mixture of 4.25 equivalents of biotin *vs.* tetrameric WT Sav, the sulfoxidation of *p*-methoxythioanisole **11** (the most active and selective substrate, Table 18, entry 1) afforded racemic product (Table 18,

entry 2). This result suggests that the reaction takes place in the proximity of the biotin-binding site.

Moreover, substituting streptavidin by avidin or bovine serum albumin (BSA) respectively afforded sulfoxidation products with very modest enantioselectivities (Table 18, entries 3-4). This suggests that Sav provides a specific binding site for the pentahydrated vanadyl ion.

Table 18. Catalysis results suggesting that the biotin-binding pocket of streptavidin specifically binds the vanadyl ion.[a]

Entry	Protein	Conv. (%)	ee (%)
1	WT Sav	100	90 (*R*)
2	Biotin (4.25 eq.) ⊂ WT Sav	96	0
3	Avidin	78	7 (*R*)
4	BSA	100	0

[a] Reaction conditions: 2.3% EtOH in HCl / KCl 0.05 M buffer at pH 2.2; protein 0.0001 M; $VOSO_4$ 0.0002 M; *p*-methoxythioanisole **11** 0.01 M; *t*-BuOOH 0.05 M; room temperature; 4 h.

Next, we proceeded to a closer investigation of the artificial enzyme, with the aim of elucidating critical aspects of the catalytic system: the coordination sphere around vanadium, the localization and geometry of the active site, the reaction kinetics and the binding affinity of the vanadyl ion to streptavidin.

2.2.5.1 EPR Studies

Electron paramagnetic resonance (EPR) spectroscopy is a technique for studying chemical species that have one or more unpaired electrons. The vanadyl ion – $[V^{IV}O]^{2+}$ – exhibits sharp eight-line EPR spectra, which are sensitive to the ligand environment around the $[VO]^{2+}$ group.This ion has therefore been used as a probe of the metal-binding sites of several proteins.[195-197] A marked pH-dependence of the EPR spectra is observed, due to different equilibria of $[VO]^{2+}$ in water.[198]

For the investigation of the coordination environment around $[VO]^{2+}$ ⊂ WT Sav, EPR experiments were performed with the help of Mrs. Carole Duboc at the University of Grenoble (FR), using $VOSO_4$ in the presence of WT Sav. At neutral pH, Sav-free and Sav-containing aqueous solutions of $VOSO_4$ show no EPR signal. This is not surprising, since it was shown that EPR inactive, probably polynuclear vanadium hydroxide species such as $VO(OH)_2$ form above pH 4.5.[198]

EPR experiments performed with $[VO]^{2+} \subset$ WT Sav at pH 2.2 (HCl / KCl buffer) yield a spectrum very similar to that of $[VO(H_2O)_5]^{2+}$ (Figure 10).[198] Frozen solutions of $[VO(H_2O)_5]^{2+}$ display powder pattern eight-line EPR spectra dominated by the hyperfine coupling of the vanadium ion (S = 1/2; I = 7/2). The spin Hamiltonian parameters used to simulate the experimental data are analogous to those found previously for $[VO(H_2O)_5]^{2+}$ (these calculations were performed by Mrs. Duboc),[199] suggesting that the first coordination sphere around vanadium does not change upon incorporation into Sav. Therefore, we hypothesize that $[VO(H_2O)_5]^{2+}$ interacts only via second coordination sphere contacts with the host protein.

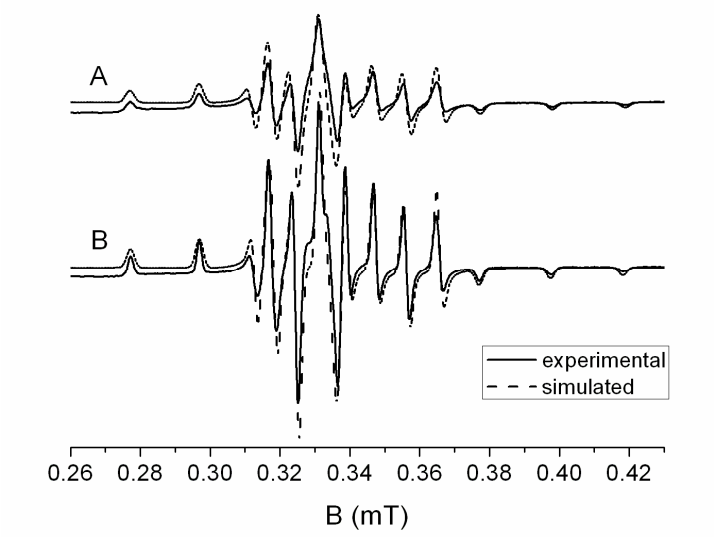

Figure 10. Frozen aqueous solution X-band EPR spectra (straight line) of $VOSO_4$ (A) and $VOSO_4 \subset$ WT Sav (B) in a 0.05 M HCl / KCl buffer solution at pH = 2.2. Experiment conditions: $VOSO_4$ 0.0002 M (A) and (B) and tetrameric WT Sav 0.0001 M (B). Powder simulation spectra (dotted line) have been calculated using the following EPR spin Hamiltonian parameters: (A) $g_{//} = 1.932$, $g_{\perp} = 1.978$, $A_{//} = 183$, $A_{\perp} = 70.10^{-4}$ cm^{-1}, $W_{//} = 22$, $W_{\perp} = 19$ G and (B) $g_{//} = 1.933$, $g_{\perp} = 1.976$, $A_{//} = 182$, $A_{\perp} = 69.10^{-4}$ cm^{-1}, $W_{//} = 25$, $W_{\perp} = 25$ G.

In nature, similar examples are provided by molybdate or tungstate anion-binding proteins, in which oriented hydrogen bonds provided by the protein play a major role in conferring exquisite specificity towards MO_4^{2-} (M = Mo, W).[200,201] Interestingly, the intensity of the EPR spectrum in the presence of Sav is noticeably higher than in its absence, suggesting a shielding of the vanadium complex within the binding site.

2.2.5.2 NMR Studies

Another spectroscopic technique used for the characterization of vanadium-containing compounds is ^{51}V NMR spectroscopy, which has become a routine tool for studying V^V complexes. By comparison with existing data, this technique can be used to predict the coordination environment around vanadium.[190]

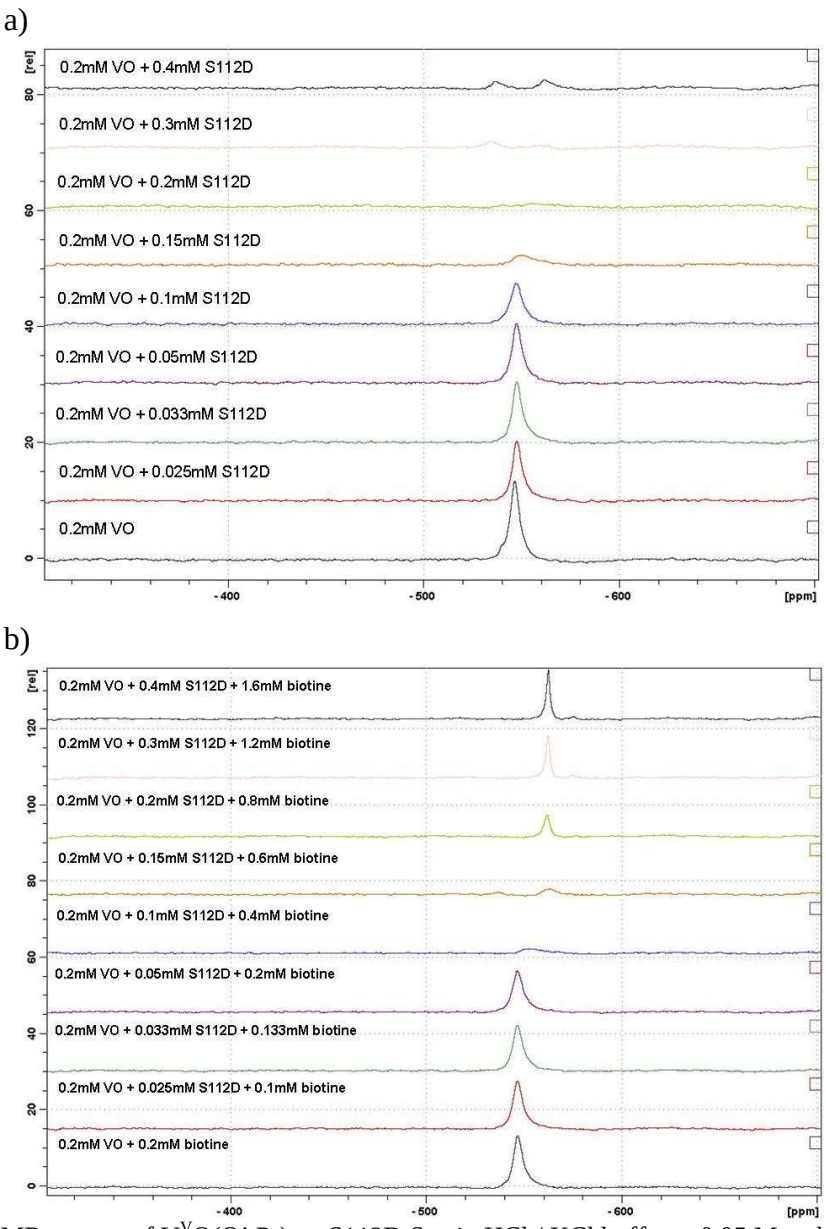

Figure 11. ^{51}V NMR spectra of $V^VO(Oi\text{-}Pr)_3 \subset$ S112D Sav in HCl / KCl buffer at 0.05 M and pH 2.2. a) Spectra obtained after gradual addition of S112D Sav to a solution of $V^VO(Oi\text{-}Pr)_3$; the final concentrations of $[VO]^{3+}$ and S112D Sav are indicated in mM; b) Spectra obtained after addition of 4 eq. of biotin *vs.* tetrameric Sav to the previously obtained solutions of $V^VO(Oi\text{-}Pr)_3 \subset$ S112D Sav; the final concentrations of $[VO]^{3+}$, S112D Sav and biotin are indicated in mM.

^{51}V NMR spectra were measured with the help of Dr. Julien Furrer at the University of Neuchâtel. Using $V^{V}O(O\textit{i}\text{-}Pr)_3$ in the presence of S112D Sav (this mutant was chosen for solubility reasons and affords similar conversion and ee, when compared to WT Sav) in HCl / KCl buffer at pH 2.2, a peak at -543 ppm was obtained, which was assigned to the $[VO(H_2O)_5]^{3+}$ species, by comparison with the spectrum of a Sav-free aqueous $V^{V}O(O\textit{i}\text{-}Pr)_3$ solution (Figure 11a).

Gradual addition of S112D Sav to a 0.0002 M solution of $V^{V}O(O\textit{i}\text{-}Pr)_3$ results in broadening of the signal and its disappearance starting with 0.15 mM concentration of tetrameric Sav (Figure 11a). It is known that the association of the ^{51}V nucleus with a large protein can broaden the signal width due to slow tumbling of the complex in a protein environment.[190] It is tempting to speculate that slow tumbling of $[VO(H_2O)_5]^{3+}$ is due to association with the protein. However, these results could not be used to study the binding of vanadyl to Sav, as no relation could be established between the concentration of S112D Sav and the area of the $[VO(H_2O)_5]^{3+}$ peak.

Interestingly, no significant shift in the ^{51}V signal was observed, suggesting that there are no changes in the first coordination sphere of vanadium.

Addition of biotin to the previous reaction mixtures was expected to restore the ^{51}V signal, as $[VO(H_2O)_5]^{3+}$ should be expelled from the binding cavity. Indeed, the ^{51}V signal reappears after biotin binding, although the integrated areas of the resulting peaks are much lower than before adding the biotin (Figure 11b) and the signal is slightly shifted. As a change in the tertiary and quaternary structure of tetrameric Sav occurs after biotin incorporation, binding of $[VO(H_2O)_5]^{3+}$ to a different location than in apo-Sav is possible. Yet, no clear conclusions can be drawn from these experiments.

2.2.5.3 Localization of the Binding Site: Docking Studies

In order to gain insight into the localization of $[VO(H_2O)_5]^{2+}$ within Sav, docking experiments were carried out in collaboration with Dr. Jaroslaw Panek at the University of Ljubljana (SLO).

Initial structures of streptavidin for the docking and further molecular dynamics modeling were based on the X-ray structures of WT Sav crystallized from a low-pH solution[202] and deposited in the PDB data bank with references 2IZC (apo-Sav at pH = 2.0) and 2IZG (biotin $\subset$ Sav complex at pH = 2.0). The two structures gave essentially the same results during the docking procedure.

Structures in which $[VO(H_2O)_5]^{2+}$ was docked outside the biotin-binding pocket were rejected from further consideration, based on the observation that $[VO(H_2O)_5]^{2+}$ in the presence of biotin-loaded Sav affords racemic sulfoxidation product. The remaining sets of coordinates (with $[VO(H_2O)_5]^{2+}$ inside the pocket) differed only slightly in orientation, but not position, of the $[VO(H_2O)_5]^{2+}$. The lowest energy docked structure was then tested for stability by molecular dynamics simulation using the full tetrameric form of Sav.

The optimized structure is depicted in Figure 12. As can be appreciated, residues critical for biotin binding (*i.e.* D128, N23, S27 and S45) are also involved in interactions with $[VO(H_2O)_5]^{2+}$. The pentahydrated vanadyl cation occupies the same position as biotin's urea group and the surrounding water molecules can act like H-donors / acceptors in interactions with binding site residues. Most importantly, the D128 residue, widely recognized as the most critical residue for biotin-Sav affinity,[172,203-205] displays the closest contact to $[VO(H_2O)_5]^{2+}$ in the docked structure.

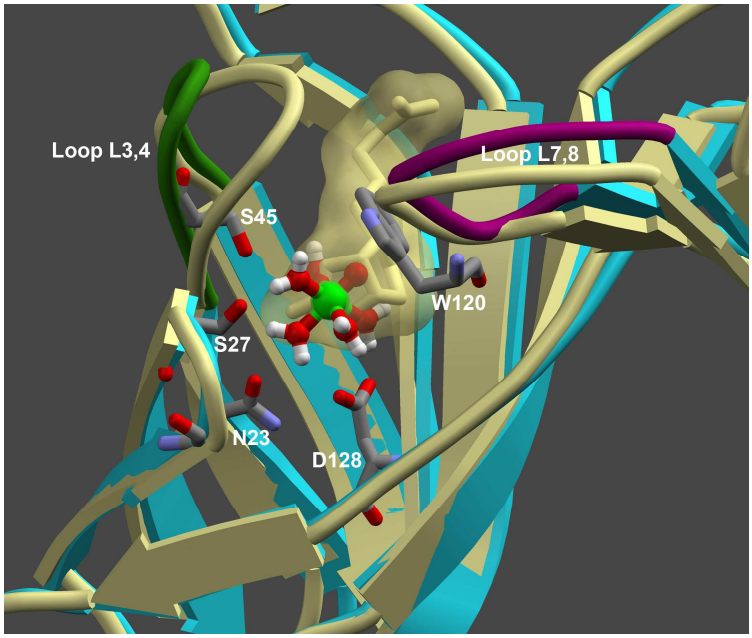

Figure 12. Superimposition of the docked structure $[VO(H_2O)_5]^{2+}$ (ball-and-stick representation) ⊂ WT Sav (monomers A and B, light blue schematic secondary structure) with the structure of biotin ⊂ WT Sav at pH = 2.0 (PDB reference code 2IZG; biotin: yellow stick, yellow transparent surface; monomers A and B: yellow schematic secondary structure). Close lying D128, N23, S27 and S45 residues are highlighted, as well as the residue W120 from the monomer B, which closes the biotin-binding site of the subunit A. Two neighbouring loops are also highlighted: the flexible L3,4 loop (residues 48-52, green) and the L7,8 loop of monomer B (residues 112-121, violet).

Inspection of the docked model also reveals that there is a significant difference in the position of the L3,4 loop compared to the biotin ⊂ streptavidin complex. Crystallographic studies of biotin ⊂ streptavidin showed that the L3,4 loop (residues 48-52) becomes ordered during binding and locks the biotin in the binding site.[171,173] In the vanadyl-containing docked structure, this loop appears to have an open conformation (Figure 12). No other major reorganization of the host protein is observed.

It is interesting to note that the L7,8 loop (residues 112-121) of the adjacent monomer B is situated in proximity to the vanadyl-binding site and could interact with the incoming prochiral sulfide (Figure 12). Residue W120 from this loop, closing the biotin lid of subunit A, also displays a close contact with the vanadyl moiety.

2.2.5.4 Influence of Site-Directed Mutations

In the absence of the chemical dimension, the optimization of the new system was based entirely on genetic modifications of the host protein. It has already been shown that introduction of point mutations in an enzyme scaffold can result in increased and even inverted enantioselectivity.[206,207]

On the basis of the docking model, several residues were identified as possibly involved either in vanadyl binding or in the catalytic reaction. Some of these residues were replaced by the small glycine or alanine amino acids, and the effect of these mutations on the reaction outcome was tested. Sulfide **11** was chosen as a model substrate, as it is provides the best results with WT Sav in terms of conversion and selectivity. In addition, we selected sulfides **9** and **15** in an attempt to optimize the moderate selectivities observed with these substrates.

The residue D128, which displays the closest contact with the vanadyl ion in the docked model, appears to be intimately involved in the binding process. The D128A Sav mutant was produced in our laboratory by Dr. Marc Creus and tested for the sulfoxidation of substrate **11**. This experiment yielded racemic product (Table 19, entry 1), thus strongly supporting the hypothesis that the active vanadyl moiety is located within the biotin-binding pocket during catalysis.

To further explore the catalytic system, we reasoned that modifications in the loop regions might provide useful information. We focused on modifications in the L3,4 loop, containing residue S45, which is also near to $[VO(H_2O)_5]^{2+}$ and possibly involved in H-bonds with coordinated water molecules. To perturb the loop structure and thus influence vanadyl binding and possibly the selectivity of the reaction, we produced a chimaeric Sav, abbreviated

Aviloop, in which the L3,4 loop of streptavidin was replaced with that of avidin (residues 38-45), thus yielding a loop three residues longer than that of the wild-type protein (Figure 13). The chimaeric Aviloop retained strong biotin-binding affinity, as previously reported.[171] Despite avidin's lack of selectivity as host protein, the artificial metalloenzyme $[VO]^{2+} \subset$ Aviloop afforded improved selectivities compared to WT Sav, both for aliphatic and for aromatic substrates (Table 19, entries 2-3).

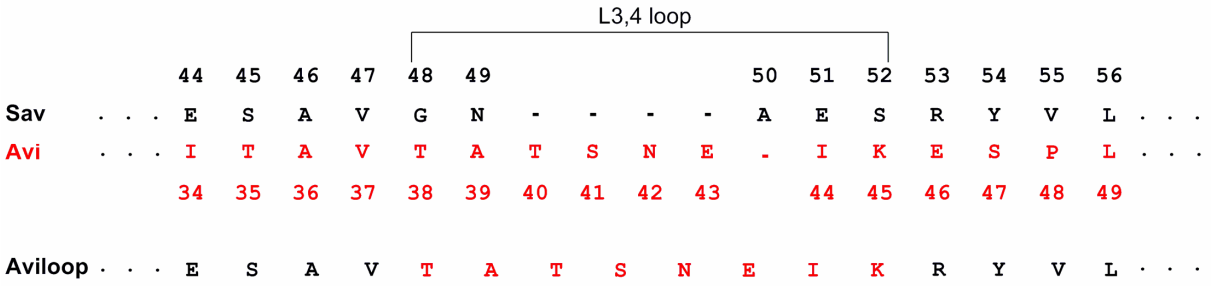

Figure 13. Partial amino acid sequence of the chimaeric Aviloop protein; the L3,4 loop of Sav (residues 48-52) was replaced with the longer L3,4 loop of avidin (residues 38-45).

The small variations in selectivity obtained with Aviloop suggest that the residues of the L3,4 loop are not crucial for vanadyl binding. They might interact with the oxidant and / or the substrate during catalysis, thus fine-tuning the selectivity of the reaction. However, the results obtained prove that the second coordination sphere, provided by close-lying residues, influences enantioselectivity. Based on these initial findings, we hypothesize that improved artificial enzymes can be evolved by directed evolution, by further mutagenesis of close-lying residues and selection of improved variants.

Table 19. Influence of site-directed mutations on the activity and selectivity of $[VO]^{2+} \subset$ Sav for the sulfoxidation reaction of selected substrates.[a]

Entry	Protein	Substrate	Conv. (%)	ee (%)
1	D128A Sav	**11**	97	0
2	Aviloop	**9**	100	60 (*R*)
3	Aviloop	**15**	54	90 (*R*)
4	T114G Sav	**11**	100	74 (*R*)
5	T115A Sav	**11**	100	84 (*R*)
6	E116A Sav	**11**	100	74 (*R*)

[a] Reaction conditions: 2.3% EtOH in HCl / KCl 0.05 M buffer at pH 2.2; Sav isoform 0.0001 M; $VOSO_4$ 0.0002 M; substrate 0.01 M; *t*-BuOOH 0.05 M; room temperature; 4 h.

In addition to the L3,4 loop, the L7,8 loop of the adjacent monomer B, situated in proximity to the hydrophobic pocket, was also expected to influence catalysis by interacting with the incoming substrate. Several Sav isoforms bearing glycine or alanine mutations in the L7,8 loop region were tested for enantioselective sulfoxidation. Some positions of the loop afforded a decrease in selectivity, suggesting that these positions might indeed interfere with the approach of the prochiral sulfide to the catalytic centre (Table 19, entries 4-6).

2.2.5.5 Kinetic Studies

Control reactions performed in the absence of Sav showed that free $[VO]^{2+}$ has a considerably lower activity than $[VO]^{2+} \subset$ WT Sav (see Table 17, entries 1-2), indicating that streptavidin acts like an accelerating ligand for the sulfoxidation reaction. Kinetic experiments were performed in order to determine the extent of this acceleration.

To investigate whether the artificial metalloenzyme follows Michaelis-Menten kinetics, the initial oxidation rate *vs.* substrate concentration was determined. As the substrate has poor solubility in water, the reactions were carried out using 43% EtOH in 0.05 M HCl / KCl buffer at pH 2.2. For solubility reasons, the S112D Sav mutant was used instead of WT Sav (and affords similar conversion and ee, when compared to WT Sav). Saturation kinetics could not be achieved under these reaction conditions, due to poor substrate solubility (Figure 14).

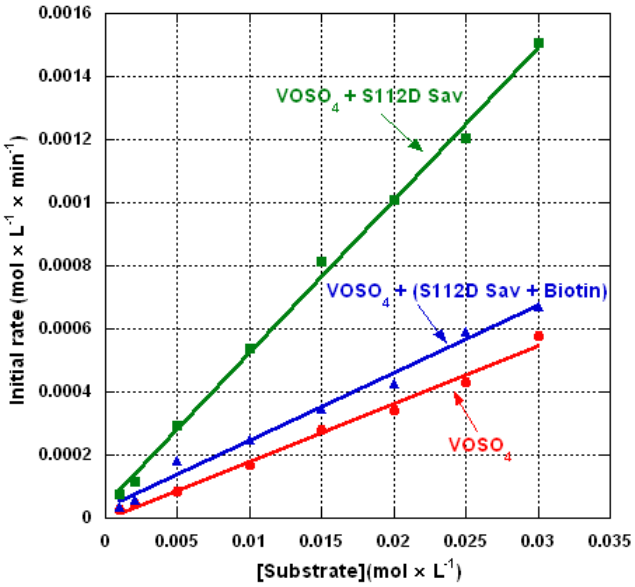

Figure 14. Initial oxidation rate *vs.* substrate concentration for $VOSO_4$ in the absence of streptavidin (•), $VOSO_4 \subset$ Sav (■) and $VOSO_4$ + (Biotin ⊂ Sav) (▲). Reaction conditions: 57% buffer HCl / KCl 0.05 M at pH 2.2; 43% EtOH; S112D Sav 0.0001 M; $VOSO_4$ 0.0002 M; *p*-methoxythioanisole **11**; *t*-BuOOH 0.05 M; room temperature.

Most interestingly, these experiments confirmed that the presence of biotin-free Sav modestly accelerates the sulfoxidation rate ($v_{init}([VO]^{2+} \subset$ WT Sav) / $v_{init}([VO]^{2+}) = 3$). In contrast, biotin-loaded streptavidin enhances the rate of the $[VO]^{2+}$-catalyzed sulfoxidation very little ($v_{init}([VO]^{2+}$ + Biotin $\subset$ Sav) / $v_{init}([VO]^{2+}) = 1.5$). This observation further supports the hypothesis that the oxidation indeed occurs within the biotin binding pocket. The initial rate constants determined for a typical reaction (0.01 M *p*-methoxythioanisole **11**) are $k_i = 2.7$ min^{-1} (for Sav-incorporated $[VO]^{2+}$) and $k_f = 0.8$ min^{-1}(for free $[VO]^{2+}$).

It is also noteworthy that the reaction with substrate **11** proceeds with nearly quantitative conversion for a range of concentrations (50, 100, 150 eq. *p*-methoxythioanisole *vs.* vanadium). These results suggest that product inhibition is insignificant under these conditions.

2.2.5.6 Attempts to Determine the Affinity Constant

Since both free $[VO]^{2+}$ and $[VO]^{2+} \subset$ Sav catalyze the sulfoxidation reaction, the ratio between the two species, established by the affinity constant, determines the total enantioselectivity of the reaction. Hence, it is important to know the affinity of the vanadyl ion for the biotin-binding pocket.

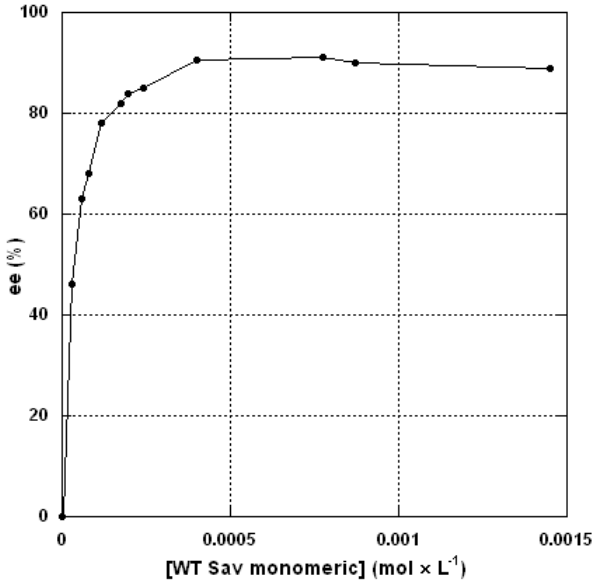

Figure 15. Variation of the selectivity with the monomeric Sav concentration. Reaction conditions: 2.3% EtOH in HCl / KCl 0.05 M buffer at pH 2.2; WT Sav variable concentration, $VOSO_4$ 0.0002 M; *p*-methoxythioanisole **11** 0.01 M; *t*-BuOOH 0.05 M; room temperature; 4 h.

In a first approach, we studied the influence of the Sav concentration on the enantioselectivity of the reaction, keeping the $[VO]^{2+}$ concentration fixed at 0.0002 M (thus varying the ratio between free $[VO]^{2+}$ and $[VO]^{2+} \subset$ Sav). Interestingly, the ee reaches a saturation point at 90% (*R*) using [WT Sav monomeric] = 0.0004 M (tetrameric concentration 0.0001 M), suggesting that maximal incorporation of $[VO]^{2+}$ into Sav occurs at these concentrations of the two species (Figure 15).

Based on this dependence of the ee on the ratio between free- and Sav-incorporated vanadyl species and considering the kinetic parameters obtained for the $[VO]^{2+}$- and $[VO]^{2+} \subset$ Sav-catalyzed sulfoxidation, we reasoned that we could estimate the affinity constant. For this purpose, we performed the previous experiment using the same reaction conditions as for the kinetic runs (*i.e.* 57% buffer HCl / KCl 0.05 M at pH 2.2; 43% EtOH; S112D Sav 0.0001 M; $VOSO_4$ 0.0002 M; *p*-methoxythioanisole **11** 0.01 M; *t*-BuOOH 0.05 M) and we obtained a maximum selectivity of 78% (*R*).

To determine K_a, the following assumptions were made:

- only two species containing $[VO]^{2+}$ are present in the reaction mixture: $[VO]^{2+}$ and $[VO]^{2+} \subset$ Sav; this hypothesis is reasonable, since upon incorporation of biotin, $[VO]^{2+}$ in the presence of Sav follows similar kinetics as free $[VO]^{2+}$ (see Figure 14);
- the intrinsic selectivity of the $[VO]^{2+} \subset$ Sav-catalyzed reaction does not depend on the concentration of $[VO]^{2+} \subset$ Sav; we reasoned that this selectivity is equal to the "saturation" selectivity, 78% ee (*R*).

Table 20. Notations used in equations 1 and 2.

Term	Expression
free $[VO]^{2+}$ concentration	$[VO^{2+}]_f$
$[VO]^{2+} \subset$ Sav concentration	$[VO^{2+}]_i$
free Sav concentration	$[Sav]_f$
total Sav concentration	$c_0^{Sav} = [Sav]_f + [VO^{2+}]_i$
total $[VO]^{2+}$ concentration	$c_0^{V} = [VO^{2+}]_f + [VO^{2+}]_i$
rate constant for free $[VO]^{2+}$	$k_f^{total} = k_f^{R} + k_f^{S}$
rate constant for $[VO]^{2+} \subset$ Sav	$k_i^{total} = k_i^{R} + k_i^{S}$

Thus, the free $[VO]^{2+}$ concentration can be expressed as a function of the ratio of *R* / *S* enantiomers and the rate constants of the reactions catalyzed by free- and Sav-bound $[VO]^{2+}$ in the following manner (the notations used for the different terms is presented in Table 20):

selectivity of $VO^{2+} \subset$ Sav ee = 78% (*R*) ⟶ 89% *R* enantiomer, 11% *S* enantiomer $\frac{k_i^R}{8.09} = k_i^S = \frac{k_i^{total}}{9.09}$

selectivity of VO^{2+} ee = 0 $k_f^R = k_f^S = \frac{k_f^{total}}{2}$

$$\frac{\%R}{\%S} = \frac{k_i^R \cdot [VO^{2+}]_i + k_f^R \cdot [VO^{2+}]_f}{k_i^S \cdot [VO^{2+}]_i + k_f^S \cdot [VO^{2+}]_f}$$

$$[VO^{2+}]_f = \frac{\frac{k_i^{total}}{9.09} \cdot c^0_V \cdot \left(8.09 - \frac{\%R}{\%S}\right)}{\frac{k_i^{total}}{9.09} \cdot \left(8.09 - \frac{\%R}{\%S}\right) + \frac{k_f^{total}}{2} \cdot \left(\frac{\%R}{\%S} - 1\right)} \quad \text{(Equation 1)}$$

On the other hand, from the equilibrium constant K_a, the following equation can be deduced for the dependence of the free $[VO]^{2+}$ concentration on the total Sav and $[VO]^{2+}$ concentrations:

$$VO^{2+} + Sav \rightleftharpoons VO^{2+} \subset Sav$$

$$K_a = \frac{[VO^{2+}]_i}{[VO^{2+}]_f \cdot [Sav]_f}$$

$$K_a \cdot [VO^{2+}]_f^2 + (K_a \cdot c^0_{Sav} - K_a \cdot c^0_V + 1) \cdot [VO^{2+}]_f - c^0_V = 0 \quad \text{(Equation 2)}$$

Knowing the kinetic parameters k_i^{total} = 2.7 min^{-1} and k_f^{total} = 0.8 min^{-1}, the total $[VO]^{2+}$ concentration (c_0^V = 0.0002 M) and the dependence of the *R* / *S* ratio on the total Sav concentration, an algorithm can be used to fit the two equations 1 and 2 that minimizes the difference between the two $[VO^{2+}]_f$ values while varying the K_a parameter. In this way, a K_a value of $1.7 \cdot 10^4$ M^{-1} was obtained, although significant differences between the experimental and the "fitted" ee were observed (Figure 16). Nevertheless, this procedure affords a rough estimate of the K_a value.

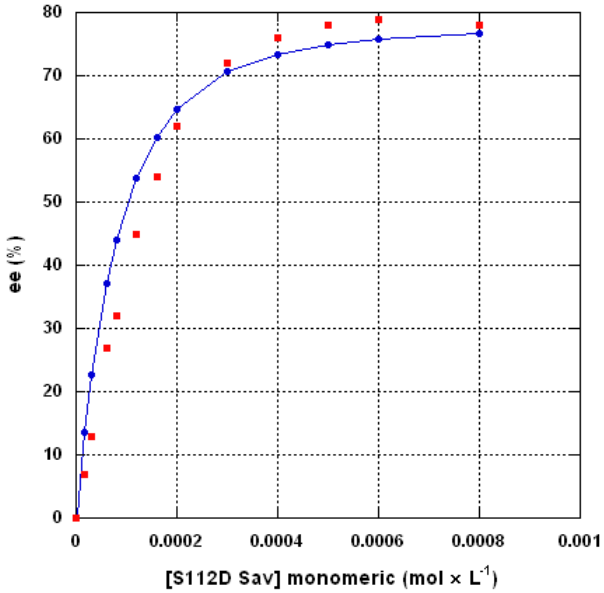

Figure 16. Comparison between experimental (●) and "fitted" ee (■), calculated from equations 1 and 2 using $K_a = 1.7 \cdot 10^4\ M^{-1}$.

2.3 Concluding Remarks

Incorporation of a vanadyl ion into the biotin-binding pocket of streptavidin affords an artificial metalloenzyme for the enantioselective oxidation of prochiral sulfides with good enantioselectivities both for dialkyl and alkyl-aryl substrates (up to 93 % ee).

Evidence provided by EPR spectroscopy, docking simulations, chemical (*i.e.* addition of biotin) or genetic modification of the host protein suggest that the active pre-catalyst $[VO(H_2O)_5]^{2+}$ interacts only via second coordination sphere contacts with the biotin-binding pocket of streptavidin.

Although our efforts to determine the affinity of $[VO(H_2O)_5]^{2+}$ for Sav did not succeed, catalysis results indicate that the selectivity reaches a maximum at a concentration of $\sim 2 \cdot 10^{-4}$ M of the two species, suggesting that maximum incorporation of $[VO(H_2O)_5]^{2+}$ into Sav occurs under these conditions.

Current efforts aim at elucidating the structure and the mechanism of this artificial peroxidase, improving its performance *via* evolutionary protocols, and investigating the crucial aspect of vanadyl and substrate binding.

Chapter 3 Conclusion and Perspectives

The *ex nihilo* creation of catalytic activity from a non-catalytic protein scaffold is a very challenging task. The design of *metallo*enzymes is especially difficult, because the construction of highly specific binding sites is necessary, tailored in function to the metal ion, its oxidation state, preferred geometry and ligand donor set.[208,209]

This study focused on two different strategies for the creation of metalloenzymes: introduction of a new metal-binding site within a protein by modifying the protein's native co-factor and exploiting the H-bonding network within the protein's binding site to incorporate a small metal ion. The performance of these enzymes was tested and optimized for two different enantioselective reactions: transfer hydrogenation of prochiral ketones and sulfide oxidation.

In the first case, supramolecular anchoring of carefully designed biotinylated organometallic fragments into streptavidin provides facile control over the first coordination sphere of the metal through chemical reactions outside the protein. This approach allows separate variation and characterization of the metal complex and the protein, followed by straightforward combination of the chemical and the genetic moieties. As a consequence, a chemogenetic optimization procedure can be easily implemented.

Starting from streptavidin-based artificial transfer hydrogenases previously created in our laboratory, a round of chemogenetic optimization enabled identification of (*R*)- and (*S*)-selective catalysts for the reduction of acetophenone derivatives. Inspired by the X-ray structure of one such (*S)*-selective variant, we implemented an additional directed evolution step that allowed us to further optimize transfer hydrogenases for the reduction of dialkyl ketones.

The general procedure for designed evolution of the artificial keto-reductase is presented in Scheme 1. The activity and selectivity trends of the reaction are ensured by the choice of the chemical fragment in a first screening round. Since several interactions are involved in the enantioselection mechanism (protein-organometallic fragment and protein-substrate), successive rounds of saturation mutagenesis at carefully selected positions of the host protein are necessary to fine-tune the selectivity.

In this way, artificial transfer hydrogenases for the enantioselective reduction of dialkyl ketones were evolved, which optimized second coordination sphere interactions between the substrate and the host protein. Such specialized enzymes were obtained from a relatively

modest screening effort and *via* a straightforward protein immobilization step performed on crude cellular extracts.

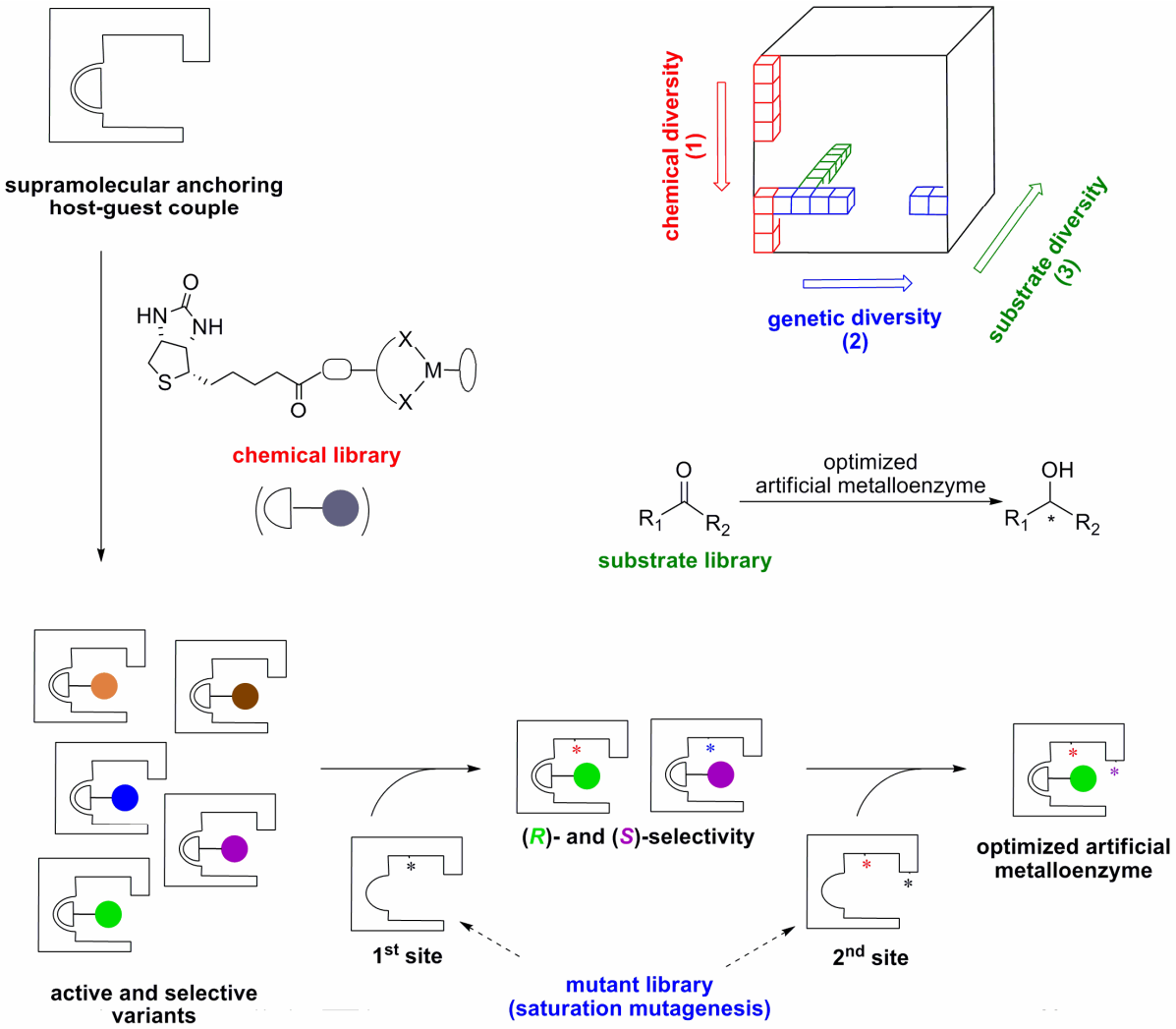

Scheme 1. Designed evolution of an artificial keto-reductase. A search strategy that does not require examination of all possibilities is used to accelerate the chemogenetic optimization procedure[23]. Rational design (choice of mutation sites) and combinatorial methods (structural variation of the chemical component combined with saturation mutagenesis) are used to evolve artificial metalloenzymes with the desired properties.

Compared to other directed evolution techniques,[178] the designed evolution of artificial metalloenzymes using chemogenetic tools offers new possibilities for protein engineering. Introducing a chemical dimension not only enriches the functionality of the protein sequence space to be explored, but also represents a variable with a significant impact on the reaction outcome. Variation of the chemical moiety results in a dramatic change in reactivity. Ideally, one could envision creating an artificial metalloenzyme for nearly any water compatible transition metal-catalyzed reaction,[210] thus broadening the scope of enzymatic catalysis. In

this spirit, we have envisaged the implementation of more challenging oxidation reactions. However, the application of artificial metalloenzymes based on the biotin-streptavidin technology in enantioselective sulfoxidation proved to be a difficult task, due to the incompatibility of the chosen chemical fragment with the genetic component (*i.e.* streptavidin).

A different strategy was therefore developed to address this challenge: the well-tailored H-bonding network of streptavidin's deep active site cavity was found to provide a suitable binding site for the small hydrated vanadyl ion. The catalytic activity of the metal centre and the enantiodiscriminating environment provided by the host protein were exploited to perform highly enantioselective oxidations of several prochiral sulfides. This study demonstrates that specific metal binding can transform a non-enzymatic protein into an enantioselective biocatalyst with synthetic utility and may thus be regarded as an example of functional promiscuity.[31,32] Moreover, the findings provide insight into how selective enzymes may first have evolved in nature from non-catalytic scaffolds.[211]

At this stage, the practical use of artificial metalloenzymes is limited due to the high cost of their development and their low activities compared to biocatalysts evolved in nature. However, their general scope, as well as the rapid optimization procedure makes their application attractive for reactions that are not possible with natural biocatalysts or for challenging substrates for homogeneous catalysts. The combination of chemical and genetic optimization techniques may result in a rapid expansion of protein functionality and a range of novel applications. We therefore believe that hybrid catalysts possess a real potential for applications in white biotechnology processes.

In addition, the well-defined binding pocket of streptavidin could be exploited to incorporate other catalytically active polar coordination compounds to perform enantioselective reactions, although the affinity between the catalyst and the protein could represent a non-negligible issue. Some studies on the alkene dihydroxylation reaction catalyzed by osmium tetroxide have shown promising results in this direction.

Chapter 4 Materials and Methods

1 Materials and Reagents

Solvents were of analytical grade and were purchased from Aldrich, Fluka or Acros and used without further purification. Water was purified to milliQ degree of purity. Other chemicals were obtained from the following suppliers:

Table 1. Origin and characteristics of the reagents.

Reagent	Supplier	Characteristics
Acetophenone	Fluka	≥ 98% (GC)
2-Acetylpyridine	Fluka	≥ 98% (GC)
Benzylmethylsulfide	Acros	98%
N-Benzylmaleimide	Aldrich	99%
4-Benzyloxy-2-butanone	Fluka	≥ 97% (GC)
D-Biotin	Chanzou Huaren	≥ 99%
D-Biotin-4-fluorescein	Sigma	-
D-Biotin-Sepharose^{TM} CL-4B, suspension in TBS buffer pH 7.4, 0.02% NaN_3	Affiland	4 mg immobilized biotin / mL wet gel binding capacity: 40 mg / mL wet gel
Boric acid, $B(OH)_3$	Fluka	99.5%
4-Bromoacetophenone	Acros	98%
tert-Butyl hydroperoxide	Lancaster	70% (w / v) aqueous solution (7.278 M)
Cyclohexylmethyl sulfide	Alfa Aesar	96%
Cumyl hydroperoxide	Aldrich	80% (techn.)
3,4-Diaminobenzoic acid	Aldrich	97%
Diethylenetriamine	Acros	98.5%
2,5-Dihydroxybenzaldehyde	Aldrich	98%
3,5-Di-*tert*-butyl-2-hydroxybenzaldehde	Aldrich	99%
EDC	Acros	98%
Ethylphenylsulfide	Acros	97%
Ethylenediamine	Fluka	≥ 99%

Reagent	Supplier	Characteristics
Guanidinium chloride	Merck	-
HOBT	Acros	98%
Hydrogen peroxide,	Sigma	30% (w / w) aqueous solution
2-Iminobiotin-Sepharose^{TM} 4 Fast Flow, suspension in EtOH 20%	Affiland	1 mg immobilized iminobiotin / mL wet gel binding capacity: 10 mg / mL wet gel
Iodosylbenzene diacetate	Acros	98%
Lithium aluminium hydride	Fluka	97%
Manganese(II) acetate tetrahydrate, $Mn(OAc)_2 \cdot 4H_2O$	Fluka	≥ 99%
4-Methoxythioanisole	Acros	99%
Methyl-2-naphtylsulfide	Alfa Aesar	98%
4-Methylacetophenone	Acros	95%
1-Methylimidazole	Fluka	>99% (GC)
4-Methylthioanisole	Aldrich	99%
3-morpholino-propanesulfonic acid, MOPS	Fluka	≥ 99.5%
Palladium on carbon, Pd / C	Aldrich	10% Pd w /w
1-Phenyl-2-butanone	Aldrich	98%
4-Phenyl-2-butanone	Aldrich	98%
Potassium chloride	Fluka	-
Pyridine	Acros	>99%
Pyridine-*N*-oxide	Aldrich	95%
Ruthenium chloride, $RuCl_3$, hydrate	Umicore	36.55% Ru
Silica, SiO_2 (32-63 60 Å)	Brunschwig	-
Sodium azide, NaN_3	Aldrich	99%
Sodium formate, HCOONa	Merck	99.5%
Sodium hypochlorite	Acros	5% Cl_2
Sodium orthovanadate	Sigma	>90%
Sodium periodate	Acros	99%

Reagent	Supplier	Characteristics
α-Tetralone	Aldrich	98% (GC)
Thioanisole	Aldrich	99% (GC)
Toluene-4-sulfonyl chloride	Fluka	99%
Triethylamine, Et_3N	Acros	99%
Trifluoroacetic acid	Aldrich	99%
Vanadium(V) oxytriisopropoxide, $VO(O\textit{i}\text{-}Pr)_3$	Aldrich	-
Vanadium(IV) oxide sulfate pentahydrate, $VOSO_4 \cdot 5H_2O$	Riedel-de-Haën	-
Vanadium(IV) oxide bis(acetylacetonate), $VO(acac)_2$	Strem Chemicals	98%

Iodosylbenzene (PhIO) was prepared from iodosylbenzene diacetate ($PhI(OAc)_2$) according to a published procedure.[212]

Protein. Avidin was obtained from Belovo (CH). Bovine serum albumin was obtained from Fluka (M~67000, purity >96%). Streptavidin (wild-type and mutants) was prepared by the team of biologists in our laboratory according to published results.[213] The concentration of streptavidin active sites in the cellular extracts, as well as the number of active binding sites in purified streptavidin were quantified in 96-well plates using a fluorescence assay (titration with biotin-4-fluorescein) adapted from the literature.[186]

2 Apparatus

Liquid chromatography: HPLC. Chiral phase HPLC chromatograms were acquired and analyzed on an HP-1100 HPLC apparatus equipped with a UV-Visible diode-array detector and a 100-position autosampler. The solvents used (hexane, *i*-PrOH) were of HPLC-grade. The selected chiral columns and the retention times of the products are described in Section 5.

Gas Chromatography: GC. Chiral GC chromatograms were acquired and analyzed on a GC HP 5890 apparatus using He as a vector gas. The selected chiral columns and the retention times of the products are described in Section 5.

Nuclear Magnetic Resonance: NMR. ^{1}H, ^{13}C and ^{51}V spectra were acquired on a 200 MHz (Varian) or on a 400 MHz (Bruker) spectrometer using deuterated chloroform (99.8% D),

dimethyl sulfoxide (99.5% D) or methanol (99.8% D) from Cambridge Isotope Laboratories. For the ^{51}V spectra, an HCl / KCl buffer at pH 2.2 was used.

Mass Spectrometry: MS. Mass spectra were recorded using an LCQ-IT (Finnigan) spectrometer and an ESI (Electron Spray) or APCI (Atmospheric Pressure Chemical) ionisation mode.

3 Description of Catalytic Experiments

3.1 Transfer Hydrogenation of Carbonyl Compounds

The following procedures are described for the catalytic runs from the second round of optimization, *i.e.* the designed evolution step. The catalysts from the first round chemogenetic optimization procedure were already described by Dr. Christophe Letondor[184] and the reaction procedures are similar to those described below for transfer hydrogenation with purified protein (in the second screen, the volumes and quantities of the reagents are divided by a factor of 3).

All the substrates were commercially available. The $HCOONa{\cdot}B(OH)_3$ mixture was obtained by dissolving $B(OH)_3$ (2.10 g, 34 mmol) and HCOONa (2.72 g, 40 mmol) in water (40 mL) and adjusting the pH to 6.25 with NaOH pellets. The resulting stock solution ($[B(OH)_3]$ = 0.85 M, [HCOONa] = 1 M) was thoroughly degassed.

For immobilization purposes, beads of D-biotin – sepharose (2350 μL wet beads; binding capacity 40 mg of avidin per mL of wet beads; Affiland, Belgium) were washed with water and then resuspended in water in a total volume of 4000 μL. The stock suspension was employed for a batch of maximum 60 catalytic experiments.

General procedure for transfer hydrogenation with immobilized streptavidin. To a solution of cell extract containing streptavidin (0.15 μmol of tetrameric protein determined by titration with biotin-4-fluorescein)[186] was added a suspension of biotin – sepharose (215 μL containing 125 μL wet beads). The resulting suspension, containing a two-fold excess of Sav relative to the biotin-sepharose, was vigorously stirred at room temperature for 60 min. The beads containing immobilized Sav (0.075 μmol of tetrameric protein) were centrifuged in 1.5 mL eppendorf tubes and washed three times with 400 μL of a 1 M guanidinium chloride solution and once with 400 μL water, then resuspended in degassed water (total volume 750 μL). The suspension was thoroughly degassed (nitrogen flushed).

The degassed immobilized protein (337 μL suspension, 0.0337 μmol of tetrameric Sav) was mixed in an eppendorf tube with the precursor complex [η^6-(arene)Ru(**Biot–*p*-L**)Cl] (4.27 μL of a 0.0395 M stock-solution in degassed DMF, 0.169 μmol Ru) and shaken at room temperature for 10 min. The beads were centrifuged in 1.5 mL eppendorf tubes, washed three times with 200 μL HCOONa·$B(OH)_3$ mixture, once with 200 μL water and then resuspended in degassed water in a total volume of 340 μL. The HCOONa·$B(OH)_3$ mixture (405 μL) and the MOPS buffer (135 μL of a 1 M stock-solution, pH adjusted to 6.25) were added. The resulting suspension was divided into two different test tubes (400 μL per test tube, containing 0.015 μmol protein, 0.045 μmol Ru, 180 μmol HCOONa) and the corresponding substrate (*p*-bromoacetophenone **2** or 4-phenyl-2-butanone **6**, 4.5 μL of a 1 M stock solution in DMF, 4.5 μmol) was added to each tube. The test tubes were placed in a magnetically-stirred multireactor, purged several times with nitrogen and heated at 55°C for 64 hours. After completion, the reaction mixture was extracted with Et_2O (4 × 0.5 mL) and dried over Na_2SO_4. The organic solution was filtered through a short silicagel plug that was thoroughly washed with Et_2O, concentrated and subjected to HPLC analysis.

General procedure for the transfer hydrogenation with purified streptavidin. Lyophilized streptavidin was dissolved in milliQ water (100 μM tetrameric concentration). The solution was thoroughly degassed (nitrogen flushed). The degassed protein (150 μL solution, 0.015 μmol of tetrameric Sav) was mixed in a test tube with the precursor complex [η^6-(arene)Ru(**Biot–*p*-L**)Cl] (1.27 μL of a 0.0395 M stock solution in DMF, 0.05 μmol Ru) and stirred at room temperature for 10 min. The HCOONa·$B(OH)_3$ mixture (200 μL), the MOPS buffer (67 μL of a 1 M stock-solution, pH adjusted to 6.25) and the corresponding substrate (5 μL of a 1 M stock solution in DMF, 5 μmol) were added to each tube. The test tubes were placed in a magnetically stirred multireactor, purged several times with nitrogen and heated at 55 °C for 64 hours. After completion, the reaction mixture was extracted with Et_2O (4 × 0.5 mL) and dried over Na_2SO_4. The organic solution was filtered through a short silicagel plug that was thoroughly washed with Et_2O, concentrated and subjected to HPLC analysis (2-acetylpyridine-containing extracts were not filtered on silica).

3.2 Sulfoxidation Reactions

3.2.1 Sulfoxidation Catalyzed by Metal-Salen Complexes

The oxidants used were prepared as described in Table 2.

Table 2. Stock solutions of the different oxidants and volumes added to the reaction mixture for the sulfoxidation catalyzed by Mn-**Sal-X** or V-**Sal-X**.

Oxidant	[Stock solution] (M)	Solvent	V added to the reaction (μL)
NaOCl	0.73	H_2O	5.5
$NaIO_4$	0.25	H_2O	16
PhIO	0.25	MeOH	16
$PhI(OAc)_2$	0.25	MeOH	16
H_2O_2 solution 1	0.11	H_2O	17.7
H_2O_2 solution 2	1.0	H_2O	4
t-BuOOH[a]	3.64	H_2O / EtOH 1 / 1	5.5

[a] The stock solution was prepared by mixing EtOH with a commercial solution of 70% *t*-BuOOH in H_2O in a 1 / 1 (v / v) ratio.

Background reaction. A suspension of thioanisole (4 μL of a 1 M DMF stock solution) in 400 μL water was mixed in a test tube with 1 equivalent of oxidant (see Table 2 for the volumes added). The test tube was closed and the reaction mixture stirred at room temperature for 4 to 5 h. After this time, the reaction mixture was extracted four times with Et_2O. The organic phase was dried over Na_2SO_4 and subjected to HPLC analysis.

Activity tests of Mn-Sal-X complexes. A solution of Mn-**Sal-X** in 400 μL water (2 μL of a 0.02 M stock solution in DMF, 100 μM final concentration) was mixed in a test tube with thioanisole (2 μL of a 1 M DMF stock solution). The reaction was initiated by adding 1 equivalent of oxidant (17.7 μL of H_2O_2 solution 1 – see Table 2 – 0.005 M final concentration) and the test tube was sealed. After 4 to 5 h stirring at room temperature, the reaction mixture was extracted four times with Et_2O. The organic phase was dried over Na_2SO_4, filtered through a short silica gel plug that was thoroughly washed with Et_2O and

subjected to HPLC analysis. Similar results were obtained with control samples that were not subjected to filtration through a silica plug.

Tests of Mn-Sal-X in presence of Sav. A solution of streptavidin in water (400 μL, 33 μM tetrameric concentration) was mixed in a test tube with the biotinylated metal complex, Mn-**Sal-X** (2 μL of a 0.02 M stock solution in DMF, 100 μM final concentration). After 5 min incubation time, thioanisole was added (2 μL of a 1 M DMF stock solution). The reaction was initiated by adding 1 equivalent of oxidant (17.7 μL of H_2O_2 solution 1 – see Table 2 –) and the test tube was sealed. After 4 to 5 h stirring at room temperature, the reaction mixture was extracted four times with Et_2O. The organic phase was dried over Na_2SO_4 and subjected to HPLC analysis.

Tests of V-Sal-X in presence of Sav. A solution of streptavidin in water (200 μL, 100 μM tetrameric concentration) was mixed in a test tube with the biotinylated metal complex, V-**Sal-X** (2 μL of a 0.02 M stock solution in DMF, 200 μM final concentration). After 5 min incubation time, thioanisole was added (4 μL of a 0.5 M DMF stock solution). The reaction was initiated by adding 5 equivalents of oxidant (2.75 μL of a 3.64 M *t*-BuOOH stock solution in MeOH, 0.05 M final concentration) and the test tube was sealed. After 4 h stirring at room temperature, the reaction mixture was extracted four times with Et_2O. The organic phase was dried over Na_2SO_4 and subjected to HPLC analysis.

3.2.2 Sulfoxidation Catalyzed by Vanadyl Ion

The 0.05 M HCl / KCl buffer at pH 2.2 was obtained by dissolving KCl (298 mg, 4 mmol) in water (80 mL) and adjusting the pH to 2.2 with concentrated HCl (36%).

General procedure for the asymmetric sulfoxidation catalyzed by vanadium-loaded streptavidin. A solution of streptavidin in buffer at pH 2.2 (200 μL, 100 μM tetrameric concentration) was mixed in a test tube (1 mL capacity) with the vanadium source (4 μL of a 0.01 M stock solution in water or EtOH, 200 μM final concentration). After 10 min incubation time, the substrate was added (4 μL of a 0.5 M stock solution in EtOH, 0.01 M final concentration). The reaction was initiated by adding the oxidant (2.75 μL of a 3.64 M *t*-BuOOH stock solution in water / EtOH 1 / 1, 0.05 M final concentration) and the test tube was sealed. After 4 h stirring at room temperature, the reaction mixture was extracted four times with Et_2O. The organic phase was dried over Na_2SO_4 and subjected to HPLC analysis.

Catalysis on a milligram quantity of *p*-methoxythioanisole 11. To a WT Sav (26.3 mg, 0.35 μmol) solution in buffer at pH 2.2 (3.5 mL) in a round-bottom flask was added an aqueous solution of $VOSO_4 \cdot 5H_2O$ (35 μL of a 0.02 M stock solution in water). After 10 min. incubation time, the substrate was added (35 μL of a 1 M stock solution in EtOH). The reaction was initiated by adding the oxidant (48 μL of a 3.64 M *t*-BuOOH stock solution in water / EtOH 1 / 1) and the flask was sealed. After 4 h stirring at room temperature, the reaction mixture was extracted four times with Et_2O. The organic phase was dried over Na_2SO_4, evaporated under vacuum and the crude product was purified by flash chromatography on silicagel using CH_2Cl_2 / MeOH (100 / 1) to afford 5 mg of methyl-*p*-methoxyphenyl sulfoxide (80% yield).

^{1}H NMR (400 MHz, Acetone-d_6, 298 K): δ_H (ppm) 2.64 (s, 3H, CH_3-S), 3.87 (s, 3H, CH_3-O), 7.12 (d, J = 8 Hz, 2H, 2 × HC$_{aromatic}$), 7.62 (d, J = 8 Hz, 2H, 2 × HC$_{aromatic}$).

Chiral HPLC: Chiralcel OB-H, hexane / *i*-PrOH 80 / 20, flow 1.0 mL / min, t_1 =15.7 min., t_2 = 31.9 min., 90% ee (*R*).

3.2.3 Kinetic Experiments

Kinetic experiments were performed in a mixture of 57% HCl / KCl buffer (0.05 M, pH 2.2) and 43% EtOH, to ensure complete solubilization of the substrate. For all the catalytic runs, *p*-methoxythioanisole **11** was used as model substrate. All the experiments were performed in duplicate and the two reactions were quenched after 2, respectively 4 minutes. During this interval, the increase in sulfoxide concentration as a function of time followed a straight line. Initial rates were calculated over a 4 minute period, starting from the conversion values obtained by HPLC analysis.

Free $VOSO_4$. A solution of *p*-methoxythioanisole **11** (200 μL, 0.001 – 0.03 M final concentration range, see Chapter 2, Section 2.2.5.5, Figure 14) in buffer / EtOH mixture (57 / 43 v / v) was mixed in a test tube (1 mL capacity) with $VOSO_4$ (4 μL of a 0.01 M stock solution in buffer, 200 μM final concentration). After 10 minutes incubation time, the reaction was initiated by adding the oxidant (2.75 μL of a 3.64 M *t*-BuOOH stock solution in water / EtOH 1 / 1, 0.05 M final concentration). After 2, respectively 4 minutes, the reaction was quenched by adding 100 μL saturated $Na_2S_2O_3$, followed by 400 μL Et_2O. The reaction mixture was extracted four times with Et_2O. The organic phase was dried over Na_2SO_4 and subjected to HPLC analysis.

$VOSO_4$ ⊂ S112D Sav. A solution (200 μL) containing S112D Sav (100 μM final tetrameric concentration) and *p*-methoxythioanisole **11** (0.001 – 0.03 M final concentration range, see Chapter 2, Section 2.2.5.5, Figure 14) in buffer / EtOH mixture (57 / 43 v / v) was mixed in a test tube (1 mL capacity) with $VOSO_4$ (4 μL of a 0.01 M stock solution in buffer, 200 μM final concentration). After 10 minutes incubation time, the reaction was initiated by adding the oxidant (2.75 μL of a 3.64 M *t*-BuOOH stock solution in water / EtOH 1 / 1, 0.05 M final concentration). After 2, respectively 4 minutes, the reaction was quenched by adding 100 μL saturated $Na_2S_2O_3$, followed by 400 μL Et_2O. The reaction mixture was extracted four times with Et_2O. The organic phase was dried over Na_2SO_4 and subjected to HPLC analysis.

$VOSO_4$ + (biotin ⊂ S112D Sav). A solution (200 μL) containing S112D Sav (100 μM final tetrameric concentration), biotin (100 μM final concentration) and *p*-methoxythioanisole **11** (0.001 – 0.03 M final concentration range, see Chapter 2, Section 2.2.5.5, Figure 14) in buffer / EtOH mixture (57 / 43 v / v) was mixed in a test tube (1 mL capacity) with $VOSO_4$ (4 μL of a 0.01 M stock solution in buffer, 200 μM final concentration). After 10 minutes incubation time, the reaction was initiated by adding the oxidant (2.75 μL of a 3.64 M *t*-BuOOH stock solution in water / EtOH 1 / 1, 0.05 M final concentration). After 2, respectively 4 minutes, the reaction was quenched by adding 100 μL saturated $Na_2S_2O_3$, followed by 400 μL Et_2O. The reaction mixture was extracted four times with Et_2O. The organic phase was dried over Na_2SO_4 and subjected to HPLC analysis.

4 Synthesis of the Biotinylated Metal-Salen Complexes

4.1 Synthesis of the Ligands Sal-1 – Sal-4

Biotin pentafluorophenol ester (BPFP) and biotinyl-*N*-hydroxysuccinimide ester (BNHS) were prepared according to reported procedures.[157,214]

4.1.1 Synthesis of Sal-1

Biotinamine.[214]

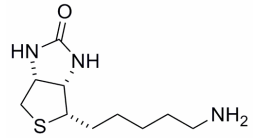

A concentrated NH_4OH solution (24%, 30 mL) was added dropwise to a solution of BPFP (700 mg, 1.8 mmol) in DMF (8 mL). The resulting suspension was stirred at room

temperature for 12 h. The white solid was filtered, washed five times with water and three times with Et_2O and dried under vacuum to give 205 mg (47%) of biotinamide as a white solid. To a suspension of biotinamide (198 mg, 0.8 mmol) in THF (15 mL) under nitrogen was added $LiAlH_4$ (155 mg, 4 mmol) and the resulting mixture was refluxed for 22 h. The reaction was then cooled with an ice bath and water (0.6 mL) was slowly added. The Al salts were filtered on celite and washed with $CHCl_3$. The filtrate was evaporated to yield the biotinamine (154 mg, 83% yield from biotinamide).

^{1}H NMR (200 MHz, DMSO-d_6, 298 K): δ_H (ppm) 1.1-1.8 (m, 10 H, CH_2CH_2CH_2CH_2, NH_2), 2.55 (m, 2H, CH_2-S), 2.82 (m, 1H, CH_2-S), 3.05-3.18 (m, 1H, C*H*-S), 3.35-3.40 (m, 2H, CH_2-NH), 4.05-4.18 (m, 1H, C*H*-N), 4.25-4.35 (m, 1H, C*H*-N), 6.36 (s, 1H, CH-N*H*), 6.45 (s, 1H, CH-N*H*).

3, 4-Diaminobenzoic acid, aminobiotinyl amide.

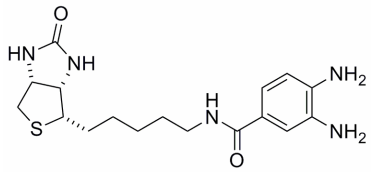

3,4-Diaminobenzoic acid (152 mg, 1mmol), EDC (233 mg, 1.5 mmol), HOBT (202 mg, 1.5 mmol), Et_3N (268 μL, 2 mmol) and biotinamine (401 mg, 1.75 mmol) were mixed in DMF (40 mL) and the resulting solution was stirred at 45°C during 24 h. After this time, the DMF was evaporated and the crude product was purified by flash chromatography on silicagel using CH_2Cl_2 / MeOH (initial mixture 9 / 1, final mixture 6 / 4) to afford the product (203 mg, 0.56 mmol, 56% yield).

^{1}H NMR (400 MHz, DMSO-d_6, 298 K): δ_H (ppm) 1.21-1.61 (m, 8H, CH_2CH_2CH_2CH_2-CH_2NH), 2.58 (d, *J* = 12.4 Hz, 1H, CH_2-S), 2.82 (dd, *J* = 12.4 Hz, *J* = 5.1 Hz, 1H, CH_2-S), 3.08-3.14 (m, 1H, C*H*-S), 3.38-3.52 (m, 2H, CH_2-NH), 4.12-4.15 (m, 1H, C*H*-N), 4.29-4.33 (m, 1H, C*H*-N), 4.95 (br, 4H, NH_2), 6.39 (s, 1H, CH-N*H*), 6.47 (s, 1H, CH-N*H*), 6.47 (d, *J* = 8.0 Hz, 1H, *H*C$_{aromatic}$), 6.95 (dd, *J* = 8.0 Hz, *J* = 1.9 Hz, 1H, *H*C$_{aromatic}$), 7.04 (d, *J* = 1.9 Hz, 1H, *H*C$_{aromatic}$), 7.88 (t, *J* = 5.6 Hz, 1H, CH$_2$-*H*N).

^{13}C NMR (100 MHz, DMSO-d_6, 298 K): δ_C (ppm) 27.4 (*C*H$_2$), 29.1 (*C*H$_2$), 29.2 (*C*H$_2$), 30.1 (*C*H$_2$), 39.7 (*C*H$_2$-NH), 40.7 (*C*H$_2$-S), 56.4 (*C*H-S), 60.1 (*C*H-N), 61.9 (*C*H-N), 113.6 (*C$_{aromatic}$*H), 114.7 (*C$_{aromatic}$*H), 117.8 (*C$_{aromatic}$*H), 124.1 (*C$_{aromatic}$*-CO), 134.7 (*C$_{aromatic}$* -NH$_2$), 139.0 (*C$_{aromatic}$*-NH$_2$), 163.6 (HN-*C*O-NH), 167.6 (*C*O-NH).

ESI$^+$-MS: 386.2 (10, $[M+Na]^+$), 365.1 (20, $[M+2H]^{2+}$), 364.1 (100, $[M+H]^+$).

***N,N'*-Bis-(3,5-di-*tert*-butylsalicylidene)-3,4-diaminobenzoic acid, aminobiotinyl amide, Sal-1**.

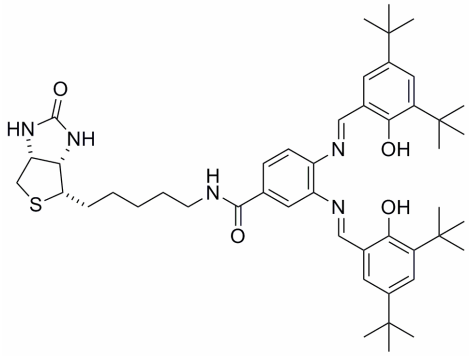

To a solution of 3,5-di-*tert*-butyl-2-hydroxybenzaldehyde (386 mg, 1.65 mmol) in MeOH (10 mL) was added a solution of 3, 4-diaminobenzoic acid, aminobiotinyl amide (200 mg, 0.55 mmol) in MeOH (10 mL) and the reaction mixture was refluxed during 48 h. After this time, MeOH was evaporated and the crude product was purified by flash chromatography on silicagel using CH_2Cl_2 / MeOH (initially pure CH_2Cl_2, final mixture 95 / 5) to afford **Sal-1** as a yellow-orange solid (287 mg, 0.36 mmol, 65% yield).

^{1}H NMR (400 MHz, $CDCl_3$, 298 K): δ_H (ppm) 1.33 (s, 18H, 2 × C(C*H*$_3$)$_3$), 1.45 (s, 18H, 2 × C(C*H*$_3$)$_3$), 1.33-1.67 (m, 8H, C*H*$_2$C*H*$_2$C*H*$_2$C*H*$_2$-CH$_2$NH), 2.62 (d, *J* = 12.8 Hz, 1H, C*H*$_2$-S), 2.82 (dd, *J* = 12.8 Hz, *J* = 4.7 Hz, 1H, C*H*$_2$-S), 3.07-3.12 (m, 1H, C*H*-S), 3.36-3.51 (m, 2H, C*H*$_2$-NH), 4.19-4.22 (m, 1H, C*H*-N), 4.39-4.42 (m, 1H, C*H*-N), 5.67 (s, 1H; CH-N*H*), 6.68 (s, 1H; CH-N*H*), 7.23-7.27 (m, 3H, *H*C$_{aromatic}$), 7.46 (d, *J* = 2.4 Hz, 1H, *H*C$_{aromatic}$), 7.48 (d, *J* = 2.4 Hz, 1H, *H*C$_{aromatic}$), 7.78 (dd, *J* = 8.2 Hz, *J* = 1.8 Hz, 1H, *H*C$_{aromatic}$), 7.84 (d, *J* = 1.8 Hz, 1H, *H*C$_{aromatic}$), 8.68 (s, 1H, C*H*=N), 8.79 (s, 1H, C*H*=N), 13.41 (s, 1H, O*H*), 13.45 (s, 1H, O*H*).

^{13}C NMR (100 MHz, $CDCl_3$, 298 K): δ_C (ppm) 27.4 (*C*H$_2$), 28.9 (*C*H$_2$), 29.0 (*C*H$_2$), 29.5 (*C*H$_2$), 29.8 (3 × *C*H$_3$), 31.9 (6 × *C*H$_3$), 34.6 (3 × *C*H$_3$), 35.5 (4 × *C*-CH$_3$), 40.3 (*C*H$_2$-NH), 40.9 (*C*H$_2$-S), 56.3 (*C*H-S), 60.5 (*C*H-N), 62.3 (*C*H-N), 118.6 (*C*$_{aromatic}$), 118.7 (*C*$_{aromatic}$), 119.4 (*C*$_{aromatic}$), 120.3 (*C*$_{aromatic}$), 126.3 (*C*$_{aromatic}$), 127.4 (*C*$_{aromatic}$), 127.6 (*C*$_{aromatic}$), 128.9 (*C*$_{aromatic}$), 129.1 (*C*$_{aromatic}$), 133.9 (*C*$_{aromatic}$), 137.5 (*C*$_{aromatic}$), 137.7 (*C*$_{aromatic}$), 141.0 (2 × *C*$_{aromatic}$), 143.0 (*C*$_{aromatic}$), 145.6 (*C*$_{aromatic}$), 159.0 (*C*$_{aromatic}$), 159.1 (*C*$_{aromatic}$), 164.6 (HN-*C*O-NH), 166.0 (2 × *C*H=N), 167.1 (*C*O-NH).

ESI$^+$-MS: 818.6 (10, $[M+Na]^+$), 798.5 (20), 797.4 (50, $[M+2H]^{2+}$), 796.5 (100, $[M+H]^+$).

4.1.2 Synthesis of Sal-2

5-(*O*-Biotinyl)-2,5-dihydroxybenzaldehyde.

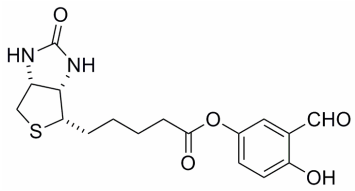

2,5-Dihydroxybenzaldehyde (1 g, 7.24 mmol), BNHS (2.06 g, 6.03 mmol) and Et_3N (1.21 mL, 9.05 mmol) were mixed in DMF (30 mL) and the resulting solution was stirred at room temperature for 48 h. After this time, the DMF was evaporated and the crude product was purified by flash chromatography on silicagel using CH_2Cl_2 / MeOH (95 / 5) to afford the product (437 mg, 1.20 mmol, 20% yield).

^{1}H NMR (400 MHz, DMSO-d_6, 298 K): δ_H (ppm) 1.57-1.40 (m, 4H, CH_2CH_2-CH_2CO), 1.63-1.70 (m, 2H, CH_2-CHS), 2.58 (t, J = 7.4 Hz, 2H, CH_2CO), 2.60 (d, J = 12.7 Hz, 1H, CH_2-S), 2.85 (dd, J = 12.7 Hz, J = 5.1 Hz, 1H, CH_2-S), 3.12-3.17 (m, 1H, CH-S), 4.14-4.18 (m, 1H, CH-N), 4.31-4.34 (m, 1H, CH-N), 6.39 (s, 1H, CH-NH), 6.48 (s, 1H, CH-NH), 7.03 (d, J = 12.7 Hz, 1H, HC$_{aromatic}$), 7.29 (dd, J = 8.9 Hz, J = 3.0 Hz, 1H, HC$_{aromatic}$), 7.35 (d, J = 3.0 Hz, 1H, HC$_{aromatic}$), 10.26 (s, 1H, CHO).

^{13}C NMR (100 MHz, DMSO-d_6, 298 K): δ_C (ppm) 25.2 (CH$_2$), 28.8 (CH$_2$), 28.9 (CH$_2$), 34.1 (CH$_2$CO), 40.7 (CH$_2$-S), 59.2 (CH-S), 60.1 (CH-N), 61.9 (CH-N), 119.1 ($C_{aromatic}$H), 121.4 ($C_{aromatic}$), 123.3 ($C_{aromatic}$), 130.8 ($C_{aromatic}$H), 143.6 ($C_{aromatic}$), 159.3 ($C_{aromatic}$), 163.6 (HN-CO-NH), 172.9 (CO-O), 191.1 (CH=O).

ESI$^+$-MS: 387.1 (100, [M+Na]$^+$), 365.1 (10, [M+H]$^+$).

***N*-((5-*O*-Biotinyl)-2,5-dihydroxysalicylidene), *N'*-(3,5-di-*tert*-butylsalicylidene)-ethylenediamine, Sal-2.**

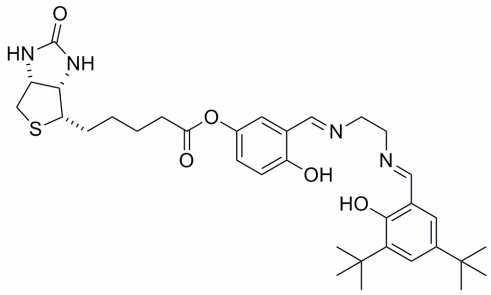

To a solution of 5-(*O*-biotinyl)-2,5-dihydroxybenzaldehyde (300 mg, 0.82 mmol) and 3,5-di-*tert*-butyl-2-hydroxybenzaldehyde (192 mg, 0.82 mmol) in MeOH (30 mL) was added a solution of Et_3N (53 μL, 0.8 mmol) in MeOH (10 mL) and the resulting reaction mixture was

stirred at room temperature for 10 minutes. The Schiff bases were precipitated by adding water (50 mL) and the solid was collected after centrifugation of the resulting suspension, dissolved in CH_2Cl_2 and dried over $MgSO_4$. After evaporation of the CH_2Cl_2, the three Schiff bases were separated by flash chromatography on silicagel using CH_2Cl_2 / MeOH (initially pure CH_2Cl_2, final mixture 97 / 3) to afford the non-symmetric Schiff base **Sal-2** as a yellow solid (141 mg, 0.23 mmol, 28% yield).

^{1}H NMR (400 MHz, CD_3OD, 298 K): δ_H (ppm) 1.29 (s, 9H, C(C*H*$_3$)$_3$), 1.41 (s, 9H, C(C*H*$_3$)$_3$), 1.42-1.82 (m, 6H, C*H*$_2$C*H*$_2$C*H*$_2$-CH$_2$CO), 2.60 (d, *J* = 12.7 Hz, 1H, C*H*$_2$-S), 2.73 (t, *J* = 7.4 Hz, 2H, C*H*$_2$-CO), 2.95 (dd, *J* = 12.7 Hz, *J* = 4.9 Hz, 1H, C*H*$_2$-S), 3.18-3.27 (m, 1H, C*H*-S), 3.94-3.96 (m, 4H, NH-C*H*$_2$C*H*$_2$-NH), 4.30-4.36 (m, 1H, C*H*-N), 4.48-4.54 (m, 1H, C*H*-N), 6.87 (d, *J* = 7.8 Hz, 1H, *H*C$_{aromatic}$), 7.04 (m, 2H; 2 × *H*C$_{aromatic}$), 7.12 (d, *J* = 2.4 Hz, 1H, *H*C$_{aromatic}$), 7.37 (d, *J* = 2.4 Hz, 1H, *H*C$_{aromatic}$), 8.41 (s, 1H, C*H*=N), 8.42 (s, 1H, C*H*=N).

4.1.3 Synthesis of Sal-3

***N*-Biotinyl-*N'*,*N"*-bis(3,5-di-*tert*-butylsalicylidene)diethylenetriamine, Sal-3.**

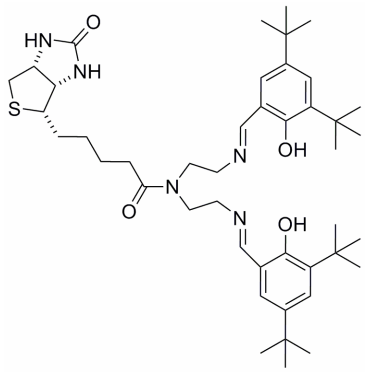

A solution of 3,5-di-*tert*-butyl-2-hydroxybenzaldehyde (150 mg, 0.64 mmol) and ethylenetriamine (34 µL, 0.32 mmol) in toluene (5 mL) was stirred during 4 h at room temperature. The solvent was evaporated and the crude product was purified by flash chromatography on silicagel using CH_2Cl_2 / MeOH (96 / 4) to afford a yellow solid (171 mg, quantitative yield). As the product hydrolyzed rapidly in solution, the purification was performed very quickly.

To a solution of *N*,*N'*-bis-(3,5-di-*tert*-butylsalicylidene)diethylenetriamine (170 mg, 0.32 mmol) and BNHS (131 mg, 0.38 mmol) in DMF (5 mL) was added Et_3N (134 µL, 1 mmol) and the reaction mixture was heated at 50 °C during 24 h. The solvent was evaporated and the

crude product was purified by flash chromatography on silicagel using CH_2Cl_2 / MeOH / Et_3N (95 / 5 / 2) to afford **Sal-3** as a yellow solid (168 mg, 69% yield).

^{1}H NMR (400 MHz, $CDCl_3$, 298 K): δ_H (ppm) 1.31 (s, 18H, 2 × C(C*H*$_3$)$_3$), 1.45 (s, 18H, 2 × C(C*H*$_3$)$_3$), 1.59-1.76 (m, 6H, C*H*$_2$C*H*$_2$C*H*$_2$-CH$_2$CO), 2.41 (t, *J* = 7.5 Hz, 2H, C*H*$_2$-CO), 2.73 (d, *J* = 12.7 Hz, 1H, C*H*$_2$-S), 2.90 (dd, *J* = 12.7 Hz, *J* = 4.9 Hz, 1H, C*H*$_2$-S), 3.11-3.16 (m, 1H, C*H*-S), 3.68-3.69 (m, 4H, C*H*$_2$-N=CH), 3.76 (t, *J* = 5.9 Hz, 2H, C*H*$_2$-N), 3.84 (t, *J* = 5.9 Hz, 2H, C*H*$_2$-N), 4.26-4.29 (m, 1H, C*H*-N), 4.47-4.50 (m, 1H, C*H*-N), 5.24 (s, 1H, CH-N*H*), 5.68 (s, 1H, CH-N*H*), 7.07 (d, *J* = 2.4 Hz, 1H, *H*C$_{aromatic}$), 7.09 (d, *J* = 2.4 Hz, 1H, *H*C$_{aromatic}$), 7.39-7.40 (m, 2H, *H*C$_{aromatic}$), 8.34 (s, 1H, C*H*=N), 8.37 (s, 1H, C*H*=N), 13.35 (s, 1H, O*H*), 13.69 (s, 1H, O*H*).

^{13}C NMR (100 MHz, $CDCl_3$, 298 K): δ_C (ppm) 25.5 (*C*H$_2$), 28.7 (*C*H$_2$), 29.8 (*C*H$_3$), 29.8 (*C*H$_3$), 31.9 (*C*H$_3$), 33.2 (*C*H$_2$), 34.4 (*C*H$_2$), 34.5 (*C*-CH$_3$), 35.4 (*C*-CH$_3$), 40.9 (*C*H$_2$-S), 48.3 (*C*H$_2$-N), 50.3 (*C*H$_2$-N), 55.7 (*C*H-S), 57.8 (*C*H$_2$-N), 58.8 (*C*H$_2$-N), 60.5 (*C*H-N), 62.1 (*C*H-N), 117.9 (*C*$_{aromatic}$), 118.2 (*C*$_{aromatic}$), 126.4 (*C*$_{aromatic}$H), 126.6 (*C*$_{aromatic}$H), 127.5 (*C*$_{aromatic}$H), 127.9 (*C*$_{aromatic}$H), 137 (*C*$_{aromatic}$), 137.1 (*C*$_{aromatic}$), 140.6 (*C*$_{aromatic}$), 140.8 (*C*$_{aromatic}$), 158.2 (*C*$_{aromatic}$), 158.4 (*C*$_{aromatic}$), 163.7 (HN-*C*O-NH), 168.1 (*C*H=N), 168.4 (*C*H=N), 173.9 (*C*O-NH).

ESI$^+$-MS: 776.4 (20), 763.5 (55, [M+2H]$^{2+}$), 762.6 (100, [M+H]$^+$).

4.1.4 Synthesis of Sal-4

(*meso*)-*N*-Benzyl-3,4-dihydroxy-2,5-pyrrolidinedione.[215]

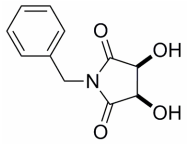

To a solution of *N*-benzylmaleimide (3 g, 16.0 mmol) in AcOEt / CH_3CN 1 / 1 (total volume 195 mL) cooled in an ice bath at 0°C was added a solution of $RuCl_3$ (233 mg, 1.13 mmol) and $NaIO_4$ in water (32 mL). The biphasic mixture was vigourously stirred for 3 minutes at 0°C, following which the reaction was quenched with 100 mL $Na_2S_2O_3$ saturated solution. The organic phase was separated and the aqueous layer was extracted three times with AcOEt. The combined organic layers were dried over $MgSO_4$ and evaporated *in vacuo* to afford the crude product, which was purified by flash chromatography on silicagel using CH_2Cl_2 / MeOH (98 / 2) to afford a white solid (2.5 g, 70% yield).

^{1}H NMR (200 MHz, CD_3OD, 298 K): δ_H (ppm) 4.48 (s, 2H, N-C*H*$_2$-Ph), 4.67 (s, 2H, 2 × C*H*-OH), 7.28-7.34 (m, 5H, *H*C$_{aromatic}$).

(*meso*)-*N*-Benzyl-3,4-dihydroxypyrrolidine.

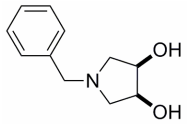

This synthesis was adapted from a published procedure.[216] All the manipulations were carried out using standard Schlenk techniques. To a suspension of $LiAlH_4$ (4.3 g, 113 mmol) in THF (130 mL) under nitrogen was added a solution of (*meso*)-*N*-benzyl-3,4-dihydroxy-2,5-pyrrolidinedione (5.0 g, 22.6 mmol) and the reaction mixture was refluxed during 62 h. The reaction was cooled with an ice bath and AcOEt (120 mL) was carefully added with vigourous stirring, followed by water (18 mL) and 3 M NaOH solution (4.25mL). After 1 h stirring at room temperature, the aluminium salts filtered on celite and washed with AcOEt. The filtrate was evaporated to yield the crude product, which was purified by flash chromatography on silicagel using AcOEt / MeOH / Et_3N (95 / 5 / 1) to afford a yellow oil (1.13 g, 26% yield).

^{1}H NMR (200 MHz, $CDCl_3$, 298 K): δ_H (ppm) 2.59 (br, 2H, O*H*), 2.68-2.70 (m, 4H, 2 × C*H*$_2$-N), 3.6 (s, 2H, N-C*H*$_2$-Ph), 4.16-4.21 (m, 2H, 2 × C*H*-OH), 7.28-7.37 (m, 5H, *H*C$_{aromatic}$).

(*meso*)-*N*-benzyl-3,4-dihydroxypyrrolidine di-*p*-toluenesulfonate.

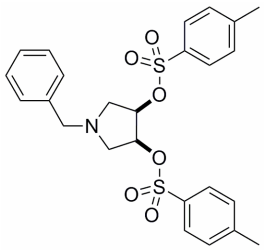

This synthesis was adapted from a published procedure.[217] To a solution of (*meso*)-*N*-benzyl-3,4-dihydroxypyrrolidine (1.13 g, 5.85 mmol) in pyridine (32 mL) was added *p*-toluenesulfonyl chloride (3.4 g, 17.8 mmol) in one portion. The resulting solution was stored at 4°C for 4 days. The mixture was then added dropwise to a cooled solution of citric acid (160 g in 1 L water) and the resulting aqueous solution was extracted four times with Et_2O. The combined organic layers were dried over Na_2SO_4 and evaporated *in vacuo*. The crude product was purified by flash chromatography on silicagel using CH_2Cl_2 / Et_3N (100 / 1) to afford a white solid (2.36 g, 81% yield).

^{1}H NMR (200 MHz, $CDCl_3$, 298 K): δ_H (ppm) 2.47 (s, 6H, 2 × C*H*$_3$), 2.69-2.76 (m, 2H, C*H*$_2$-N), 3.02-3.11 (m, 2H, C*H*$_2$-N), 3.6 (s, 2H, N-C*H*$_2$-Ph), 4.71-4.83 (m, 2H, 2 × C*H*-OH), 7.19-7.36 (m, 9H, *H*C$_{aromatic}$), 7.74 (s, 2H, *H*C$_{aromatic}$), 7.78 (s, 2H, *H*C$_{aromatic}$).

(*meso*)-*N*-benzyl-3,4-diazidopyrrolidine.

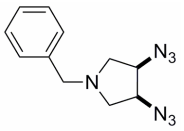

This synthesis was adapted from a published procedure.[218] All the manipulations were carried out using standard Schlenk techniques. To a solution of (*meso*)-*N*-benzyl-3,4-dihydroxypyrrolidine di-*p*-toluenesulfonate (2.0 g, 4.0 mmol) in DMF (22 mL) under nitrogen was added solid NaN_3 (1.04 g, 16.0 mmol). The resulting suspension was heated at 100°C for 22 h and then cooled at room temperature. Water (40 mL) was added and the mixture was extracted four times with CH_2Cl_2. The organic layers were dried over Na_2SO_4 and evaporated *in vacuo*. The crude product was purified by flash chromatography on silicagel using hexane / AcOEt (80 / 20) to afford an incolor oil (880 mg, 90% yield).

^{1}H NMR (400 MHz, $CDCl_3$, 298 K): δ_H (ppm) 2.70 (dd, *J* = 10.2 Hz, *J* = 4.7 Hz, 2H, 2 × C*H*$_2$-N), 3.01 (dd, *J* = 10.2 Hz, *J* = 6.5 Hz, 2H, 2 × C*H*$_2$-N), 3.69 (s, 2H, N-C*H*$_2$-Ph), 4.04-4.07 (m, 2H, 2 × C*H*-N_3), 7.32-7.38 (m, 5H, *H*C$_{aromatic}$).

^{13}C NMR (100 MHz, $CDCl_3$, 298 K): δ_C (ppm) 57.5 (2 × *C*H_2-N), 60.1 (N-*C*H_2-Ph), 62.2 (2 × *C*H-N_3), 127.8 (*C*$_{aromatic}$H), 128.9 (2 × *C*$_{aromatic}$H), 129.1 (2 × *C*$_{aromatic}$H), 138.2 (*C*$_{aromatic}$).

(*meso*)-3,4-(*N*,*N*'-Bis(3,5-di-*tert*-butylsalicylidene))-pyrrolidine.

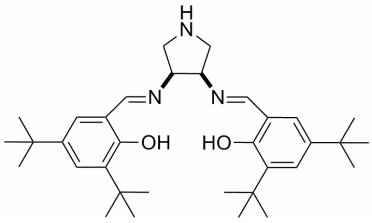

This synthesis was adapted from a published procedure.[219] All the manipulations were carried out using standard Schlenk techniques. A suspension of palladium on charcoal (10% w/w, 47 mg, 0.02 mmol) in EtOH / CF_3COOH (8 / 2 v / v) was added to a solution of (*meso*)-*N*-benzyl-3,4-diazidopyrrolidine (100 mg, 0.41 mmol) in EtOH / CF_3COOH (8 / 2 v / v, total volume 2 mL). The suspension was shaken under 5 bar H_2 for 16 h, filtered through celite and concentrated under vacuum to afford a white solid. The crude residue was dissolved in EtOH (3 mL) and neutralized with a solution of NaOH 4.7 M (0.32 mL). Neat 3,5-di-*tert*-butyl-2-

hydroxybenzaldehyde (197 mg, 0.84 mmol) was added at once and the reaction was refluxed for 2 h. The reaction mixture was then poured into 3.3 mL saturated NaCl solution and extracted three times with CH_2Cl_2. The organic layers were combined, washed with saturated NaCl solution, dried over Na_2SO_4 and evaporated under vacuum. The product was purified by flash chromatography on silicagel using AcOEt / MeOH (initially pure AcOEt, then 95 / 5) to yield a foamy yellow glass (110 mg, 54% yield over the two steps).

^{1}H NMR (400 MHz, $CDCl_3$, 298 K): δ_H (ppm) 1.28 (s, 18H, 2 × C(C*H*$_3$)$_3$), 1.29 (s, 18H, 2 × C(C*H*$_3$)$_3$), 3.39-3.41 (m, 4H, 2 × C*H*$_2$-N), 4.05-4.07 (m, 2H, C*H*-N=CH), 7.04 (d, *J* = 2.44 Hz, 2H, *H*C$_{aromatic}$), 7.35 (d, *J* = 2.44 Hz, 2H, *H*C$_{aromatic}$), 8.36 (s, 2H, 2 × C*H*=N), 13.34 (s, 2H, 2 × O*H*).

^{13}C NMR (100 MHz, $CDCl_3$, 298 K): δ_C (ppm) 29.8 (C-(*C*H$_3$)$_3$), 31.9 (C-(*C*H$_3$)$_3$), 34.5 (2 × *C*-CH$_3$), 35.4 (2 × *C*-CH$_3$), 53.4 (2 × *C*H$_2$-N), 73.6 (2 × *C*H-N), 118.0 (2 × *C*$_{aromatic}$), 126.2 (2 × *C*$_{aromatic}$H), 127.5 (2 × *C*$_{aromatic}$H), 137.1 (2 × *C*$_{aromatic}$), 140.2 (2 × *C*$_{aromatic}$), 158.5 (*C*$_{aromatic}$), 166.7 (2 × *C*H=N).

APCI$^+$-MS: 546.5 (30), 535.5 (50, $[M+2H]^{2+}$), 534.5 (100, $[M+H]^+$).

(*meso*)-*N*-Biotinyl-3,4-(*N'*,*N"*-bis(3,5-di-*tert*-butylsalicylidene))-pyrrolidine, Sal-4.

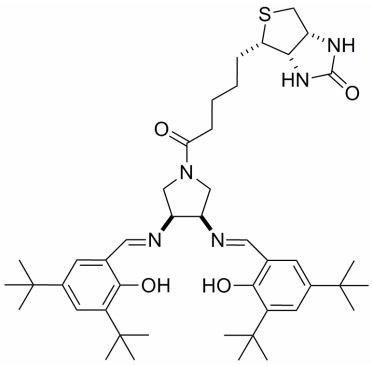

To a solution of **(***meso*)-3,4-(*N*,*N'*-bis(3,5-di-*tert*-butylsalicylidene))-pyrrolidine (36 mg, 0.07 mmol) and BNHS (25 mg, 0.07 mmol) in DMF (1 mL) was added Et_3N (14 µL, 0.1 mmol) and the reaction mixture was stirred at room temperature during 24 h. The solvent was evaporated and the crude product was purified by flash chromatography on silicagel using CH_2Cl_2 / MeOH (90 / 10) to afford **Sal-4** as a yellow solid (45 mg, 86% yield).

^{1}H NMR (200 MHz, $CDCl_3$, 298 K): δ_H (ppm) 1.27-1.37 (m, 36H, 4 × C(C*H*$_3$)$_3$), 1.40-1.90 (m, 6H, C*H*$_2$C*H*$_2$C*H*$_2$-CH$_2$CO), 2.41 (m, 2H, C*H*$_2$-CO), 2.6-3.0 (m, 2H, C*H*$_2$-S), 3.11-3.25 (m, 1H, C*H*-S), 3.8-3.97 (m, 4H, 2 × C*H*$_2$-N), 4.0-4.25 (m, 2H, 2 × C*H*-N=CH), 4.30-4.40 (m,

1H, C*H*-N), 4.45-4.50 (m, 1H, C*H*-N), 5.30 (d, *J* = 5.6 Hz, 1H, CH-N*H*), 5.97 (d, *J* = 9.6 Hz 2H, CH-N*H*), 7.05 (dd, *J* = 2.4 Hz, *J* = 4.4 Hz, 2H, 2 × *H*$C_{aromatic}$), 7.36 (d, *J* = 2.4 Hz, 2H, 2 × *H*$C_{aromatic}$), 8.35 (s, 1H, C*H*=N), 8.42 (s, 1H, C*H*=N), 13.0 (s, 1H, O*H*), 13.07 (s, 1H, O*H*).

ESI$^-$-MS: 758.7 (100, [M-H]$^-$), 759.7 (50, M), 794.5 (80, [M–H+2H_2O]$^-$), 795.4 (40, M+2H_2O).

4.2 Preparation of the Metal-Salen Complexes

(*meso*)-*N*-Biotinyl-3,4-(*N'*,*N"*-bis(3,5-di-*tert*-butylsalicylidene))-pyrrolidine, manganese^{III} chloride complex, Mn-Sal-4.

This synthesis was adapted from a published procedure.[220] To a solution of Mn(OAc)$_2$·4H_2O (44 mg, 0.18 mmol) in EtOH (1.5 mL) was added a solution of **Sal-4** in toluene (1.8 mL) and the resulting mixture was refluxed for 1 h. Saturated aqueous NaCl (0.2 mL) was then added and air was bubbled through the solution during 30 minutes. The reaction mixture was cooled to room temperature, toluene (4 mL) and CH_2Cl_2 (10 mL) were added and the organic phase was separated and washed two times with water. The aqueous phase was extracted with CH_2Cl_2 until it was colourless and the collected organic layers were dried over Na_2SO_4 and evaporated under vacuum. The Mn complex was purified by flash chromatography on silicagel using CH_2Cl_2 / MeOH (75 / 15) to afford a brown solid (28.5 mg, 56% yield).

ESI$^+$-MS: 812.5 (100, [M-Cl]$^+$), 813.5 (40, [M–Cl+H]$^+$), 814.3 (10, [M–Cl+2H]$^+$).

Mn-Sal-1 – Mn-Sal-3.

The three Mn-**Sal-X** complexes were prepared by mixing solutions of known concentrations of Mn(OAc)$_2$·4H_2O (0.08 M) and **Sal-X** (0.04 M) in DMF (1 / 1 volumes of the two solutions) and heating the resulting mixtures in closed tubes at 65°C. Thus, the corresponding Mn-**Sal-X** complexes were available in 0.02 M solutions in DMF and were used without further isolation and purification.

V-Sal-1 – V-Sal-3.

The V-**Sal-X** complexes were prepared by adapting a published procedure,[194] by mixing solutions of known concentrations of VO(acac)$_2$ (0.04 M) and **Sal-X** (0.04 M) in DMF (1 / 1 volumes of the two solutions) and heating the resulting mixtures in closed tubes at 65°C. Thus, the corresponding V-**Sal-X** complexes were available in a 0.02 M solutions in DMF and were used without further isolation and purification.

5 Analysis of the Reduction and Oxidation Products

The conversions and enantioselectivities of the catalytic runs were determined by HPLC analysis using either the Chiralcel OD-H, OB-H or OJ-H columns (Daicel Chemical Industries, Tokyo) with hexane / isopropanol as solvent or a (*S*,*S*)-ULMO column (Regis Technologies Inc., Illinois, U.S.A.) with hexane / 1,2-dimethoxyethane as solvent.

For each substrate / product couple, a calibration curve was established, relating the ratio of the HPLC integrated surfaces of the corresponding peaks ($S_{substrate}$ / $S_{enantiomer\ products}$) to the substrate / product molar ratio. Thus, the conversions were determined by comparison of the HPLC areas with the calibration curve. The enantioselectivities were directly determined from the HPLC integrated surfaces.

For the sulfoxidation catalytic runs, control experiments were performed using acetophenone as internal standard. The yields of sulfoxides determined in this manner were very similar to the conversions obtained by the previous method.

5.1 Analytical Data for the Reduction Products

Racemic alcohols were prepared from the corresponding starting ketones by reduction with $NaBH_4$ in EtOH and used for HPLC reference purposes. The analytical data for the reduction products is presented in Table 3.

For the catalytic runs with 2-acetylpyridine **5** affording enantioselectivities >90% ee (*S*), the ee's were determined by GC analysis on a β-Dex capillary column (Supelco, 30 m × 0.25 mm × 0.25 μm, 100kPa He) using the following program: initial T(°C) / time(min.) / slope(°C / min.) / T(°C) / time(min.) / slope(°C/min.) / T(°C) / time(min.) / slope(°C/min.) / T(°C) / time (min.) : 60 / 5 / 1 / 80 / 10 / 1.5 / 100 / 15 / 5 / 190 / 1. The retention times for the alcohols were: t_1 = 63.7 min. (*R*), t_2 = 64.7 min. (*S*).

Table 3. HPLC conditions, retention times and absolute configurations for the reduction products [a].

Alcohol	Column	Conditions	t_1 (min)	t_2 (min)	Detection
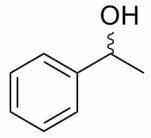	OD-H	hexane / *i*-PrOH 95 / 5 flow 0.7 mL / min	17.8 (*R*)	22.7 (*S*)	215 nm
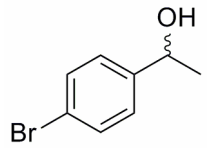	OD-H	hexane / *i*-PrOH 95 / 5 flow 0.7 mL / min	11.6 (*S*)	12.9 (*R*)	225 nm
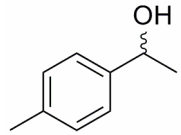	(*S*,*S*)-ULMO	hexane / DME 100 / 1.5 flow 1 mL / min	16.6 (*R*)	19.5 (*S*)	215 nm
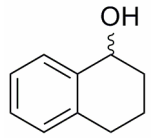	OD-H	hexane / *i*-PrOH 100 / 2 flow 0.9 mL / min	17.2[b] (*S*)	18.5[b] (*R*)	215 nm
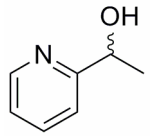	OD-H	hexane / *i*-PrOH 100 / 2 flow 0.9 mL / min	19.5[b] (*R*)	22.2[b] (*S*)	215 nm
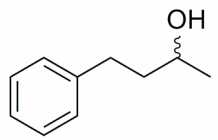	OD-H	hexane / *i*-PrOH 95 / 5 flow 0.7 mL / min	13.9[b] (*R*)	20.6[b] (*S*)	215 nm
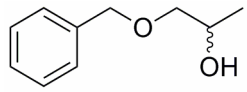	OD-H	hexane / *i*-PrOH 95 / 5 flow 0.7 mL / min	11.9[c] (*S*)	13.5[c] (*R*)	215 nm
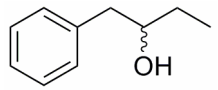	OD-H	hexane / *i*-PrOH 100 / 2 flow 0.9 mL / min	11.2 (*S*)	16.6 (*R*)	215 nm

[a] The absolute configuration was assigned by comparison with published results.[179]
[b] The absolute configuration was assigned by comparison with an enantiopure sample.
[c] The absolute configuration was assigned by comparison with an enantiopure sample prepared from (*R*)-butanediol.

5.2 Analytical Data for the Oxidation Products

Racemic sulfoxides were prepared from the corresponding starting sulfides by oxidation with vanadium sulfate and *t*-BuOOH in CH_2Cl_2 and used for HPLC reference purposes.

For the sulfoxidation with $[VO]^{2+} \subset$ Sav, the analytical data of the sulfoxides are presented in Table 4.

Table 4. HPLC conditions, retention times and absolute configurations for the sulfoxidation products [a].

Sulfoxide	Column	Conditions	t_1 (min)	t_2 (min)
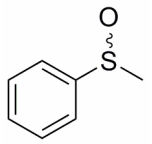	OD-H	hexane / *i*-PrOH 90 / 10 flow 0.8 mL / min	13.1 (*R*)	17.1 (*S*)
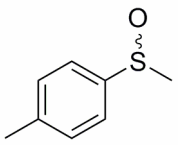	OB-H	hexane / *i*-PrOH 80 / 20 flow 1.0 mL / min	9.2 (*S*)	20.0 (*R*)
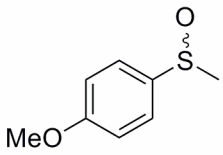	OB-H	hexane / *i*-PrOH 70 / 30 flow 1.0 mL / min	11.0 (*S*)	21.3 (*R*)
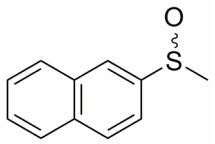	OB-H	hexane / *i*-PrOH 80 / 20 flow 1.0 mL / min	13.6 (*S*)	19.7 (*R*)
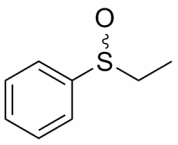	OD-H	hexane / *i*-PrOH 95 / 5 flow 0.8 mL / min	15.0 (*R*)	20.7 (*S*)
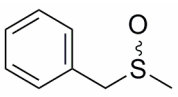	OB-H	hexane / *i*-PrOH 70 / 30 flow 1.0 mL / min	8.7 (*S*)	11.1 (*R*)
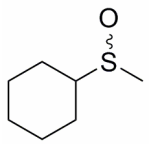	OB-H	hexane / *i*-PrOH 95 / 5 flow 1.0 mL / min	15.4 (*S*)	19.0 (*R*)

[a] UV detection at 215 nm; the absolute configurations were assigned by comparison with published results.[117]

For the sulfoxidation of thioanisole with the biotinylated metal-salen complexes, the ee's and conversions were determined either on an OD-H column with hexane / *i*-PrOH 90 / 10 at

0.8 mL / min (t_1 = 15.5 min. (*R*), t_2 = 20.5 min (*S*)), or on an OJ-H column with hexane / *i*-PrOH 100 / 2 at 1.0 mL / min (t_1 = 32.5 min. (*S*), t_2 = 34.9 min (*R*)).

Chapter 5 References

1. Lindström, B.; Pettersson, L. J. *CATTECH* **2003**, *7*, 130.
2. Evans, D.; Osborn, J. A.; Jardine, F. H.; Wilkinson, G. *Nature* **1965**, *208*, 1203.
3. Beller, M.; Bolm, C., *Transition Metals for Organic Synthesis*. 2nd ed.; Wiley-VCH: Weinheim, 2004.
4. Schoemaker, H. E.; Mink, D.; Wubbolts, M. G. *Science* **2003**, *299*, 1694.
5. Fersht, A., *Structure and Mechansim in Protein Science*. W.H. Freeman & Co.: New York, 1999.
6. Rouhi, A. M. *Chem. Eng. News* **2003**, *81*, 45.
7. Kagan, H. B. *L'actualité chimique* **2003**, 10.
8. Pàmies, O.; Bäckvall, J.-E. *Chem. Rev.* **2003**, *103*, 3247.
9. Blaser, H. U.; Spindler, F.; Studer, M. *Appl. Catal., A* **2001**, *221*, 119.
10. Blaser, H.-U.; Pugin, B.; Spindler, F. *J. Mol. Cat. A: Chemical* **2005**, *231*, 1.
11. Thayer, A. *Chem. Eng. News* **2006**, *84*, 15.
12. Dalko, P. I.; Moisan, L. *Angew. Chem. Int. Ed.* **2001**, *40*, 3726.
13. Knowles, W. S. *Angew. Chem. Int. Ed.* **2002**, *41*, 1998.
14. Kagan, H. B.; Dang, T.-P. *J. Am. Chem. Soc.* **1972**, *94*, 6429.
15. Knowles, W. S.; Sabacky, M. J.; Vineyard, B. D.; Weinkauff, D. J. *J. Am. Chem. Soc.* **1975**, *97*, 2567.
16. Noyori, R. *Angew. Chem. Int. Ed.* **2002**, *41*, 2008.
17. Sharpless, K. B. *Angew. Chem. Int. Ed.* **2002**, *41*, 2024.
18. Jacobsen, E. N.; Pfaltz, A.; Yamamoto, H., *Comprehensive Asymmetric Catalysis*. Springer: Berlin, 1999; Vol. 1-3.
19. Yoon, T. P.; Jacobsen, E. N. *Science* **2003**, *299*, 1691.
20. Knowles, W. S. *Acc. Chem. Res.* **1983**, *16*, 106.
21. Vogl, E. M.; Gröger, H.; Shibasaki, M. *Angew. Chem. Int. Ed.* **1999**, *38*, 1570.
22. Loeb, S. J., In *Comprehensive Supramolecular Chemistry*, Lehn, J.-M.; Atwood, J. L.; Davies, J. E. D.; McNichol, D. D.; Vögtle, F.; Gokel, G. W., Eds. Pergamon: Oxford, 1996.
23. Shimizu, K. D.; Snapper, M. L.; Hoveyda, A. H. *Chem. Eur. J.* **1998**, *4*, 1885.
24. Gennari, C.; Piarulli, U. *Chem. Rev.* **2003**, *103*, 3071.
25. Jandeleit, B.; Schaefer, D. J.; Powers, T. S.; Turner, H. W.; Weinberg, W. H. *Angew. Chem. Int. Ed.* **1999**, *38*, 2494.

26. Reetz, M. T. *Angew. Chem. Int. Ed.* **2001**, *40*, 284.
27. Schmid, A.; Dordick, J. S.; Hauer, B.; Kiener, A.; Wubbolts, M.; Witholt, B. *Nature* **2001**, *409*, 258.
28. Koeller, K. M.; Wong, C. H. *Nature* **2001**, *409*, 232.
29. Arnold, F. H. *Nature* **2001**, *409*, 253.
30. Sylvestre, J.; Chautard, H.; Cedrone, F.; Delcourt, M. *Org. Process Res. Dev.* **2006**, *10*, 562.
31. Kazlauskas, R. J. *Curr. Opin. Chem. Biol.* **2005**, *9*, 195.
32. Khersonsky, O.; Roodveldt, C.; Tawfik, D. S. *Curr. Opin. Chem. Biol.* **2006**, *10*, 498.
33. Goldberg, K.; Schroer, K.; Lütz, S.; Liese, A. *Appl. Microbiol. Biotechnol.* **2007**, *76*, 249.
34. Goldberg, K.; Schroer, K.; Lütz, S.; Liese, A. *Appl. Microbiol. Biotechnol.* **2007**, *76*, 237.
35. Noyori, R.; Okhuma, T. *Angew. Chem. Int. Ed.* **2001**, *40*, 40.
36. Brown, H. C.; Ramachandran, P. V. *Acc. Chem. Res.* **1992**, *25*, 16.
37. Noyori, R.; Tomino, I.; Tanimoto, Y.; Nishizawa, M. *J. Am. Chem. Soc.* **1984**, *106*, 6709.
38. Corey, E. J.; Helal, C. J. *Angew. Chem. Int. Ed.* **1998**, *37*, 1986.
39. Blaser, H.-U.; Malan, C.; Pugin, B.; Spindler, F.; Steiner, H.; Studer, M. *Adv. Synth. Catal.* **2003**, *345*, 103.
40. Meerwein, H.; Schmidt, R. *Justus Liebigs Ann. Chem.* **1925**, *444*, 221.
41. Verley, A. *Bull. Soc. Chim. Fr.* **1925**, *37*, 537.
42. Ponndorf, W. *Angew. Chem.* **1926**, *39*, 138.
43. Noyori, R.; Hashiguchi, S. *Acc. Chem. Res.* **1997**, *30*, 97.
44. Palmer, M. J.; Wills, M. *Tetrahedron: Asymmetry* **1999**, *10*, 2045.
45. Gladiali, S.; Alberico, E. *Chem. Soc. Rev.* **2006**, *35*, 226.
46. Hashiguchi, S.; Fujii, A.; Takehara, J.; Ikariya, T.; Noyori, R. *J. Am. Chem. Soc.* **1995**, *117*, 7562.
47. Wu, X.; Xiao, J. *Chem. Commun.* **2007**, 2449.
48. Puentener, K.; Schwink, L.; Knochel, P. *Tetrahedron Lett.* **1996**, *37*, 8165.
49. Everaere, K.; Mortreux, A.; Carpentier, J.-F. *Adv. Synth. Catal.* **2003**, *345*, 67.
50. Palmer, M.; Walsgrove, T.; Wills, M. *J. Org. Chem.* **1997**, *62*, 5226.
51. Sammakia, T.; Stangeland, E. L. *J. Org. Chem.* **1997**, *62*, 6104.
52. Nishibayashi, Y.; Takei, I.; Uemura, S.; Hidai, M. *Organometallics* **1999**, *18*, 2291.
53. Reetz, M. T.; Li, X. *J. Am. Chem. Soc.* **2006**, *128*, 1044.

54. Yamakawa, M.; Ito, H.; Noyori, R. *J. Am. Chem. Soc.* **2000**, *122*, 1466.
55. Haack, K.-J.; Hashiguchi, S.; Fujii, A.; Ikariya, T.; Noyori, R. *Angew. Chem. Int. Ed.* **1997**, *36*, 285.
56. Fujii, A.; Hashiguchi, S.; Uematsu, N.; Ikariya, T.; Noyori, R. *J. Am. Chem. Soc.* **1996**, *118*, 2521.
57. Koike, T.; Ikariya, T. *Adv. Synth. Catal.* **2004**, *346*, 37.
58. Clapham, S. E.; Hadzovic, A.; Morris, R. H. *Coord. Chem. Rev.* **2004**, *248*, 2201.
59. Samec, J. S. M.; Bäckvall, J.-E.; Andersson, P. G.; Brandt, P. *Chem. Soc. Rev.* **2006**, *35*, 237.
60. Noyori, R.; Yamakawa, M.; Hashiguchi, S. *J. Org. Chem.* **2001**, *66*, 7931.
61. Pàmiès, O.; Bäckvall, J.-E. *Chem. Eur. J.* **2001**, *7*, 5052.
62. Yamakawa, M.; Yamada, I.; Noyori, R. *Angew. Chem. Int. Ed.* **2001**, *40*, 2818.
63. Bubert, C.; Blacker, J.; Brown, S. M.; Crosby, J.; Fitzjohn, S.; Muxworthy, J. P.; Thorpe, T.; Williams, J. M. J. *Tetrahedron Lett.* **2001**, *42*, 4037.
64. Wu, X.; Li, X.; Hems, W.; King, F.; Xiao, J. *Org. Biomol. Chem.* **2004**, *2*, 1818.
65. Ogo, S.; Abura, T.; Watanabe, Y. *Organometallics* **2002**, *21*, 2964.
66. Wu, X.; Li, X.; King, F.; Xiao, J. *Angew. Chem. Int. Ed.* **2005**, *44*, 3407.
67. Schlatter, A.; Kundu, M. K.; Woggon, W. D. *Angew. Chem. Int. Ed.* **2004**, *43*, 6731.
68. Hayes, A. M.; Morris, D. J.; Clarkson, G. J.; Wills, M. *J. Am. Chem. Soc.* **2005**, *127*, 7318.
69. Langer, T.; Helmchen, G. *Tetrahedron Lett.* **1996**, *37*, 1381.
70. Jiang, Y.; Jiang, Q.; Zhu, G.; Zhang, X. *Tetrahedron Lett.* **1997**, *38*, 215.
71. Rubach, J. K.; Plapp, B. V. *Biochemistry* **2002**, *41*, 15770.
72. Kroutil, W.; Mang, H.; Edegger, K.; Faber, K. *Curr. Opin. Chem. Biol.* **2004**, *8*, 120.
73. Moore, J. C.; Pollard, D. J.; Kosjek, B.; Devine, P. N. *Acc. Chem. Res.* **2007**, *40*, 1412.
74. Caron, S.; Dugger, R. W.; Ruggeri, S. G.; Ragan, J. A.; Ripin, D. H. B. *Chem. Rev.* **2006**, *106*, 2943.
75. Noyori, R.; Aoki, M.; Sato, K. *Chem. Commun.* **2003**, 1977.
76. Bäckvall, J.-E., *Modern Oxidation Methods*. Wiley-VCH Verlag GmbH&Co. KGaA: Weinheim, 2004.
77. Jorgensen, K. A. *Chem. Rev.* **1989**, *89*, 431.
78. Stahl, S.; Labinger, J. A.; Bercaw, J. E. *Angew. Chem. Int. Ed.* **1998**, *37*, 2181.
79. Bonini, C.; Righi, G. *Tetrahedron* **2002**, *58*, 4981.

80. Gao, Y.; Klunder, J. M.; Hanson, R. M.; Masamune, H.; Ko, S. Y.; Sharpless, K. B. *J. Am. Chem. Soc.* **1987**, *109*, 5765.
81. Zhang, W.; Loebach, J. L.; Wilson, S. R.; Jacobsen, E. N. *J. Am. Chem. Soc.* **1990**, *112*, 2801.
82. Irie, R.; Noda, K.; Ito, Y.; Matsumoto, N.; Katsuki, T. *Tetrahedron Lett.* **1990**, *31*, 7345.
83. Jacobsen, E. N.; Wu, M. H., Epoxidation of alkenes other than allylic alcohols. In *Comprehensive Asymmetric Catalysis*, Jacobsen, E. N.; Pfaltz, A.; Yamamoto, H., Eds. Springer: Berlin, 1999; Vol. 2.
84. Jacobsen, E. N.; Zhang, W.; Guler, M. L. *J. Am. Chem. Soc.* **1991**, *113*, 6703.
85. McGarrigle, E. M.; Gilheany, D. G. *Chem. Rev.* **2005**, *105*, 1563.
86. Katsuki, T. *J. Mol. Catal. A: Chem.* **1996**, *113*, 87.
87. Nakajima, K.; Kojima, M.; Fujita, J. *Chem. Lett.* **1986**, 1483.
88. Matsumoto, K.; Sawada, Y.; Saito, B.; Sakai, K.; Katsuki, T. *Angew. Chem. Int. Ed.* **2005**, *44*, 4935.
89. Nakata, K.; Takeda, T.; Mihara, J.; Hamada, T.; Irie, R.; Katsuki, T. *Chem. Eur. J.* **2001**, *7*, 3776.
90. Kureshy, R. I.; Khan, N. H.; Abdi, S. H. R.; Bhatt, A. K.; Iyer, P. *J. Mol. Catal. A: Chem.* **1997**, *121*, 25.
91. Kureshy, R. I.; Khan, N. H.; Abdi, S. H. R.; Patel, S. T.; Iyer, P.; Suresh, E.; Dastidar, P. *J. Mol. Catal. A: Chem.* **2000**, *160*, 217.
92. Noda, K.; Hosoya, N.; Yanai, K.; Irie, R.; Katsuki, T. *Tetrahedron Lett.* **1994**, *35*, 1887.
93. Palucki, M.; Hanson, P.; Jacobsen, E. N. *Tetrahedron Lett.* **1992**, *33*, 7111.
94. Hamada, T.; Irie, R.; Mihara, J.; Hamachi, K.; Katsuki, T. *Tetrahedron* **1998**, *54*, 10017.
95. Sun, W.; Wang, H.; Xia, C.; Li, J.; Zhao, P. *Angew. Chem. Int. Ed.* **2003**, *42*, 1042.
96. Li, Z.; Tang, Z. H.; Hu, X. X.; Xia, C. G. *Chem. Eur. J.* **2005**, *11*, 1210.
97. Adolfsson, H., Transition metal-catalyzed epoxidation of alkenes. In *Modern Oxidation Methods*, Bäckvall, J.-E., Ed. Wiley-VCH Verlag GmbH&Co. KGaA: Weinheim, 2004.
98. Brandes, B. D.; Jacobsen, E. N. *J. Org. Chem.* **1994**, *59*, 4378.
99. Hamada, T.; Fukuda, T.; Imanishi, H.; Katsuki, T. *Tetrahedron* **1996**, *52*, 515.
100. Bäckvall, J.-E., Selective oxidation of amines and sulfides. In *Modern Oxidation Methods*, Bäckvall, J.-E., Ed. Wiley-VCH Verlag GmbH&Co. KGaA: Weinheim, 2004.
101. Carreño, M. C. *Chem. Rev.* **1995**, *95*, 1717.

102. Fernandez, I.; Khiar, N. *Chem. Rev.* **2003**, *103*, 3651.

103. Legros, J.; Dehli, J. R.; Bolm, C. *Adv. Synth. Catal.* **2005**, *347*, 19.

104. Bolm, C.; Muniz, K.; Hildebrand, J. P., Oxidation of sulfides. In *Comprehensive Asymmetric Catalysis*, Jacobsen, E. N.; Pfaltz, A.; Yamamoto, H., Eds. Springer: Berlin, 1999.

105. Pitchen, P.; Kagan, H. B. *Tetrahedron Lett.* **1984**, *25*, 1049.

106. Di Furia, F.; Modena, G.; Seraglia, R. *Synthesis* **1984**, 325.

107. Zhao, S. H.; Samuel, O.; Kagan, H. B. *Tetrahedron* **1987**, *43*, 5135.

108. Komatsu, N.; Hashizume, M.; Sugita, T.; Uemura, S. *J. Org. Chem.* **1993**, *58*, 4529.

109. Kokubo, C.; Katsuki, T. *Tetrahedron* **1996**, *52*, 13895.

110. Halterman, R. L.; Jan, S. T.; Nimmons, H. L. *Synlett* **1991**, 791.

111. Bolm, C.; Bienewald, F. *Angew. Chem. Int. Ed.* **1995**, *34*, 2640.

112. Bolm, C. *Coord. Chem. Rev.* **2003**, *237*, 245.

113. Groves, J. T.; Viski, P. *J. Org. Chem.* **1990**, *55*, 3628.

114. Duboc-Toia, C.; Menage, S.; Lambeaux, C.; Fontecave, M. *Tetrahedron Lett.* **1997**, *38*, 3727.

115. Legros, J.; Bolm, C. *Angew. Chem. Int. Ed.* **2004**, *43*, 4225.

116. Legros, J.; Bolm, C. *Chem. Eur. J.* **2005**, *11*, 1086.

117. Egami, H.; Katsuki, T. *J. Am. Chem. Soc.* **2007**, *129*, 8940.

118. van Deurzen, M. P. J.; van Rantwijk, F.; Sheldon, R. A. *Tetrahedron* **1997**, *53*, 13183.

119. Colonna, S.; Gaggero, N.; Carrea, G.; Pasta, P. *Chem. Commun.* **1997**, 439.

120. van de Velde, F.; Arends, I. W.; Sheldon, R. A. *J. Inorg. Biochem.* **2000**, *80*, 81.

121. ten Brink, H. B.; Tuynman, A.; Dekker, H. L.; Hemrika, W.; Izumi, Y.; Oshiro, T.; Schoemaker, H. E.; Wever, R. *Inorg. Chem.* **1998**, *37*, 6780.

122. Turner, N. J. *Curr. Opin. Biotechnol.* **2003**, *14*, 401.

123. Toscano, M. D.; Woycechowsky, K. J.; Hilvert, D. *Angew. Chem. Int. Ed.* **2007**, *46*, 3212.

124. Reetz, M. T. *Proc. Natl. Acad. Sci. U.S.A.* **2004**, *101*, 5716.

125. Arnold, F. H.; Volkov, A. A. *Curr. Opin. Chem. Biol.* **1999**, *3*, 54.

126. Taylor, S. V.; Kast, P.; Hilvert, D. *Angew. Chem. Int. Ed.* **2001**, *40*, 3310.

127. Chen, R. *Trends Biotechnol.* **2001**, *19*, 13.

128. Morley, K. L.; Kazlauskas, R. J. *Trends Biotechnol.* **2005**, *23*, 231.

129. Reetz, M. T.; Zonta, A.; Schimossek, K.; Liebeton, K.; Jaeger, K.-E. *Angew. Chem. Int. Ed.* **1997**, *36*, 2830.

130. Reetz, M. T. *Tetrahedron* **2002**, *58*, 6595.

131. Hendrickson, T. L.; de Crecy-Lagard, V.; Schimmel, P. *Annu. Rev. Biochem.* **2004**, *73*, 147.

132. Davis, B. G. *Curr. Opin. Biotechnol.* **2003**, *14*, 379.

133. Qi, D.; Tann, C. M.; Haring, D.; Distefano, M. D. *Chem. Rev.* **2001**, *101*, 3081.

134. Pauling, L. *Nature* **1948**, *161*, 707.

135. Pollack, S. J.; Jacobs, J. W.; Schultz, P. G. *Science* **1986**, *234*, 1570.

136. Tramontano, A.; Janda, K. D.; Lerner, R. A. *Science* **1986**, *234*, 1566.

137. Wentworth, P.; Janda, K. D. *Curr. Opin. Chem. Biol.* **1998**, *2*, 138.

138. Hilvert, D. *Annu. Rev. Biochem.* **2000**, *69*, 751.

139. Lu, Y. *Inorg. Chem.* **2006**, *45*, 9930.

140. Holm, R. H.; Kennepohl, P.; Solomon, E. I. *Chem. Rev.* **1996**, *96*, 2239.

141. Thomas, C. M.; Ward, T. R. *Chem. Soc. Rev.* **2005**, *34*, 337.

142. Letondor, C.; Ward, T. R. *ChemBioChem* **2006**, *7*, 1845.

143. Yamamura, K.; Kaiser, E. T. *J. Chem. Soc., Chem. Commun.* **1976**, 830.

144. Okrasa, K.; Kazlauskas, R. J. *Chem. Eur. J.* **2006**, *12*, 1587.

145. Fernández-Gacio, A.; Codina, A.; Fastrez, J.; Riant, O.; Soumillion, P. *ChemBioChem* **2006**, *7*, 1013.

146. Kokubo, T.; Sugimoto, T.; Uchida, T.; Tanimoto, S.; Okano, M. *J. Chem. Soc., Chem. Commun.* **1983**, 769.

147. van de Velde, F.; Könemann, L.; van Rantwijk, F.; Sheldon, R. A. *Chem. Commun.* **1998**, 1891.

148. Kaiser, E. T.; Lawrence, D. S. *Science* **1984**, *226*, 505.

149. Davies, R. R.; Distefano, M. D. *J. Am. Chem. Soc.* **1997**, *119*, 11643.

150. Carey, J. R.; Ma, S. K.; Pfister, T. D.; Garner, D. K.; Kim, H. K.; Abramite, J. A.; Wang, Z.; Guo, Z.; Lu, Y. *J. Am. Chem. Soc.* **2004**, *126*, 10812.

151. Mahammed, A.; Gross, Z. *J. Am. Chem. Soc.* **2005**, *127*, 2883.

152. Reetz, M. T.; Jiao, N. *Angew. Chem. Int. Ed.* **2006**, *45*, 2416.

153. Dzyuba, S. V.; Klibanov, A. M. *Tetrahedron: Asymmetry* **2004**, *15*, 2771.

154. Das, P. K.; Caaveiro, J. M. M.; Luque, S.; Klibanov, A. M. *Biotech. Bioeng.* **2002**, *78*, 104.

155. Ohashi, M.; Koshiyama, T.; Ueno, T.; Yanase, M.; Fujii, H.; Watanabe, Y. *Angew. Chem. Int. Ed.* **2003**, *42*, 1005.

156. Ueno, T.; Koshiyama, T.; Ohashi, M.; Kondo, K.; Kono, M.; Suzuki, A.; Yamane, T.; Watanabe, Y. *J. Am. Chem. Soc.* **2005**, *127*, 6556.

157. Wilchek, M.; Bayer, E. A., *Methods in Enzymology: Avidin-Biotin Technology*. Academic Press: San Diego, 1990; Vol. 184.

158. Wilson, M. E.; Whitesides, G. M. *J. Am. Chem. Soc.* **1978**, *100*, 306.

159. Lin, C.-C.; Lin, C.-W.; Chan, A. S. C. *Tetrahedron: Asymmetry* **1999**, *10*, 1887.

160. Ward, T. R. *Chem. Eur. J.* **2005**, *11*, 3798.

161. Creus, M.; Ward, T. R. *Org. Biomol. Chem.* **2007**, *5*, 1835.

162. Loosli, A.; Rusbandi, U. E.; Gradinaru, J.; Bernauer, K.; Schlaepfer, C. W.; Meyer, M.; Mazurek, S.; Novic, M.; Ward, T. R. *Inorg. Chem.* **2006**, *45*, 660.

163. Gonzalez, M.; Argarana, C. E.; Fidelio, G. D. *Biomol. Eng.* **1999**, *16*, 67.

164. Green, N. M. *Adv. Protein Chem.* **1975**, *29*, 85.

165. Sano, T.; Pandori, M. W.; Chen, X.; Smith, C. L.; Cantor, C. R. *J. Biol. Chem.* **1995**, *270*, 28204.

166. Zocchi, A.; Jobe, A. M.; Neuhaus, J.-M.; Ward, T. R. *Protein Expr. Purif.* **2003**, *32*, 167.

167. Zocchi, A.; Humbert, N.; Berta, T.; Ward, T. R. *Chimia* **2003**, *57*, 589.

168. Dixon, R. W.; Radmer, R. J.; Kuhn, B.; Kollman, P. A.; Yang, J.; Raposo, C.; Wilcox, C. S.; Klumb, L. A.; Stayton, P. S.; Behnke, C.; Le Trong, I.; Stenkamp, R. *J. Org. Chem.* **2002**, *67*, 1827.

169. Weber, P. C.; Wendoloski, J. J.; Pantoliano, M. W.; Salemme, F. R. *J. Am. Chem. Soc.* **1992**, *114*, 3197.

170. Laitinen, O. H.; Hytonen, V. P.; Nordlund, H. R.; Kulomaa, M. S. *Cell. Mol. Life Sci.* **2006**, *63*, 2992.

171. Eisenberg-Domovich, Y.; Pazy, Y.; Nir, O.; Raboy, B.; Bayer, E. A.; Wilchek, M.; Livnah, O. *Proc. Natl. Acad. Sci. USA* **2004**, *101*, 5916.

172. Weber, P. C.; Ohlendorf, D. H.; Wendoloski, J. J.; Salemme, F. R. *Science* **1989**, *243*, 85.

173. Livnah, O.; Bayer, E. A.; Wilchek, M.; Sussman, J. L. *Proc. Natl. Acad. Sci. U.S.A.* **1993**, *90*, 5076.

174. Schmidt, T. G. M.; Skerra, A. *Protein Eng.* **1993**, *6*, 109.

175. Klein, G.; Humbert, N.; Gradinaru, J.; Ivanova, A.; Gilardoni, F.; Rusbandi, U. E.; Ward, T. R. *Angew. Chem. Int. Ed.* **2005**, *44*, 7764.

176. Collot, J.; Gradinaru, J.; Humbert, N.; Skander, M.; Zocchi, A.; Ward, T. R. *J. Am. Chem. Soc.* **2003**, *125*, 9030.

177. Skander, M.; Humbert, N.; Collot, J.; Gradinaru, J.; Klein, G.; Loosli, A.; Sauser, J.; Zocchi, A.; Gilardoni, F.; Ward, T. R. *J. Am. Chem. Soc.* **2004**, *126*, 14411.

178. Reetz, M. T.; Peyeralans, J. J.-P.; Maichele, A.; Fu, Y.; Maywald, M. *Chem. Commun.* **2006**, 4318.

179. Letondor, C.; Humbert, N.; Ward, T. R. *Proc. Natl. Acad. Sci. U.S.A.* **2005**, *102*, 4683.

180. Letondor, C.; Pordea, A.; Humbert, N.; Ivanova, A.; Mazurek, S.; Novic, M.; Ward, T. R. *J. Am. Chem. Soc.* **2006**, *128*, 8320.

181. Creus, M.; Pordea, A.; Rossel, T.; Sardo, A.; Letondor, C.; Ivanova, A.; Le Trong, I.; Stenkamp, R. E.; Ward, T. R. *Angew. Chem. Int. Ed.* **2008**, *47*, 1400.

182. Thomas, C. M.; Letondor, C.; Humbert, N.; Ward, T. R. *J. Organomet. Chem.* **2005**, *690*, 4488.

183. Pierron, J.; Malan, C.; Creus, M.; Gradinaru, J.; Hafner, I.; Ivanova, A.; Sardo, A.; Ward, T. R. *Angew. Chem. Int. Ed.* **2008**, *47*, 701.

184. Letondor, C. Création de Métalloenzymes Artificielles Basées sur la Technologie Biotine-Avidine pour la Réduction Asymétrique de Dérivés Carbonylés par Transfert Hydrogénant. PhD Thesis, Université de Neuchâtel, Neuchâtel, 2006.

185. Voigt, C. A.; Mayo, S. L.; Arnold, F. H.; Wang, Z. G. *Proc. Natl. Acad. Sci. U. S. A.* **2001**, *98*, 3778.

186. Gruber, H. J.; Kada, G.; Marek, M.; Kaiser, K. *Biochim. Biophys. Acta.* **1998**, *1381*, 203.

187. Hofmann, K.; Wood, S. W.; Brinton, C. C.; Montibeller, J. A.; Finn, F. M. *Proc. Natl. Acad. Sci. U. S. A.* **1980**, *77*, 4666.

188. Schwenkreis, T.; Berkessel, A. *Tetrahedron Lett.* **1993**, *34*, 4785.

189. Pietikäinen, P. *Tetrahedron Lett.* **1994**, *35*, 941.

190. Crans, D. C.; Smee, J. J.; Gaidamauskas, E.; Yang, L. *Chem. Rev.* **2004**, *104*, 849.

191. Ma, R.; Bakac, A.; Espenson, J. H. *Inorg. Chem.* **1992**, *31*, 1925.

192. Perrin, D. D.; Dempsey, B., *Buffers for pH and Metal Ion Control*. Chapman and Hall Ltd: London, 1974.

193. Sams, C. K.; Jorgensen, K. A. *Acta Chem. Scand.* **1995**, *49*, 839.

194. Nakajima, K.; Kojima, K.; Kojima, M.; Fujita, J. *Bull. Chem. Soc. Jpn.* **1990**, *63*, 2620.

195. Chasteen, N. D.; DeKoch, R. J.; Rogers, B. L.; Hanna, M. W. *J. Am. Chem. Soc*. **1973**, *95*, 1301.

196. DeKoch, R. J.; West, D. J.; Cannon, J. C.; Chasteen, N. D. *Biochemistry* **1974**, *13*, 4347.

197. Grady, J. K.; Shao, J.; Arosio, P.; Santambrogio, P.; Chasteen, N. D. *J. Inorg. Biochem.* **2000**, *80*, 107.

198. Francavilla, J.; Chasteen, N. D. *Inorg. Chem.* **1975**, *14*, 2860.

199. Mustafi, D.; Galtseva, E. V.; Krzystek, J.; Brunel, L.-C.; Makinen, M. W. *J. Phys. Chem. A* **1999**, *103*, 11279.

200. Hu, Y.; Rech, S.; Gunsalus, R. P.; Rees, D. C. *Nat. Struct. Biol.* **1997**, *4*, 703.

201. Lawson, D. M.; Williams, C. E. M.; Mitchenall, L. A.; Pau, R. N. *Structure* **1998**, *6*, 1529.

202. Katz, B. A. *J. Mol. Biol.* **1997**, *274*, 776.

203. DeChancie, J.; Houk, K. N. *J. Am. Chem. Soc.* **2007**, *129*, 5419.

204. Hyre, D. E.; Le Trong, I.; Merritt, E. A.; Eccleston, J. F.; Green, N. M.; Stenkamp, R. E.; Stayton, P. S. *Protein Sci.* **2006**, *15*, 459.

205. Freitag, S.; Chu, V.; Penzotti, J. E.; Klumb, L. A.; To, R.; Hyre, D.; Le Trong, I.; Lybrand, T. P.; Stenkamp, R. E.; Stayton, P. S. *Proc. Natl. Acad. Sci. U.S.A.* **1999**, *96*, 8384.

206. Chen-Goodspeed, M.; Sogorb, M. A.; Wu, F.; Raushel, F. M. *Biochemistry* **2001**, *40*, 1332.

207. May, O.; Nguyen, P. T.; Arnold, F. H. *Nat. Biotechnol.* **2000**, *18*, 317.

208. Lu, Y. *Curr. Opin. Chem. Biol.* **2005**, *9*, 118.

209. Benson, D. E.; Wisz, M. S.; Hellinga, H. W. *Curr. Opin. Biotechnol.* **1998**, *9*, 370.

210. Sinou, D. *Adv. Synth. Catal.* **2002**, *344*, 221.

211. Seelig, B.; Szostak, J. W. *Nature* **2007**, *448*, 828.

212. Saltzman, H.; Sharefkin, J. G. *Org. Synth.* **1963**, *43*, 60.

213. Skander, M.; Humbert, N.; Collot, J.; Gradinaru, J.; Klein, G.; Loosli, A.; Sauser, J.; Zocchi, A.; Gilardoni, F.; Ward, T. R. *J. Am. Chem. Soc.* **2004**, *126*, 14411.

214. Wilbur, D. S.; Chyan, M.-K.; Pathare, P. M.; Hamlin, D. K.; Frownfelter, M. B.; Kegley, B. B. *Bioconjugate Chem.* **2000**, *11*, 569.

215. Couturier, M.; Andresen, B. M.; Jorgensen, J. B.; Tucker, J. L.; Busch, F. R.; Brenek, S. J.; Dube, P.; Ende, D. J.; Negri, J. T. *Org. Process Res. Dev.* **2002**, *6*, 42.

216. Rocha Gonsalves, A. M. d. A.; Serra, M. E. S.; Murtinho, D.; Silva, V. F.; Matos Beja, A.; Paixao, J. A.; Ramos Silva, M.; Alte Da Veiga, L. *J. Mol. Catal. A: Chem.* **2003**, *195*, 1.

217. Baker, G. L.; Fritschel, S. J.; Stille, J. R.; Stille, J. K. *J. Org. Chem.* **1981**, *46*, 2954.

218. Choudary, B. M.; Chowdari, N. S.; Kantam, M. L.; Santhi, P. L. *Catal. Lett.* **2001**, *76*, 213.

219. Konsler, R. G.; Karl, J.; Jacobsen, E. N. *J. Am. Chem. Soc.* **1998**, *120*, 10780.

220. Larrow, J. F.; Jacobsen, E. N.; Gao, Y.; Hong, Y.; Nie, X.; Zepp, C. M. *J. Org. Chem.* **1994**, *59*, 1939.